Naval Research Laboratory

Washington, DC 20375-5000 NRL Memorandum Report 5901 December 31, 1986

Cosmic Ray Effects on Microelectronics, Part IV

JAMES H. ADAMS, JR.

Gamma and Cosmic Ray Astrophysics Branch
Space Science Division

Approved for public release; distribution unlimited.

SECURITY CLASSIFICATION OF THIS PAGE

AD-A176611

REPORT DOCUMENTATION PAGE

1a. REPORT SECURITY CLASSIFICATION UNCLASSIFIED	1b. RESTRICTIVE MARKINGS
2a. SECURITY CLASSIFICATION AUTHORITY	3. DISTRIBUTION/AVAILABILITY OF REPORT Approved for public release; distribution unlimited.
2b. DECLASSIFICATION/DOWNGRADING SCHEDULE	
4. PERFORMING ORGANIZATION REPORT NUMBER(S) NRL Memorandum Report 5901	5. MONITORING ORGANIZATION REPORT NUMBER(S)
6a. NAME OF PERFORMING ORGANIZATION Naval Research Laboratory 6b. OFFICE SYMBOL (If applicable)	7a. NAME OF MONITORING ORGANIZATION
6c. ADDRESS (City, State, and ZIP Code) Washington, DC 20375-5000	7b. ADDRESS (City, State, and ZIP Code)
8a. NAME OF FUNDING/SPONSORING ORGANIZATION Office of Naval Technology 8b. OFFICE SYMBOL (If applicable)	9. PROCUREMENT INSTRUMENT IDENTIFICATION NUMBER
8c. ADDRESS (City, State, and ZIP Code) Arlington, VA 22217	10. SOURCE OF FUNDING NUMBERS PROGRAM ELEMENT NO. 62712N; PROJECT NO. XF12142 100; TASK NO.; WORK UNIT ACCESSION NO.
11. TITLE (Include Security Classification) Cosmic Ray Effects on Microelectronic, Part IV	
12. PERSONAL AUTHOR(S) Adams, James H., Jr.	
13a. TYPE OF REPORT Final	13b. TIME COVERED FROM 10/83 TO 10/86
14. DATE OF REPORT (Year, Month, Day) 1986 December 31	15. PAGE COUNT 114
16. SUPPLEMENTARY NOTATION	

17. COSATI CODES		
FIELD	GROUP	SUB-GROUP

18. SUBJECT TERMS (Continue on reverse if necessary and identify by block number)
Soft upsets, Cosmic rays, Geomagnetic cutoff, Soft errors, Propagation, Single event upsets, Microelectronics

19. ABSTRACT (Continue on reverse if necessary and identify by block number)

Single Event Upset (SEU) vulnerability must be considered in the design of all modern digital electronic systems for use in space. This has resulted in a need to accurately estimate the SEU rate for each type of digital microelectronic component used in the electronic system of any spacecraft on any orbit.

This report presents a method of making such estimates. This method, considers the effects of device parameters, material shielding, orbital parameters, interplanetary weather conditions and solar activity.

20. DISTRIBUTION/AVAILABILITY OF ABSTRACT ☒ UNCLASSIFIED/UNLIMITED ☐ SAME AS RPT. ☐ DTIC USERS	21. ABSTRACT SECURITY CLASSIFICATION UNCLASSIFIED
22a. NAME OF RESPONSIBLE INDIVIDUAL James H. Adams, Jr.	22b. TELEPHONE (Include Area Code) (202) 767-2747 22c. OFFICE SYMBOL Code 4154

DD FORM 1473, 84 MAR 83 APR edition may be used until exhausted. All other editions are obsolete

SECURITY CLASSIFICATION OF THIS PAGE

☆U.S. Government Printing Office: 1986—607-047

CONTENTS

COSMIC RAY EFFECTS ON MICROELECTRONICS
PART IV

1.0 INTRODUCTION

This report is intended to provide some of the tools needed to estimate single event upset (SEU) rates. An SEU occurs when a single ionizing radiation event produces a burst of hole-electron pairs in a digital microelectronic circuit that is large enough to cause the circuit to change state. In space, these unplanned changes of state usually result from the direct ionization of single heavy ions originating outside the spacecraft. SEU's may also be caused by the products of nuclear reactions initiated by particles that originated outside the spacecraft.

SEU's are causing operational difficulties of various kinds on more than a dozen spacecraft. Obviously, vulnerability to SEU's must be considered in the design of future spacecraft. In order to assess the vulnerability of any proposed design, engineers must have a reliable means of estimating the SEU rates in the radiation environments that can be expected during the mission. This requires experimental measurements and circuit modeling to establish the parameters that determine the SEU sensitivity of each device in the circuit. It also requires a reliable model of the near-earth particle radiation environment.

The first report in this series (Adams et. al., 1981a) provided a model of the near-earth particle environment at the orbit of the earth, but outside the magnetosphere. The second report (Adams et. al., 1983) described a method for computing the orbit-averaged geomagnetic cutoff transmission function that is used to modulate the environment outside the magnetosphere to any spacecraft orbit. The third report of the series (Tsao et. al., 1984) described the radiation environment high in the earth's atmosphere.

This report first describes some improvements in the model of the near-earth particle environment and extends the method of calculating the geomagnetic cu off transmission function to elliptical orbits. Next, the method of transporting the radiation environment through the walls of the spacecraft is presented. The report goes on to describe the transformation from energy spectra to LET spectra and the computation of single event upset rates caused by the direct ionization of particles originating outside the spacecraft. Several examples of SEU rate calculations are given and the SEU rates due to direct ionization are compared with those that result from the products of nuclear reactions caused by particles that originate outside the spacecraft. Computer programs are given that allow the user to compute the SEU rate of any device inside any spacecraft on any orbit.

Manuscript approved November 6, 1986.

2.0 REVISIONS AND EXTENSIONS OF PREVIOUS WORK

Our earlier work on cosmic ray effects on microelectronics has been revised and extended as described in the following sections.

2.1 Update of the near-earth particle environment

Since the publication of the first report in this series (Adams et. al., 1981a), new data on the near-earth particle environment has been published. Using these results and others, the model presented in the first report has been improved and extended (see Appendix 1).

We used the data from the French-Danish experiment on HEAO-3 (Engelmann et. al., 1983, and Juliusson et. al., 1983) to improve the fits to the galactic cosmic ray data for the elements up to nickel.

Figures 1 and 2 give the new fits to the helium and iron differential energy spectra for galactic cosmic rays. The lower solid curves in each figure are fits to the pure galactic cosmic ray spectra at solar maximum. This is the mildest radiation environment in the 11-year solar cycle. As can be seen in figure 2, no data have yet been published on the Fe spectrum at solar maximum. The upper solid curves are fits to pure galactic cosmic ray spectra at solar minimum. The galactic cosmic ray flux is highest at the minimum of the solar activity cycle. The dashed curves are spectra that include contributions from co-rotating interaction regions, the anomalous component, and small solar flares. These spectra are chosen to present fluxes that are so high at each energy that flux levels exceeding these occur only 10% of the time. The new fits should predict the absolute cosmic ray flux within a factor of two. This uncertainty arises primarily from our inability to predict future levels of solar modulation. The new fits predict the relative abundances of the elements below nickel to ±15%, on average, at the energies where the particle fluxes are most intense.

The model was extended to include all the elements up to uranium. This was done in the following way: The data from the HEAO-3 Heavy Nuclei Experiment (Binns et. al., 1981; Binns et. al., 1982, and Binns et. al., 1983) provided measurements of the elemental abundances for the elements heavier than nickel. These measurements did not, however, resolve the individual elements. It was necessary to determine the individual elemental abundances, in most cases, by matching a cosmic ray propagation calculation (for an example, see Tsao et. al., 1981) to the HEAO measurements. The cosmic ray source composition was initally taken to be the general abundance of elements (Cameron, 1980) and then the source composition and propagation conditions were adjusted to reproduce the measured abundances at earth. The "arriving" elemental abundances at earth from this propagation calculation were taken as the correct elemental abundances for galactic cosmic rays.

The description of the contribution from the anomalous component (Adams et. al., 1981) has been extended to allow investigation of the effect it would have on spacecraft, were it to be singly-ionized. This has been done by independently modeling the anomalous component spectra, based on the data of Webber et. al. (1979). Both the singly-ionized anomalous component and the galactic cosmic ray component of each particle spectrum must be modulated to the orbit-averaged geomagnetic cutoff (Adams et. al., 1983) for the spacecraft according to their different magnetic rigidities at the same energies. The two modulated components are then combined to form the orbit-averaged differential energy spectrum incident on the skin of the spacecraft.

Proton differential energy spectra for three solar flare models were presented in Adams et. al. (1981a). The ordinary and worst case flare models were for large flares, i.e., those with one week integral proton fluxes above 10 MeV exceeding 2.5×10^7 protons/cm^2. These models were based on fits to the log-normal distributions of fluxes above three energy thresholds. We have revised these fits by extending the data base for integral proton fluxes above 10 MeV through April, 1984 using GOES satellite data (Coffey, 1984). This allowed the amplitudes of the model spectra to be adjusted. See eqs. 33 and 34 of Appendix 1 for details.

The solar flare particle event descriptions in the original model (Adams et. al., 1981a) used the proton spectra, scaled by the heavy ion to proton ratios, to obtain the spectra of heavier ions. These ratios have been revised on the basis of additional data on solar energetic particle composition (Mewaldt, 1980; Zinner, 1980; Briggs, 1979; and Van Hollebeke, 1975). They have also been extended to include the spectra for all the elements heavier than nickel. The mean composition was extended using the data on the general abundances of the elements from Cameron (1980). To get the worst-case composition for these same elements, we used the charge-dependent enhancement factor suggested by Dietrich and Simpson (1978), and assumed that it could be extended to uranium. The only data on heavy ion enrichment beyond zinc comes from tracks in meteoritic and lunar olivine samples (Goswami et. al., 1980). These data show an even greater heavy ion enrichment than predicted by the formula we used here. We will, however, continue to use the Dietrich and Simpson formula until solar flare composition measurements, made with detectors designed for this purpose, become available. In this report, we have dropped the descriptions of the mean flux from various flares given in Adams et. al. (1981), because only instantaneous flare fluxes are relevant to the SEU problem.

We also introduced another flare spectral model (Adams and Gelman, 1984). This model is intended to display all the worst features of all the recorded flares in the last thirty years. Lingenfelter and Hudson (1980) investigated the statistical data on solar flare particle fluxes. They concluded that there is a maximum size for solar particle events and that events larger than those thus far observed are very rare. We therefore will assume that our composite worst-case flare model is the most extreme event that can occur. As such, it presents the kind of environment that spacecraft should be designed to endure if they are intended to function without interruption.

The updated model is given in Appendix 1. We have compared this model with the results of Chenette and Dietrich (1984). We find that its predictions are in agreement with the results reported by these authors. This updated model should be compared with Appendix 1 of Adams et. al. (1981a) to see the detailed changes.

In recent years, evidence has been accumulating that solar energetic heavy ions may not be fully ionized. This is certainly the case in the $0.5 \leq E \leq 2.5$ MeV/u energy range, as has been shown by A. Luhn et al. (1984). At the higher energies of interest here solar energetic heavy ions may not be fully ionized (as has been generally assumed up to now). Although heavy ions with energy >10 MeV/u would be fully ionized by passing through sufficient matter, the available data only place an upper limit their pathlength in matter (Mewaldt and Stone, 1983).

Fischer et al. (1984) report evidence that solar energetic heavy ions in the energy range $5 \leq E \leq 20$ MeV/u are not fully ionized. These authors report upper limits on the charge to mass ratio of heavy ions as low as 0.1 (this ratio is ~0.5 for fully ionized heavy ions). Breneman and Stone (1985) have obtained indirect evidence that solar energetic heavy ions in the energy range 3.5 to 50 MeV/u have the same distribution of charge states as measured for 0.5 to 2.5 MeV/u ions by Luhn et al. These authors have shown that the systematic abundance variations in SEP heavy ions compared to solar coronal abundance can be understood if the change state distributions measured by Luhn et al. are assumed for these higher energy heavy ions.

The SEP model described in this report assumes that the SEP heavy ions are fully ionized. This assumption may be incorrect from the evidence discussed above. If this is the case, the SEU rates due to SEP's will be systematically underestimated for spacecraft in low earth orbit, because geomagnetic shielding will not be as effective as the present model assumes.

Under the present circumstances, the charge state of SEP's is uncertain, so it's not clear how the model for SEP's should be altered to account for the SEP charge states. Therefore, we recommend continuing to use the present model. A conservative calculation can always be made by neglecting the protection afforded by the geomagnetic cutoff (assuming the geomagnetic cutoff transmission function is 1.0 for all energies).

2.2 Extension of the geomagnetic cutoff transmission function

The technique for calculating the geomagnetic cutoff transmission function described in Adams et. al. (1983) has been extended to elliptical orbits. See Appendix 2 for the details.

3.0 RADIATION TRANSPORT THROUGH THE WALLS OF THE SPACECRAFT

The orbit-averaged differential energy spectrum of each element at the skin of the spacecraft can be found using the model spectra from Appendix 1, and modulating them to the orbit of spacecraft, using the geomagnetic cutoff transmission function calculated by the method described in Adams et. al. (1983) and Appendix 2. To find the differential energy spectra at the microelectronic components inside the spacecraft, a transport calculation must be performed. This is best done by the method of Adams (1983). This method takes into account the effects of energy loss and particle losses through total inelastic collisions. No account is taken of the way in which the projectile fragments from these collisions contribute to the differential energy spectra of lighter ions. This omission results in a systematic underestimate of the particle fluxes, especially for the elements from argon through manganese. This underestimate is so small, it can be neglected for shielding thicknesses typically found in spacecraft.

The differential energy spectrum, f(E), inside the spacecraft and behind a thickness, t (in g/cm^2 of aluminum or equivalent) of shielding is,

$$f(E) = f'(E')[S(E')/S(E)]\exp(-\sigma t), \text{ and} \quad (1)$$

$$\sigma = [5X10^{-26}\ \eta(A^{1/3} + 27^{1/3} - 0.4)^2]/27. \quad (2)$$

Where:

f'(E') is the differential energy spectrum at the skin of the spacecraft;

E' is the energy at the skin of the spacecraft, i.e., $E' = R^{-1}[R(E) + t]$, where R(E) is the residual range of an ion having an energy E and R^{-1} is the inverse function of R(E);

E is the energy inside the spacecraft;

S(E) is the stopping power of an ion having an energy E;

A is the atomic mass of the ion; and

η is Avogadro's number.

The range-energy and stopping power data come from Adams et. al. (1987). The tables needed for aluminum are reproduced in Appendices 3 and 4. Equations (1) and (2) give estimates of the differential energy spectra inside spacecraft that are satisfactory for estimating SEU rates provided the shielding thickness does not exceed 50 g/cm^2. For greater shielding thicknesses, the method of Adams (1983) seriously underestimates the SEU rate. For further discussion of this point, see Adams (1983). Precise estimates can be made by an exact transport calculation, following the methods of Tsao et. al. (1984).

4.0 CALCULATION OF THE LET SPECTRUM

The next step is to calculate the linear energy transfer (LET) spectrum from the differential energy spectra at the microelectronic components inside the spacecraft. LET is the rate at which energy is deposited per unit pathlength of an ionizing particle. For the present purpose, it is equivalent to the rate of energy loss per unit pathlength for the same particle, i.e., dE/dx or stopping power. Figure 3 shows the stopping power, S, versus energy (taken from Adams et. al., 1987) for several ions in silicon. Appendix 5 gives these same data in tabular form.

The transformation from a differential energy spectrum to a differential LET spectrum is simply,

$$f(S) = f(E)[dE/dS]. \qquad (3)$$

By examining Figure 3, it can be seen that Eq. 3 has three and sometimes four singularities, at the points where dS/dE becomes zero (and therefore dE/dS becomes infinite). When the transformation is done on a computer, the ratio of finite differentials is used to approximate dE/dS and if the boundaries of the intervals in E and S are properly chosen, the ratio can be kept finite.

To see an example of how this is done, consider the three iron differential energy spectra in Figure 4. The lowest is pure cosmic ray iron at solar maximum, the middle curve is pure cosmic ray iron at solar minimum, and the upper curve is the 90% worst case environment spectrum for iron. Each of these spectra is behind 0.025 inches of aluminum shielding and outside the magnetosphere, so there is no geomagnetic cutoff. Figure 5 shows the result

of the transformation of these spectra to differential LET spectra. Three spikes can be seen in these spectra, corresponding to the three singularities in dE/dS. These singularities make differential LET spectra awkward to handle on a computer. We prefer, instead, to use integral LET spectra. Figure 6 shows these same three spectra in integral form.

The final step is to repeat the application of Eq. 3 to the differential energy spectra for all the elements in cosmic rays (i.e., protons to uranium) and sum the resulting integral LET spectra to form one composite integral LET spectrum. This spectrum can then be used to estimate SEU rates that result from the direct ionization of charged particles.

5.0 CALCULATION OF SEU RATES FROM THE DIRECT IONIZATION OF CHARGED PARTICLES

An SEU occurs when a sufficiently large burst of charge is collected on a critical node in one of the digital microcircuits on a chip. The minimum charge required to produce an SEU is called the critical charge. This burst of charge can come from a segment of the ionized trail left by the passage of an intensely ionizing particle. It is assumed that each critical node is surrounded by a sensitive volume (idealized as a rectangular parallelepiped) and that the charge deposited in this volume gets collected (Pickel and Blandford, 1980). The dimensions of the sensitive volume are related to those of the critical node. The sensitive volume is not, however, just the dimensions of this feature. Charge is also collected from the silicon surrounding the node by diffusion. The efficiency of charge collection from beyond the node falls off with distance. Pickel and Blandford (1980) discuss how the critical charge and the dimensions of the sensitive volume are found. In general, experimental measurements of the operational SEU cross section for the device, as well as design data supplied by the manufacturer, are required. It is often necessary to interpret these data using detailed circuit modeling computer programs before the device SEU parameters can be determined (see Price et. al., 1981, Zoutendyk, 1983, and Zoutendyk et. al., 1984, for example).

This simple model, described above, predicts that when the critical charge has been collected, an SEU will occur. The amount of charge collected depends linearly on the LET of the ionizing particle and the length of its path within the sensitive volume. There is, however, another effect that extends the size of the sensitive volume. The intense trail of ionization left by the charged particle alters the electric field pattern in the neighborhood of the feature. The field forms a funnel along the particle's track and this enhances the efficiency with which charge is collected (Hsieh et. al., 1981). This funnel effect can be partly accounted for in the simple model discussed above if the dimensions of the sensitive volume are experimentally determined. Several attempts have been made to model the funnel effect explicitly (see McLean and Oldham, 1982; Messenger, 1982; and Oldham and McLean, 1983). The model of Oldham and McLean (1983) appears to correctly describe the experimental data qualitatively, and is in quanitative agreement for lightly ionizing particles. This model predicts that the collected charge will vary with LET to the 4/3 power and that SEU sensitivity may depend on the charge collection time, that in turn depends on LET. These are the practical differences between the model of Mclean and Oldham (1983) and the Pickel and Blandford model. Because detailed models that explicitly include the funnel effect have not yet "matured", the simpler model of Pickel and Blandford will be used here.

This method for estimating soft upset rates due to the direct ionization by particles originating outside the spacecraft is given below in the form presented by Adams (1983). The upset rate, N_e, in upsets/bit-sec is:

$$N_e = 22.5\pi A\, Q_{crit} \int_{22.5Q_{crit}/P_{max}}^{L_{max}} D[p(L)]F(L)/L^2\, dL, \qquad (4)$$

where,

A is the surface area of the sensitive volume in m^2,

Q_{crit} is the minimum charge required to produce an upset, in picocoulombs,

$L_{max} = 1.05 \times 10^5$ MeV cm^2/g, the highest LET any stopping ion can deliver,

P_{max} is the largest diameter of the sensitive volume in g/cm^2,

L is LET in MeV cm^2/g,

F(L) is the integral LET spectrum in Particles/m^2 ster-sec,

and

D[p(L)] is the differential pathlength distribution in the sensitive volume of each memory cell in cm^2/g,

where,

$p(L) = 22.5\, Q_{crit}/L$ is the pathlength over which an ion of LET, L, will produce a charge Q_{crit}. The constant 22.5 is the conversion from picocoulombs to MeV, assuming 3.6 ev per hole-electron pair.

Equation (4) contains the implicit assumption that the LET of each ion is essentially constant over the dimensions of the critical volume. Of course, this is not true for stopping ions very near the end of their range. Eq. (4) will assume that the maximum LET of the stopping ion applies over its entire pathlength in the sensitive volume. This assumption can result in calculated energy depositions that exceed the residual energy of the ion. The problem is especially acute for large sensitive volume dimensions, and threshold LET values just below the maximum LET of an ion that is much more abundant than all heavier ions. Fortunately, this circumstance arises rarely. Eq. (4) will be accurate if the flux of stopping ions is small compared to fast ions having the same LET. Care should be taken in the use of this formula when the threshold LET is just below the edge of a "cliff" in the integral LET spectrum.

Eq. (4) assumes one continuously sensitive critical node per bit. In general, there may be several critical nodes per bit, each with its own sensitive volume dimensions and critical charge. In addition, these nodes may

only be sensitive part of the time, making it necessary to calculate partial upset rates for each node and then combine the results, weighted by the fractional "live" time of each node. The reader is referred to Nichols et. al. (1983) for a collection of test data and to Pickel and Blandford (1980), Price et. al. (1981), Kolasinski et. al. (1983), Zoutendyk (1983), and Zoutendyk et. al. (1984) for examples of how device SEU parameters can be determined.

6.0 CALCULATION OF SEU'S RESULTING FROM NUCLEAR REACTIONS, CAUSED BY PROTONS

The intensely ionizing particles that cause an SEU can be the fragments of a silicon nucleus struck by a particle originating outside the spacecraft. The most common particle in space capable of causing such a nuclear reaction is the proton. At present, the most practical method for calculating proton-induced SEU's is to measure the operational SEU cross section at one proton energy and then use the method of Bendel and Petersen (1983) to find the SEU rate in any proton environment. Bendel and Petersen give the SEU operational cross section in upsets per proton/cm^2 per bit as,

$$\sigma = 1 \times 10^{12} \, (24/A)^{14} \, [1-\exp(-0.18Y^{0.5})]^4 \qquad (5)$$

where,

$$Y = [(18/A)^{0.5}](E-A), \qquad (6)$$

where E and A are in MeV.

Proton differential energy spectra can be obtained from Sawyer and Vette (1976) for the trapped radiation, and Appendix 1 of this report for the exomagnetospheric components. The exomagnetospheric components can then be modulated to any orbit by the method discussed in Adams et. al. (1983) and Appendix 2. The combined proton differential energy spectrum incident on the skin of the spacecraft can then be propagated to the electronics inside using a simplified version of Eq. 1, given below:

$$f(E) = f'(E')[S(E')/S(E)] \qquad (7)$$

The final step is to integrate the cross section over the proton differential energy spectrum, i.e.,

$$R = (1 \times 10^{-4}) \, 4\pi \int_0^{\infty} f(E)\sigma(E)dE \qquad (8)$$

where f(E) is in protons/(m^2 ster.sec. MeV) and R is in upsets per bit-sec.

7.0 DESCRIPTION OF THE CREME COMPUTER PROGRAMS

The CREME programs are a group of FORTRAN routines that calculate differential and integral energy and LET spectra of cosmic rays incident on the electronics inside any spacecraft in any earth orbit and the single event upset rates that result. Input parameters for running these programs describe

the interplanetary and magnetospheric weather conditions, the spacecraft's orbit, the shielding surrounding the electronics, and the characteristics of the device under consideration. Input data files contain tabulations of stopping powers and ranges of cosmic ray nuclei in aluminum and silicon, and geomagnetic cutoffs. The program's output files containing energy and LET spectra, and single event upset rates. Descriptions and instructions on how to run the CREME programs are given below. The various options given by the programs are described here following the descriptions of the programs themselves. Listings of all of the CREME programs are given in Appendix 7 of this report.

7.1 How to run the CREME programs

First, compile all the programs and subroutines, and link the programs with all appropriate subroutines. (See Sections 7.2 and 7.3 to see which subroutines must be linked with each program). For each run of the CREME programs, follow the below instructions:

1. Decide all the options you want in your run. These deal with: your spacecraft's orbit; which cosmic ray environment to consider; material shielding surrounding your device; and specifics about the device. (See Section 7.5 for details).

2. If you wish to consider geomagnetic cutoff and trapped proton effects (see Section 7.5), then run the two auxiliary programs STASS and GEOMAG2 (see Section 7.3).

3. To get differential or integral cosmic ray flux for any element versus particle energy, run SPEC (see Section 7.2).

4. For differential or integral cosmic ray flux versus particle LET, run LET (see Section 7.2).

5. To find upset rates from nuclear reactions caused by protons, run BENDEL (see Section 7.2).

6. To find upset rates caused by direct ionization, you must run two programs. First run LET to get an integral LET spectrum; then run UPSET to get the upset rate (see Section 7.2).

7.2 The main CREME programs

The main CREME programs are SPEC, LET, BENDEL, and UPSET. SPEC and LET produce spectra; UPSET and BENDEL produce upset rates.

SPEC outputs the differential and/or integral energy spectra for a single element. SPEC options are: name(s) of output file(s); number of data points in output file(s); the atomic number of the ion whose spectra you want; the year; whether to include geomagnetic cutoff and trapped protons; the interplanetary weather index; and the thickness of material shielding. SPEC must be linked with the subroutines INSIDE, CUT, CRF, DEDXAL, and RAL. If geomagnetic cutoff and trapped protons are included, the intermediate data files GTRANS.DAT and STASS.DAT (created by the auxiliary programs GEOMAG2 and STASS) must be present. The output files of SPEC are in two columns: the

first column is differential flux in particles/(m^2 .ster.sec)/(MeV/u) or integral flux in particles/(m^2 .ster.sec); the second column is energy in MeV/u.

LET outputs differential and/or integral LET spectra from a range of elements. Unlike SPEC, which simply tabulates the results of its subroutines, LET must reparameterize the fluxes. Using stopping power functions, LET transforms the energy spectra into LET spectra. The LET program has the same options as SPEC. In addition, the range of atomic numbers of elements to be included in the LET spectra is required. LET must be linked with the subroutines INSIDE, CUT, CRF, DEDXAL, RAL, and DEDXSI. As with SPEC, the intermediate data files GTRANS.DAT and STASS.DAT are needed if cutoff and trapped protons are to be included. The output files of LET have the same format as those of SPEC, but with different units: differential flux in particles/(m^2 .ster.sec)/(MeV.cm^2/g) or integral flux in particles/(m^2 .ster.sec); versus LET in MeV.cm^2/g.

BENDEL outputs the upset rate of a microelectronic device due to nuclear reactions caused by protons. The program integrates the formula of Bendel and Petersen (1983) over the differential energy spectrum of protons. BENDEL options are: number of points used to calculate the proton energy spectrum; the year; whether to include geomagnetic cutoff and trapped protons; the interplanetary weather index; the thickness of material shielding; and either Bendel's parameter A or a measured upset cross-section, in upsets/(bit proton/cm^2), at some energy, in MeV. BENDEL uses the same subroutines and data files as SPEC. It outputs upsets/(bit.sec) and upsets/(bit.day).

UPSET is a more complicated program that calculates the upset rate from the direct ionization of particles originating outside the spacecraft. UPSET assumes that each bit is stored in a microcircuit which has one continuously sensitive node. This node is surrounded by a sensitive region which is assumed to have the shape of a rectangular parallelepiped. To calculate the upset rate using UPSET, one must first use LET to create an integral LET spectrum. UPSET then integrates this spectrum over the differential distribution of pathlengths through the sensitive region of the one sensitive node in the microcircuit to obtain the SEU rate. UPSET's input parameters are: the critical charge required to produce an SEU in the device; the linear dimensions of the parallelipiped representing sensitive region of a microcircuit; and the name of the file containing the input integral LET spectrum. UPSET must be linked with the subroutine DIFPLD. UPSET outputs upsets/(bit.sec) and upsets/(bit.day).

7.3 Auxiliary CREME programs

STASS provides input data to LET, SPEC, and BENDEL on the trapped proton flux, averaged around the spacecrafts' orbit. It is a simple program that transforms unformatted hand input into formatted output for use as input data in CREME main programs. Data for STASS should come from the "Averaged Differ. Flux, #/cm**2/sec/keV" column of "Composite Orbit Spectrum" tables. These are typically included in a National Space Science Data Center report such as Stassinopoulos (1981) or Stassinopoulos (1982). STASS needs no subroutines or input data files. It outputs a two-column file: the first column is energy in MeV; the second column is differential flux in protons/(cm^2 sec)/keV. This file must be renamed to STASS.DAT before it can be used as input. (The

subroutine CRF converts the units in this file to the units used in the main programs). Note that the trapped proton contribution to SPEC, LET, or BENDEL can be omitted by creating a STASS.DAT file with zero fluxes.

GEOMAG2 is a long, complicated program that computes the geomagnetic cutoff transmission function corresponding to a given orbit. The program traces the orbit in small time steps for two days of the orbit, calculating the position and then the cutoff 200 times. These cutoffs are integrated into a "transmission function", see Adams et. al. (1983) and Appendix 2 of this report for details on this process. GEOMAG2 options are just those parameters of the orbit that are mentioned in Section 7.5. They should describe the orbit corresponding to the STASS.DAT file being used. GEOMAG2 does not need to be linked with any other program files; it uses the input file CUTOFF.DAT, a table of cutoffs at 20 km altitude (see Appendix 6). GEOMAG2 outputs a two-column data file: the first column is cutoff in GeV/ec; the second column is the transmission function, which varies from 0 to 1. This file, called GTRANS.DAT, is used as input, along with a corresponding STASS.DAT file, for the main programs--if the "geomagnetic cutoff and trapped protons" option is chosen.

7.4 CREME subprograms

INSIDE is a subroutine that accounts for the effect of material shielding on particle fluxes and energies. It considers energy loss effects and nuclear fragmentation, but does not keep track of the fragments. The shielding is assumed to be aluminum. INSIDE is called by SPEC, LET, and BENDEL; it calls CRF, CUT, RAL, and DEDXAL.

CUT applies the geomagnetic cutoff transmission function to individual particle fluxes and adds the singly-ionized anomalous cosmic rays (if that weather condition has been chosen). CUT is only called when the "geomagnetic cutoff and trapped protons" option has been chosen. In this case, CUT is called by INSIDE; it calls CRF and uses the GTRANS.DAT data file.

CRF uses formulas to calculate the differential energy spectrum of solar flare particles and/or cosmic rays of a given element, energy, year, and "weather condition". In addition, CRF has an entry point called PROTON that extracts orbit-averaged trapped proton fluxes from STASS.DAT. CRF is called by INSIDE or CUT; it calls no subroutines and uses the data file STASS.DAT (if the "geomagnetic cutoff and trapped protons" option has been chosen).

DEDXSI, DEDXAL, and RAL are subroutines that interpolate from range and stopping power tables (see Appendixes 3, 4, 5). DEDXSI is called by LET; DEDXAL and RAL are called by INSIDE. The subroutines use the input data files SILICN.DT1, ALUMNM.DT1, and ALUMNM.DT2, respectively.

DIFPLD computes the differential distribution of linear path lengths in a rectangular parallelepiped, from the formula of Bendel (1984). DIFPLD is called by UPSET; it calls no subroutines.

7.5 Options and parameters in the CREME programs

The auxiliary program GEOMAG2 requires an exact description of the satellite's orbit, which the program traces. To describe the orbit, one must input the altitude at apogee, the altitude at perigee, and the orbital inclination. To describe the satellite's position at the start of the calculation, one must specify the initial longitude of the ascending node, the initial latitude of the ascending node, and the displacement of the perigee from the ascending node. (This last parameter is not needed for a circular orbit). In addition, GEOMAG2 asks whether there is a "magnetic storm" and whether to take into account the fact that the earth casts a shadow on the spacecraft in cosmic rays. See Adams, et. al. (1983), for details.

The main CREME programs (those that output energy spectra, LET spectra, or upset rates) require further information: First, the cosmic ray flux subroutines require the date, the range of nuclear charges considered, and an "interplanetary weather index". The date (in years) tells where one should be in the solar cycle. The weather index M picks which of several sources and solar conditions to use in calculating the cosmic ray flux near the earth. A weather index of M=1 gives our best approximation to the galactic cosmic ray flux at the given date. This flux is included in all other "weather conditions", except for 3. This value (M=3) gives worst-case galactic cosmic ray fluxes that allow uncertainties in flux data and solar activity. These fluxes are so severe that they have only a 10% chance of being exceeded by actual fluxes at any moment. When M=2, the anomalous component, assumed fully ionized, is added to galactic cosmic rays. When M=4, a singly-ionized anomalous component is assumed. The singly-ionized particles are affected differently than fully-ionized particles by geomagnetic cutoff. When this weather condition is chosen, the "geomagnetic cutoff and trapped protons" option must be chosen as well.

Weather indexes from 5 through 12 add solar flare particles to the galactic cosmic rays:

M=5: peak ordinary flare flux and mean composition;
M=6: peak ordinary flare flux and worst-case composition;
M=7: peak 10% worst-case flare flux and mean composition;
M=8: peak 10% worst-case flare flux and worst-case composition;
M=9: peak Aug. 4, 1972, flare flux and mean composition;
M=10: peak Aug. 4, 1972, flare flux and worst-case composition;
M=11: peak composite worst-case flare flux and mean composition;
M=12: peak composite worst-case flare flux and worst-case composition.

The four flare options--ordinary, 10% worst-case, Aug. 1972, and composite--describe different flares. The "peak" flux is the maximum flux resulting from the flare. "Mean" and "worst-case" composition describe flares with normal and worst-case (high) ratios, respectively, of heavy ion fluxes to proton fluxes. See Appendix 1 for details on all of these cases.

The thickness of shielding surrounding the device must be entered in the runs of the main programs. Shielding thickness is entered as the thickness equivalent in inches of aluminum, which the programs convert into g/cm^2. Shielding of other materials can be approximated by the equivalent thickness of aluminum; i.e., corresponding to the same thickness in mass per unit area.

Another option of the main programs is whether to account for the geomagnetic cutoff and trapped protons. This decision should be made based on the spacecraft's orbit: calculations for low orbits should include these effects, while high orbits (near geosynchronous and beyond) need not. The CREME programs do not compute trapped proton fluxes; these must be entered using the auxiliary program STASS.

Finally, the programs that calculate upset rates need device parameters. BENDEL, which computes the upset rate due to proton-induced fragmentation, needs the parameter A. If A is unknown, a measured value of upset cross-section, in upsets/(bit proton/cm^2), and the proton energy, in MeV, corresponding to this measurement may be given (see Bendel and Petersen, 1983). UPSET, which finds the total upset rate due to direct ionization, requires the linear dimensions of the rectangular parallelipiped representing the sensitive region associated with each bit and the critical charge required to produce an upset.

8.0 DISCUSSION OF RESULTS OBTAINED WITH THE CREME PROGRAMS

The set of programs described in section 7.0 has been used to investigate the effects of interplanetary weather conditions and geomagnetic and material shielding on SEU rates. As Adams and Gelman (1984) discussed, the critical charge of a device corresponds approximately to a threshold value of LET required to produce an SEU. It follows then that the particle flux above this LET threshold is approximately proportional to the SEU rate. With this in mind, integral LET spectra can be compared directly to see their relative effect on the SEU rate of any proposed device.

Adams (1982) discusses how the integral LET spectrum changes under various conditions. Figure 1 of his paper shows the enormous dynamic range in the LET spectra that may occur outside the earth's magnetosphere. The particle flux behind 0.025 inches of aluminum shielding and above any LET threshold can change up to 5 orders of magnitude depending on the interplanetary weather. Fortunately, most of this dynamic range is due to infrequent solar flare particle events. The largest of these occur only once a decade, and are at their worst for only a few hours. These facts lead to the first important conclusion: "It's much easier to build a spacecraft to work 99% of the time than it is to build one that will work 100% of the time".

Figure 2 of Adams (1982) demonstrates the effect of material shielding on the solar particle event resulting from the August 4, 1972 flare for the elemental spectra of hydrogen through nickel. Figure 2 of Adams (1983) shows the effects of material shielding on a Aug. 4-like flare particle event with a 90% worst case enrichment in the heavy element spectra. These results include the contributions of the elemental spectra of all the elements found in nature. Adams and Gelman (1984) present a composite worst-case flare particle event model. In Figure 4 of their of their paper, they show the effect of material shielding on this flare. In each of the above examples, it can be seen that material shielding is quite effective in reducing the SEU rate in these severe environments. The second conclusion: "Material shielding is useful in moderating solar flare particle environments and reducing the dynamic range of SEU rates, where no geomagnetic shielding is involved".

It should be noted, however, that even large amounts of shielding cannot reduce the SEU rate to the levels normally occurring in the interplanetary medium. Comparing Figures 2 and 3 of Adams (1983), we can see that 4 cm (1.6 inches) of aluminum shielding will still leave the SEU rate from the Aug. 4 - like flare 1000 times worse than the cosmic ray background environment. If we compare Figure 3 of Adams (1983) with Figure 4 of Adams and Gelman (1984), it is clear that even 2 inches of aluminum shielding will leave the composite worst-case flare particle event 10,000 times more severe than the cosmic ray background. Conclusion 1 is still valid for any practical shielding thickness.

Adams (1983) also investigated the effect of material shielding on the cosmic ray background. Figure 3 of Adams (1983) demonstrates that thick shielding is required to obtain even modest reductions in the cosmic ray induced SEU rate. The third conclusion: "Material shielding is ineffective against galactic cosmic rays".

Besides material shielding, the earth's magnetic field provides protection for spacecraft that are at low altitude and near the equator. Adams (1983) shows how the orbit-averaged LET spectrum is affected by orbital altitude and inclination. While SEU's resulting from direct ionization will be less for lightly shielded devices at lower inclinations over the normal range of values of the critical charge, the degree of reduction will increase, generally, with the critical charge (see Fig. 4 of Adams, 1983). Secondly, at low inclinations, and for lightly shielded devices, there is a range of critical charge, above 2×10^4 MeV cm^2/g, for which devices appear to be immune to SEU's. It is unlikely that such devices would really be free from upsets because in practical spacecraft electronic components will not be lightly shielded from all sides. Figure 8 of Adams (1983) demonstrates that heavy shielding will restore the LET spectrum in the 2×10^4 to 1×10^5 MeV cm^2/g range. Figure 11 of the same paper demonstrates that the SEU rate for a SBP-9900 in fact goes through a minimum and then increases at greater shielding depths. In such cases, additional shielding can actually cause the SEU rate to increase! The fourth conclusion: "One must always consider the combined effects of magnetic and material shielding on the SEU rate".

The effectiveness of geomagnetic shielding depends on the charge to mass ratio of the ions. If these heavy ions are completely stripped of their electrons, this ratio will be approximately 0.5 and magnetic shielding will be as effective as discussed above. It is certainly true that galactic cosmic rays are fully stripped of their electrons. The chemical and isotopic composition of arriving galactic cosmic rays can only be explained if these particles have passed through approximately 7 g/cm^2 of interstellar gas before reaching us (Adams et. al., 1981a). That is more than enough matter to bring these ions into their equilibrium charge state, and their energy is so high outside the heliosphere that their equilibrium charge state is fully ionized.

There is a component of the particle radiation outside the magnetosphere that may be singly ionized. It is called the anomalous component. It is discussed in detail by Adams et. al. (1981a). If this component is singly ionized it will penetrate the earth's magnetic field with greater ease and reach a spacecraft as lower energy, higher LET radiation. The existing data shows some indirect evidence that the anomalous component is singly ionized. Its charge state will not be known for certain until an experiment currently

in space, onboard the NASA's LDEF spacecraft (Adams et. al., 1981b) is analyzed. Figure 11 of Adams (1983) shows that some devices like the SBP-9900 are quite sensitive to the charge state of the anomalous component when they are in a spacecraft that's in a 28.5° inclination orbit. The SEU rate for the SBP-9900 is a couple of orders of magnitude higher than normal for light shielding, if the anomalous component is in fact singly ionized. In general, the charge state of the anomalous component will influence the SEU rate for low altitude orbits below 60° inclination. The fifth conclusion: "Until the charge-state of the anomalous component has been determined, it's prudent to assume that it's singly ionized."

Unlike cosmic rays, solar flare particles have not been through much matter before reaching earth. Mewalt and Stone (1983) report that solar flare particles at 50 MeV/u have traversed less than 30 mg/cm^2 of matter. In light of this result one must consider the possibility that solar flare particles are not fully ionized. Gloeckler et. al. (1981) measured the charge state of various solar flare ions from He to Fe in the energy range from 0.3 to 2.4 MeV/u. The ionic charge states of Fe were found to be distributed from +5 to +20, with a broad maximum around +13. At higher energies, Fischer et. al. (1984) recently reported, many ions in the 5 to 20 MeV/u range from the solar flare of Feb. 13, 1978, were not fully ionized. Using the geomagnetic cutoff, these authors were able to determine the maximum ionic charge that the observed ions could have possessed. They report upper limits on the ionic charge as low as +3 for silicon and +2 for oxygen. Based on these results, we cannot be certain of the ionic charge of solar flare ions at any energy. Further experiments will be needed to establish the charge state of solar flare particles as a function of atomic number and energy. The sixth conclusion: "The effectiveness of geomagnetic shielding for heavy ions from solar flare particle events is uncertain. A conservative approach is to ignore geomagnetic shielding for solar flare heavy ions."

Spacecraft in earth orbit are exposed to the trapped radiation which contains protons and possibly heavier ions. The trapped proton population has been modeled by Sawyer and Vette (1976). There may also be significant numbers of heavier ions trapped in the inner belt. This subject has been explored by Adams and Partridge (1982). These authors found that, based on the scanty data available, the contribution to the SEU rate from upsets caused by trapped heavy ions is likely to be important at least under some conditions and that they could not rule out the possibility that trapped heavy ions may cause SEU rates that are orders of magnitude larger than those predicted from the trapped proton population. Our present knowledge of trapped heavy ions at the energies needed to produce SEU's is so poor that it's not possible to set a credible upper limit on them. Recently, Adams et al. have reported detecting trapped He ions but no heavier trapped ions at space shuttle altitudes. At the low altitudes investigated by these authors, the trapping lifetime for heavy ions is quite short (Blake and Fresen, 1977). As a result, the failure of Adams et al. to detect them does not imply their absence at somewhat higher altitudes. Seventh Conclusion: "Estimates of the SEU rate for orbits below 7000 and 200 m.mi. are likely to only be lower limits".

Within the magnetosphere, SEU's may result from the direct ionization of heavy ions coming in from outside the magnetosphere, or from heavy ions trapped in the earth's magnetic field. SEU's may also result from the intensely ionizing fragments from nuclear reactions caused by protons. This

indirect mechanism may be important in the inner Van Allen belt due to the intense proton fluxes trapped there. Unfortunately, too little is known about trapped heavy ions to assess their relative contribution to SEU rates (perhaps this question will be resolved by the Chemical Release and Radiation Effects Satellite mission). The relative importance of the other radiation components will be investigated below.

The SEU rates for three devices will be examined as a function of orbital altitude for circular orbits at 60° inclination. Calculations were done at orbital altitudes of 200, 400, 600, 800, 1200, 1667, 2593, 3889, 5186, 6389, and 10371 km. The trapped proton environments were obtained from Stassinopoulos(1981) and Stassinopoulos and Barth (1982). The parameters for these devices are listed in Table 1. These parameters are intended only for use in the example calculations presented here and may not be accurate enough to obtain exact SEU rates.

Table 1: The Device Parameters Used to Calculate the SEU Rates in Figs. 7, 8, 9, 11, 12, and 13.

DEVICE	SENSITIVE VOLUME (in micrometers)	CRITICAL CHARGE (in picocoulombs)	"A" PARAMETER	REFERENCES
HM6508RH	20x15x2.2	0.82	-	1
SBP9989	10x10x1.8	0.36(30%)	25.2	2,3,4
	10x10x1.8	0.10(70%x15%)		5,1
	1x1x1.8	0.02(70%x15%)		
AMD2901B	80x80x3	0.25	23	5,1,6,7,8

NOTE: In the SBP9989 entry, 30% and 70% refer to the fraction of critical collectors of each type. The 15% refers to the fraction of time the collector is sensitive. The last two entries for the SBP9989 reflect the reduced cross sections with which these low values of critical charge are observed.

REFERENCES:

1. Petersen et. al. (1983).
2. Price et. al. (1981).
3. Pickel (1981).
4. Pickel (1983).
5. Nichols et. al. (1983).
6. Zoutendyk (1983).
7. Zoutendyk et. al.(1984)
8. Zoutendyk (1984).

Figure 7 compares the SEU rates for a AMD-2901B from trapped protons and heavy ions from outside the magnetosphere as a function of orbital altitude for a 60 degree inclination orbit. The environment in the interplanetary medium is assumed to be the 90% worst case environment, and the electronic components are assumed to be shielded uniformly by 0.1 inches of aluminum. Because of the large critical volume, this device presents a large target for

cosmic rays. At the same time, the relatively high critical charge limits the sensitivity of the device to proton-induced upsets. The result is that proton-induced upsets are dominant only in the heart of the inner belt, between 1700 and 3600 km.

In this calculation, it was found that Eq. (4) incorrectly took into account contributions from trapped protons. This problem arose, as discussed in Section 5, because of the large device dimensions and the value of the critical charge. The corner to corner distance across the sensitive volume is 113 micrometers. Multiplying this length by the maximum LET of a stopping proton (see Appendix 5), we get an energy deposition of 13.8 MeV or .62 pC, which is greater than the critical charge. However, the energy of a proton having a residual range of 113 micrometers is only 3.35 MeV or 0.15 pC, therefore protons cannot actually cause SEU's in a AMD2901B by their own direct ionization. The problem was solved by omitting the proton contribution from the integral LET spectra used to calculate SEU rates with the UPSET routine.

Figure 8 gives the same results, as Figure 7 for the SBP-9989. Here both sources of SEU's are lower, but this time the proton-induced SEU's are more important. This is because the relatively small device dimensions limit the cosmic ray contribution, while the low critical charge means that proton-induced SEU's depend more on the device dimensions. Figure 9 compares the total SEU rates for these devices with the rate for the HM6508RH that is not vulnerable to proton-induced SEU's. The HM6508RH is the least sensitive of the three devices considered here. Since the HM6508RH is not sensitive to proton-induced SEU's, its SEU rate declines smoothly with orbital altitude, while the other devices show peak SEU rates at about 2600 km. It should be emphasized here that Figure 9 should be regarded as a lower limit on the SEU rate, especially below 7000 km since the contribution from trapped heavy ions was not included.

So far this discussion has delt with orbit-averaged spectra. It is important to note that the geomagnetic cutoff is far from constant around an orbit. The geomagnetic cutoff will be lowest at the northern- and southern-most extremes of the orbit, and highest at the points where the orbit crosses the geomagnetic equator. This means that the SEU rate due to particles coming from outside the magnetosphere will vary around the orbit, more dramatically so at high orbital inclinations. SEU's from particles trapped in the magnetosphere will also vary around the orbit. Stassinopoulos (1981) and Stassinopoulos and Barth (1982) computed the fraction of mission time that satellites spend in regions that are free from trapped radiation (<1 proton/cm^2 sec). Figure 10 shows a plot of one minus this fraction (i.e. the fraction of time spent in the belts) and the fraction spent in the high intensity regions of the belts (>1×10^3 protons/cm^2 sec) as a function of orbital altitude for 60 degree inclination orbits. From this plot, it's clear that proton-induced SEU's occur in only a portion of the orbits, and a small portion at low altitude orbits.

To explore this further, we compute the instantaneous SEU rate around one orbit of a satellite in a 60^o inclination orbit at 1667 km altitude for each of the devices in Table 1. As above, the 90% worst case environment is assumed to exist beyond the magnetosphere and the components are assumed to be behind 0.1 inches of aluminum. The instantaneous trapped proton flux was

:en from Stassinopoulos (1981). Figure 11 compares the SEU rates due to mic rays and trapped protons for an AMD-2901B as a function of mission ime. We see that trapped protons appear to dominate only in the heart of the radiation belt passes. Cosmic rays are at their worst near the magnetic poles and their mildest at the equator, as expected. Figure 12 shows the same comparison for the SBP9989. Here the peak SEU rates in the radiation belt passes are more pronounced, though lower than in Figure 11. Figure 13 compares the total SEU rates versus mission time for the AMD2901B, the SBP-9989 and the HM6508RH. Because the HM6508RH is not vulnerable to trapped protons, its SEU rate is at a minimum when the SEU rates in the other devices are at their peaks. The SEU rates of the AMD2901B and the SBP9989 are much closer in the radiation belts than near the magnetic poles because their sensitivity to cosmic rays differs more than their sensitivity to proton-induced upsets.

For all these devices, however, the SEU rates are so low that much less than one upset is expected per orbit in each device. At the SEU rates calculated for these devices, the SEU rate should be no more than one per 10,000 bits per orbit. Therefore variations in SEU rate around an orbit cannot be easily observed in real time, unless very sensitive memory devices are used to construct very large memories. Conclusion 8: "While the instantaneous SEU rate can vary dramatically around an orbit, these variations occur on time scales that are usually small compared to the mean time between SEU's. Therefore the orbit-averaged SEU rate is a useful guide for designing spacecraft digital electronics. Only when the orbit averaged SEU rate gets as large as the inverse of the orbital period should the designer be concerned with the instantaneous rate around the orbit."

9.0 REFERENCES

Adams, Jr., James H., "The Natural Radiation Environment Inside Spacecraft", IEEE Trans. on Nucl. Sci., Vol. NS-29, 2095-2100, 1982.

Adams, Jr., James H., "The Variability of Single Event Upset Rates in the Natural Environment, IEEE Trans. on Nucl. Sci., Vol. NS-30, 4475-4480, 1983.

Adams, Jr., J.H. and K. Partridge, "Do Trapped Heavy Ions Cause Soft Upsets on Spacecraft?", NRL Memorandum Report 4846, Oct. 12, 1982. (AD-A119909)

Adams, Jr., James H., and Andrew Gelman, "The Effects of Solar Flares on Single Event Upset Rates", IEEE Trans. on Nuclear Science Vol. NS-31, 1212-1216

Adams, Jr., James H., R. Silberberg, and C. H. Tsao, "Cosmic Ray Effects on Microelectronics, Part I: The Near-Earth Particle Environment", NRL Memorandum Report 4506, August 25, 1981a. (AD-A103897)

Adams, Jr., James H., M. M. Shapiro, R. Silberberg, and C. H. Tsao, "Fast Heavy Ions in the Heliosphere", Adv. in Space Res., Vol. 1, 169-172, 1981b.

Adams, Jr., James H., J. R. Letaw, and D. F. Smart, "Cosmic Ray Effects on Microelectronics, Part II: The Geomagnetic Cutoff Effects", NRL Memorandum Report 5099, May 26, 1983.(AD-128601)

Adams, Jr., James H., James Bellingham, and Peter E. Graney, "A Comprehensive Table of Ion Stopping Powers and Ranges", NRL Memorandum Report (to be published), 1987.

Bendel, W. L., "Length Distribution of Chords Through a Rectangular Volume," NRL Memorandum Report 5369, July 3, 1984. (AD-A143302)

Bendel, W. L., and E. L. Petersen, "Proton Upsets in Orbit", IEEE Trans. on Nucl. Sci., Vol. NS-30, 4481-5, 1983.

Binns, W. R., R. K. Fickle, T. L. Garrard, M. H. Israel, J. Klarmann, E. C. Stone, and C. J. Waddington, "Cosmic-ray Abundances of Elements with Atomic numbers $26 \leq Z \leq 40$" Astrophysical Journal, Vol. 247, L115-L118, 1981.

Binns, W. R., R. K. Fickle, T. L. Garrard, M. H. Israel, J. Klarmann, E. C. Stone, and C. J. Waddington, "The Abundance of the Actinides in the Cosmic Radiation as Measured on HEAO-3", Astrophysical Journal, Vol. 261, L117-L120, 1982.

Binns, W. R., R. K. Fickle, T. L. Garrard, M. H. Israel, J. Klarmann, K. E. Krombel, E. C. Stone, and C. J. Waddington, "Cosmic-ray Abundances of Sn, Te, Xe, and Ba Nuclei Measured on HEAO 3", Astrophysical Journal, Vol. 267, L93-L96, 1983.

Blake, J. B. and L. M. Friesen, "A Technique to Determine the Charge State of the Anomalous Low-Energy Cosmic Rays", Proc. of the 15th International Cosmic Ray Conference Plovdic, 1977, Volume 2, p. 341

Breneman, H. H. and E. C. Stone, "Solar and Photospheric Abundance from Solar Energetic Particle Measurements," Astrophysical Journal, Vol. 299, L57-L61, 1985.

Priggs, P. R., T.P. Armstrong and S. M. Krimigis, "Hydrogen Over Helium Enhancement in Successive Solar Flare Particle Events From the Same Active Region", Astrophysical Journal, Vol. 228, L83-L87, 1979.

Cameron, A. G. W., "Elementary and Nuclidic Abundances in the Solar System", Harvard-Smithsonian Center for Astrophysics Preprint Series No. 1357 (1980).

Chenette, D. L., and W. F. Dietrich, "The Solar Flare Heavy Ion Environment for Single Event Upsets", IEEE Trans on Nucl Sci, Vol. NS-31, 1217-1222, 1984

Coffey, Helen A., ed., Solar Geophysical Data, No. 476, Part II, Published by the Environmental and Information Data Service, NOAA, Boulder, Colorado, April, 1984.

Dietrich, W. F., and J. A. Simpson, "Preferential Enhancements of the Solar Flare Accelerated Nuclei Carbon to Zinc from ~20-300 MeV/Nucleon", Astrophysical Journal, Vol. 225, L41-L45, 1978.

Engelmann, J. J., P. Goret, E. Juliusson, L. Koch-Miramond, P.Masse, A. Soutoul, B. Byrnak, N. Lund, B. Peters, I. L. Rassmussen, M. Rotenberg, and N. J. Westergaard, "Elemental Composition of Cosmic Rays from Be to Ni as Measured by the French-Danish Instrument on HEAO-3", Proceedings of the 18th Inter. Cosmic Ray Conf., Vol. 2, 17-20, Bangalore, India, 1983.

Fischer, S., M. Vandas, K. Kudela, S. N. Kuznetsov, V. N. Lutsenko, "Determination of the Effective Charge of Solar Cosmic Ray Nuclei Using the Earth's Magnetic Field", Advances in Space Research, Vol. 4, 169-172, 1984.

Gloeckler, G., H. Weiss, D. Hovestadt, F. M. Ipavich, B. Klecker, L. A. Fisk, M. Scholer, C. Y. Fan, and J. J. O'Gallagher, "Observations of the Ionization States of Energetic Particles Accelerated in Solar Flares", Proc. of the 17th Intl. Cosmic Ray Conf., Paris, Vol. 3, 136-9, 1981.

Goswami, J.N., D. Lal, and J. D. Macdougall, "Charge Composition and Energy Spectra of the Ancient Solar Flare Heavy Nuclei", in "The Ancient Sun", Ed. by R. O. Pepin, J. A. Eddy and R.B.Merrill, 347-64, Pergamon Press, 1980.

Hsieh, C.M., P. C. Murley, and R. R. O'Brien, "A Field-funneling Effect on the Collection of Alpha-particle Generated Carriers in Silicon Devices", IEEE Electron Device Letters, Vol. EDL-2, 103, 1981.

Juliusson, E., J. J. Engelmann, J. Jorrand, L. Koch-Miramond, P. Masse, N. Petrou, N. Lund, I. L. Rassmussen, and M. Rotenberg, "The Galactic Cosmic Ray Energy Spectra as Measured by the French-Danish Instrument on HEAO-3", Proceedings of the 18th Intl. Cosmic Ray Conf., Vol. 2, 21-24, Bangalore, India, 1983.

Kolasinski, W. A., R. Koga, D. L. Chenette, "Heavy-Ion Induced Single Event Upsets in a Bipolar Logic Device", IEEE Trans. on Nucl. Sci., Vol. NS-30, 4470-4, 1983.

Lingenfelter, R.E., and H. S. Hudson, "Solar Particle Fluxes and the Ancient Sun", in "The Ancient Sun", Ed. by R. O. Pepin, J. A. Eddy and R.B.Merrill, 69-79, Pergamon Press, 1980.

Luhn, A., B. Klecker, D. Hovestadt, G. Gloeckler, F. M. Ipavich, M. Scholer, C. Y. Fan and L. A. Fisk, "Ionic Charge States of N, Ne, Mg, Si, and S in Solar Energetic Particle Events", Advances in Space Research, Vol. 4 161-164, 1984.

Messenger, G. C., "Collection of Charge on Junction Nodes from Ion Tracks", IEEE Trans. on Nucl. Sci., Vol. NS-29, 2024-31, 1982.

Mewaldt, R. A., and E. C. Stone, "A Search for Deuterium, Tritium, and ^{3}He in Large Solar Flares", Bull. of the Am. Phys. Soc., Vol. 28, 742, 1983.

Mewaldt, R. A., "Spacecraft Measurements of the Elemental and Isotopic Composition of Solar Energetic Particles", in "The Ancient Sun", Ed. by R. O. Pepin, J. A. Eddy and R.B.Merrill, 81-101, Pergamon Press, 1980.

McLean, F. B., and T.R. Oldham, "Charge Funneling in N- and P-Type Si Substrates", IEEE Trans. on Nucl. Sci., Vol. NS-29, 2018-23, 1982.

Nichols, D. K., W. E. Price, and C. J. Malone, "Single Event Upset (SEU) of Semiconductor Devices - A Summary of JPL Test Data", IEEE Trans. on Nucl. Sci., Vol. NS-30, 4520-5, 1983.

Oldham, T. R., and F. B. McLean, "Charge Collection Measurements for Heavy Ions Incident on n- and p-Type Silicon", IEEE Trans. on Nucl. Sci., Vol. NS-30, 4493-4500, 1983.

Petersen E. L., J. B. Langworthy, and S. E. Diehl, "Suggested Single Event Upset Figure of Merit", IEEE Trans. on Nucl Sci., Vol. NS-30, 4533-9, 1983.

Pickel, James C., "Cosmic Ray Effects in Integrated Injection Logic Devices", General Order No. 6301, Rockwell Intl. Science Center, Anaheim, CA. June, 1981.

Pickel, James C., private communication, 1983.

Pickel, James C., and James T. Blandford, Jr., "Cosmic-Ray-Induced Errors in MOS Devices", IEEE Trans. on Nucl. Sci., Vol. NS-27, 1006-1015, 1980.

Price, W. E., J. C. Pickel, T. Ellis, and F. B. Frazee, "Cosmic Ray Induced Errors in $I^{2}L$ Microprocessors and Logic Devices", IEEE Trans. on Nucl. Sci., Vol. NS-28, 3946-3954, 1981.

Sawyer, D. M, and J. I. Vette, "AP-8 Trapped Proton Environment for Solar Maximum and Solar Minimum", Report NSSDC/WDC-A-R&S 76-06, Greenbelt, Md., 1976.

Shea, M.E. and D.F. Smart, "Tables of Asymptotic Directions and Vertical Cutoff Rigidities for a Fine Degree by Fifteen Degree World Grid as Calculated Using the International Geomagnetic Reference Field for Epoch 1975.0", AFCRL-TR-75-0185, Hanscom, AFB, Mass., 1975.(AD-A012509)

Stassinopoulos, E. G., "Orbital Radiation Study for Inclined Circular Trajectories", NASA-X-601-81-28, Goddard Space Flight Center, Greenbelt, Md., 1981.(AD-A141849)

Stassinopoulos, E. G., and J. M. Barth, "Non-Equatorial Terrestrial Low Altitude Charged Particle Radiation Environment", NASA-X-601-82-9, Goddard Space Flight Center, Greenbelt, Md.,1982.

Sterne,T.E.,"An Introduction to Celestial Mechanics," Interscience Publishers, 1960.

Tsao, C. H., R. Silberberg, M. M. Shapiro, and J. H. Adams, Jr., "Origin, Transformations and Propagation of Cosmic Rays with $Z \geq 50$", Proc. of the 17th Intl. Cosmic Ray Conf., Vol. 9, 130-3, Paris, 1981.

Tsao, C. H., R. Silberberg, J. H. Adams, Jr., and J. R. Letaw, "Cosmic Ray Effects on Microelectronics, Part III: Propagation of Cosmic rays in the Atmosphere", NRL Memorandum Report 5402, 1984.(AD-A145026)

Van Hollebeke, M. A. I., "Relative Abundance of Proton to Helium Nuclei in Solar Cosmic Ray Events", Proc. of the 14th Intl. Cosmic Ray Conf., Vol. 5, 1563-7, 1975.

Webber, W. R., E. C. Stone, and R. E. Vogt, "The Elemental Composition of Quiet Time Low Energy Cosmic Rays Measured on the Voyager Spacecraft", Proc. of the 16th Intl. Cosmic Ray Conf., Vol. 5, 357-362, Kyoto, 1979.

Zinner, E, "On the Constancy of Solar Particle Fluxes from Track, Thermoluminescence and Solar Wind Measurements", in "The Ancient Sun", Ed. by R. O. Pepin, J. A. Eddy and R.B. Merrill, 201-26, Pergamon Press, 1980.

Zoutendyk, J. A., "Modeling of Single-Event Upset in Bipolar Integrated Circuits", IEEE Trans. on Nucl. Sci., Vol. NS-30, 4540-5, 1983.

Zoutendyk, J. A., private communication, 1984.

Zoutendyk, J. A., C. J. Malone, and L. S. Smith, "Experimental Determination of Single-Event Upset (SEU) as a Function of Collected Charge in Bipolar Integrated Circuits," IEEE Trans. on Nucl. Sci. Vol. NS-31, 1167-1174 Dec., 1984.

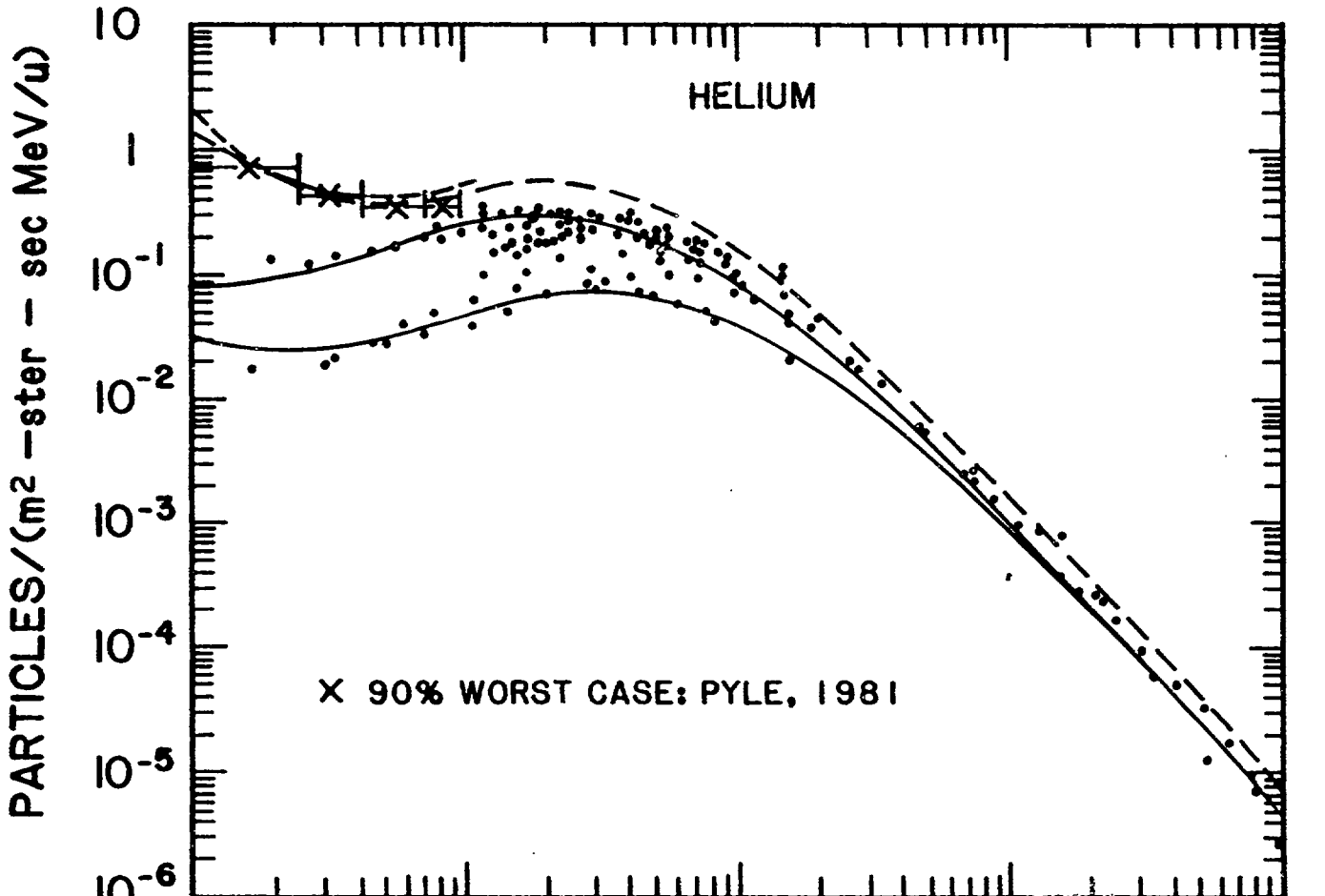

Figure 1: The cosmic ray helium spectrum: The solid curves are for solar maximum (lower) and solar minimum (upper). The dashed curve is the 90% worst-case helium spectrum. The data points are from Adams et al. (1981a).

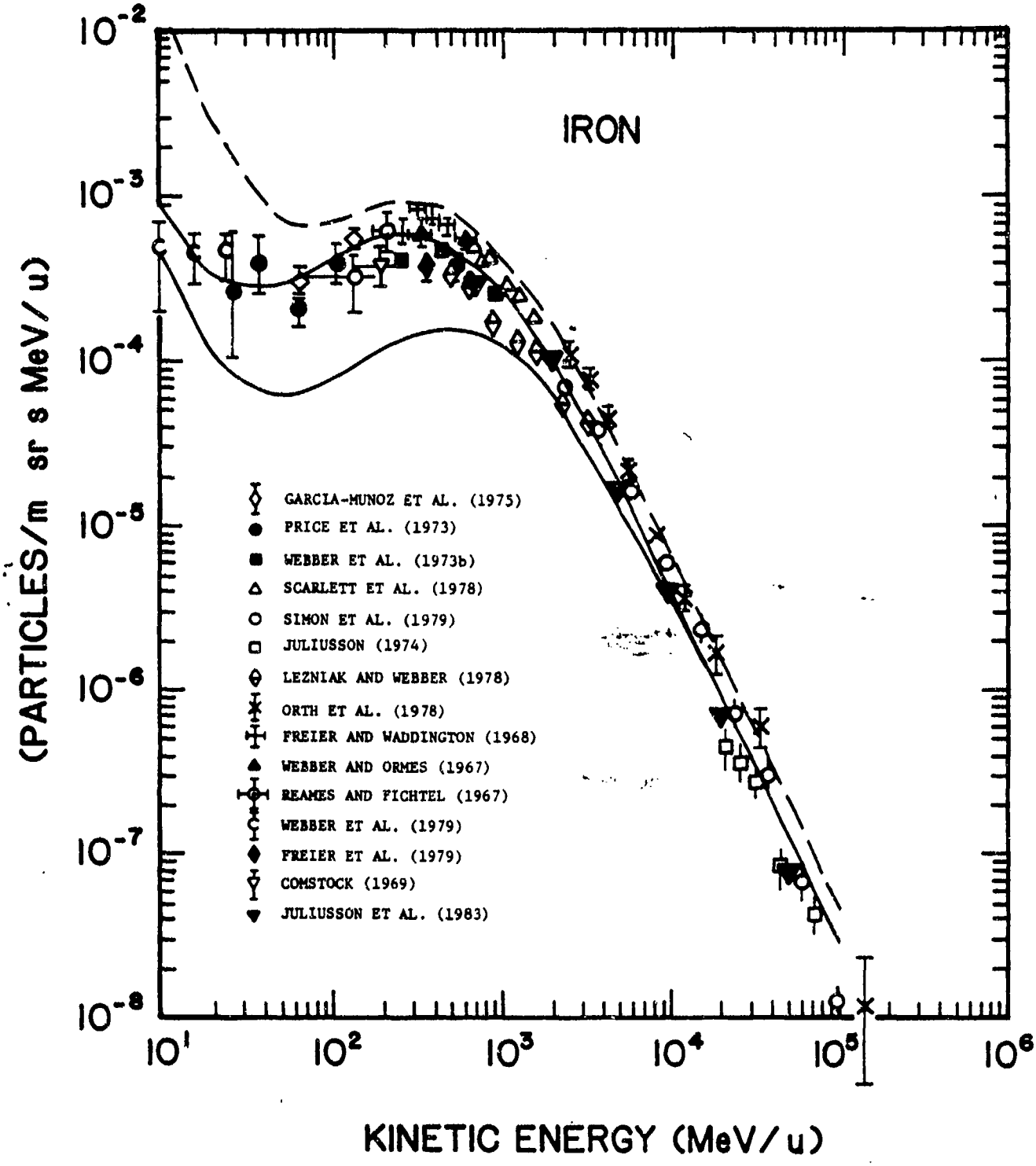

Figure 2: The cosmic ray iron spectrum: The solid curves are for solar maximum (lower) and solar minimum (upper). The dashed curve is the 90% worst-case iron spectrum, which is implied by comparison with the cosmic ray helium spectrum.

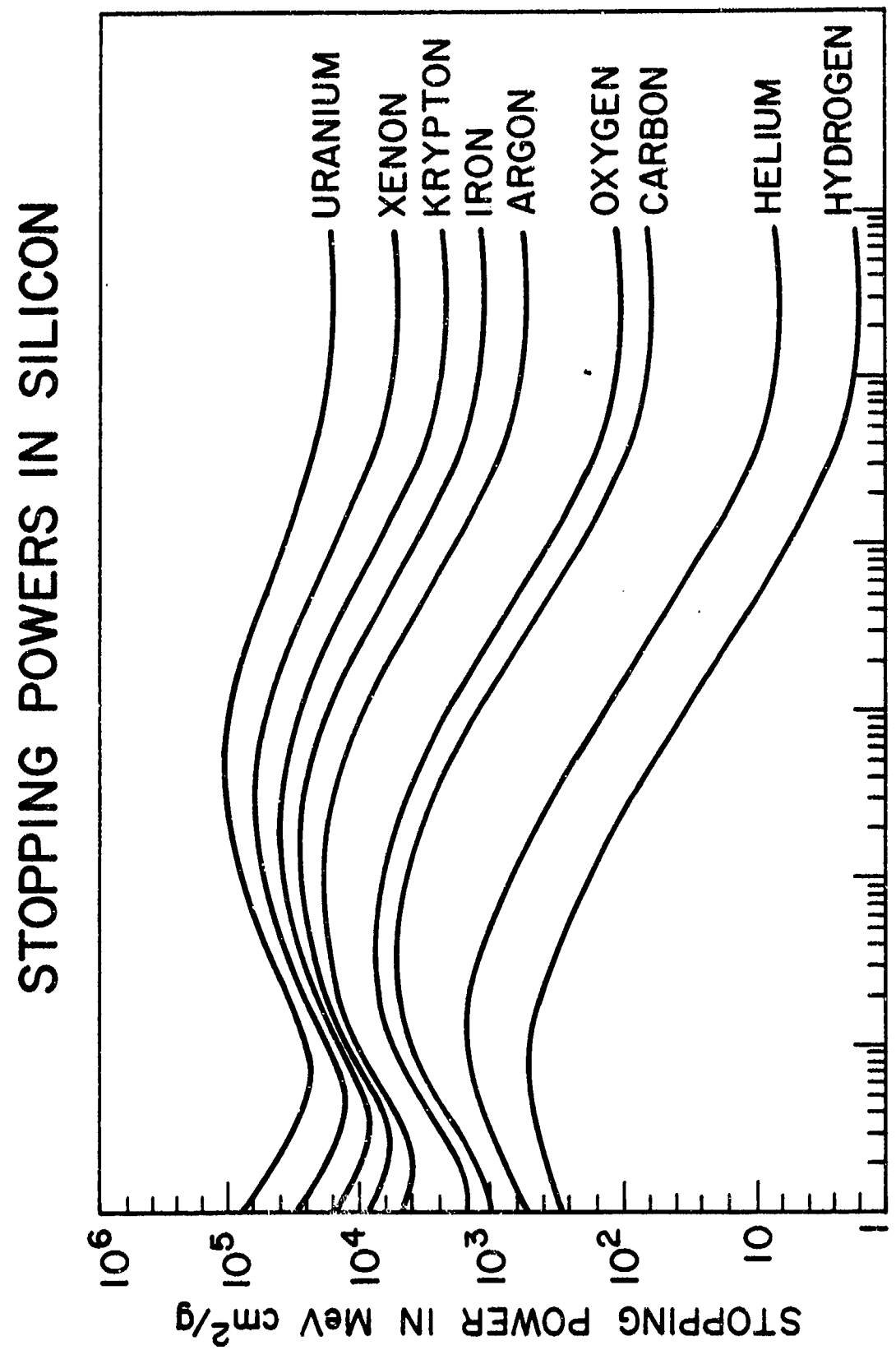

Figure 3: The stopping power (or LET) versus energy per atomic mass unit for a variety of ions.

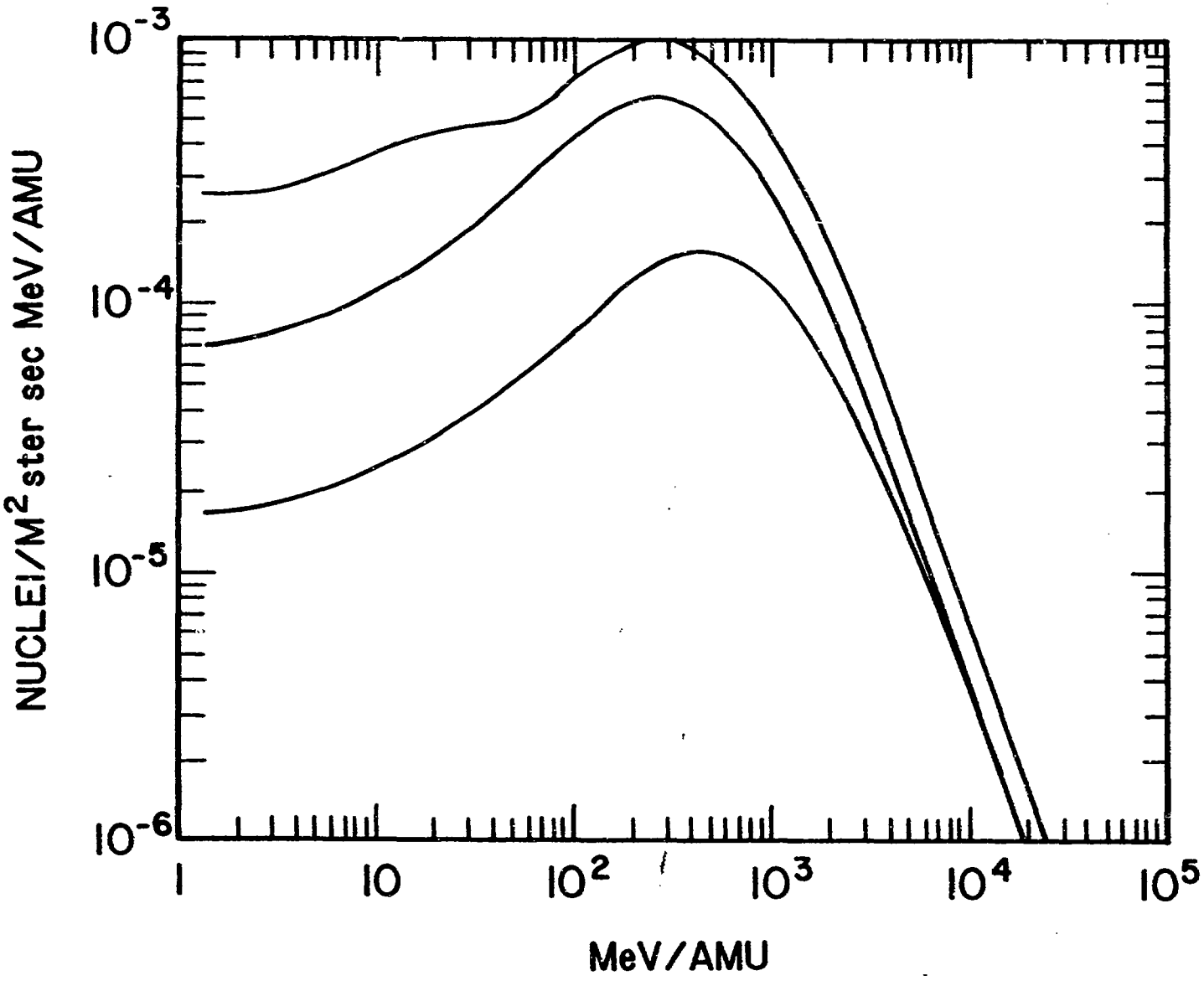

Figure 4: Cosmic ray differential iron spectra for 3 cases: 90% worst case (upper), solar minimum (middle) and solar maximum (lower). These spectra are at the orbit of the earth, but outside the earth's magnetosphere. They are behind 0.025 inches of aluminum shielding.

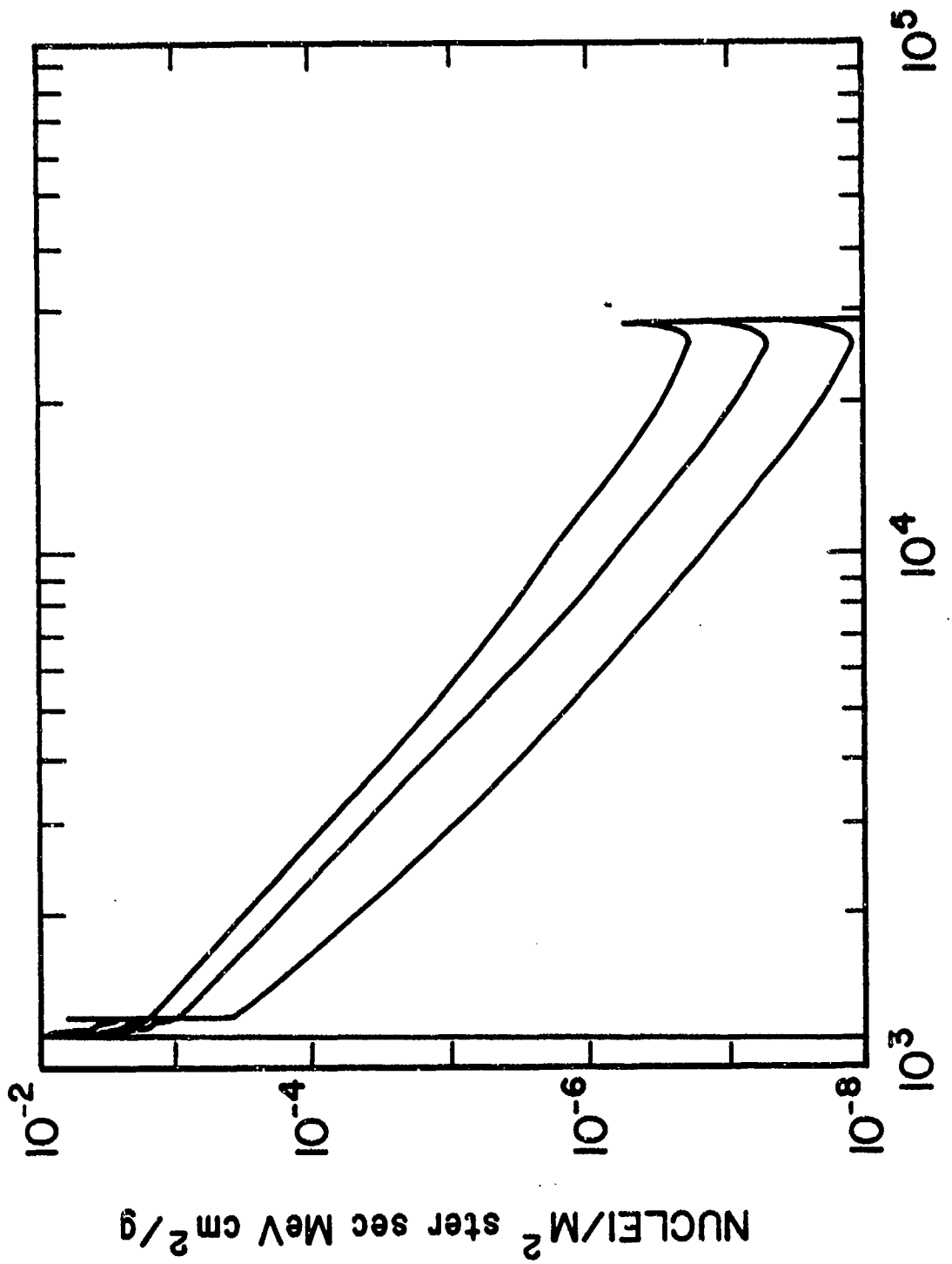

Figure 5: The same three cases as in Figure 4, but now the spectra have been transformed into differential LET spectra.

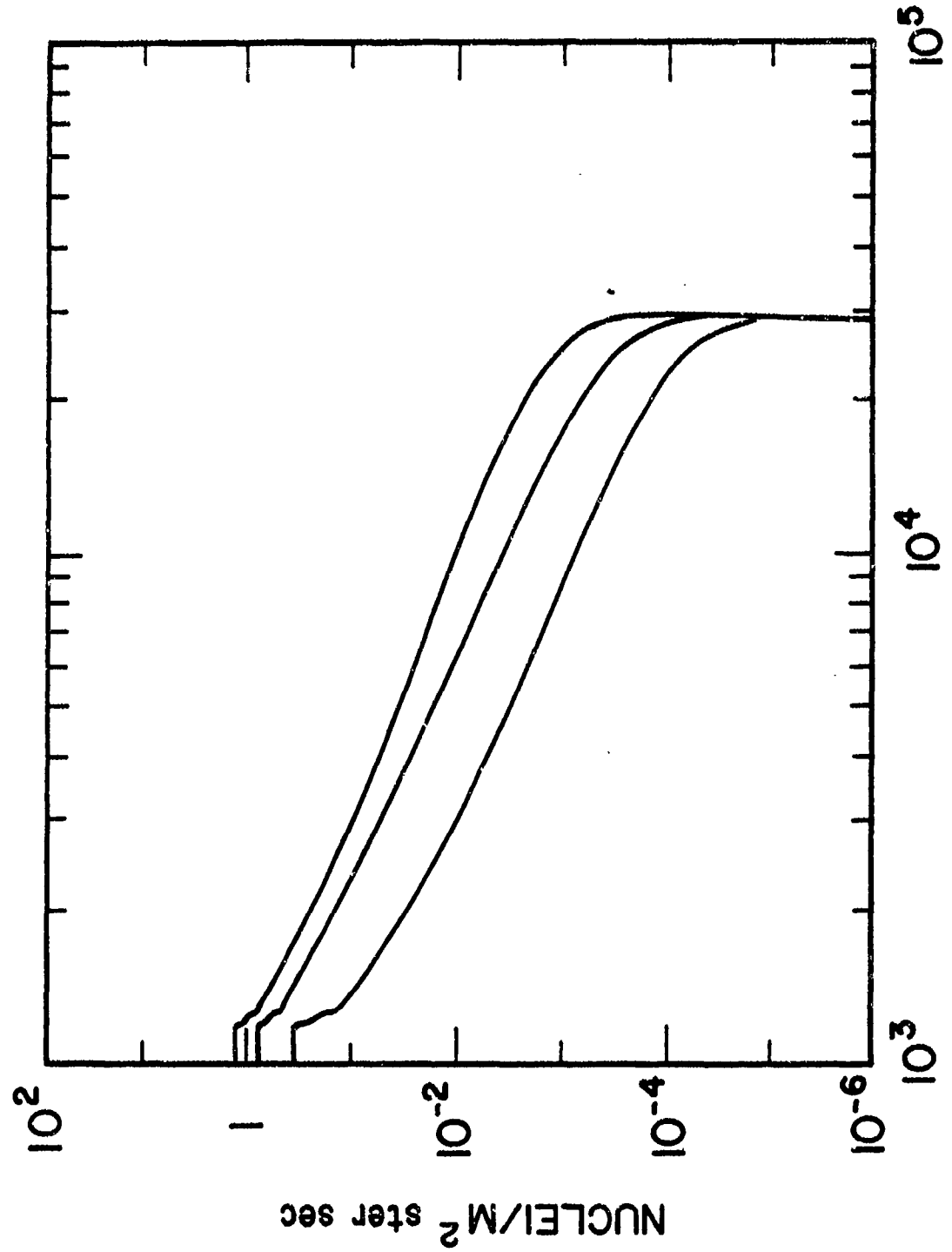

Figure 6: The same three cases as in Figures 4 and 5, but now the spectra of Figure 5 have been integrated to form integral LET spectra.

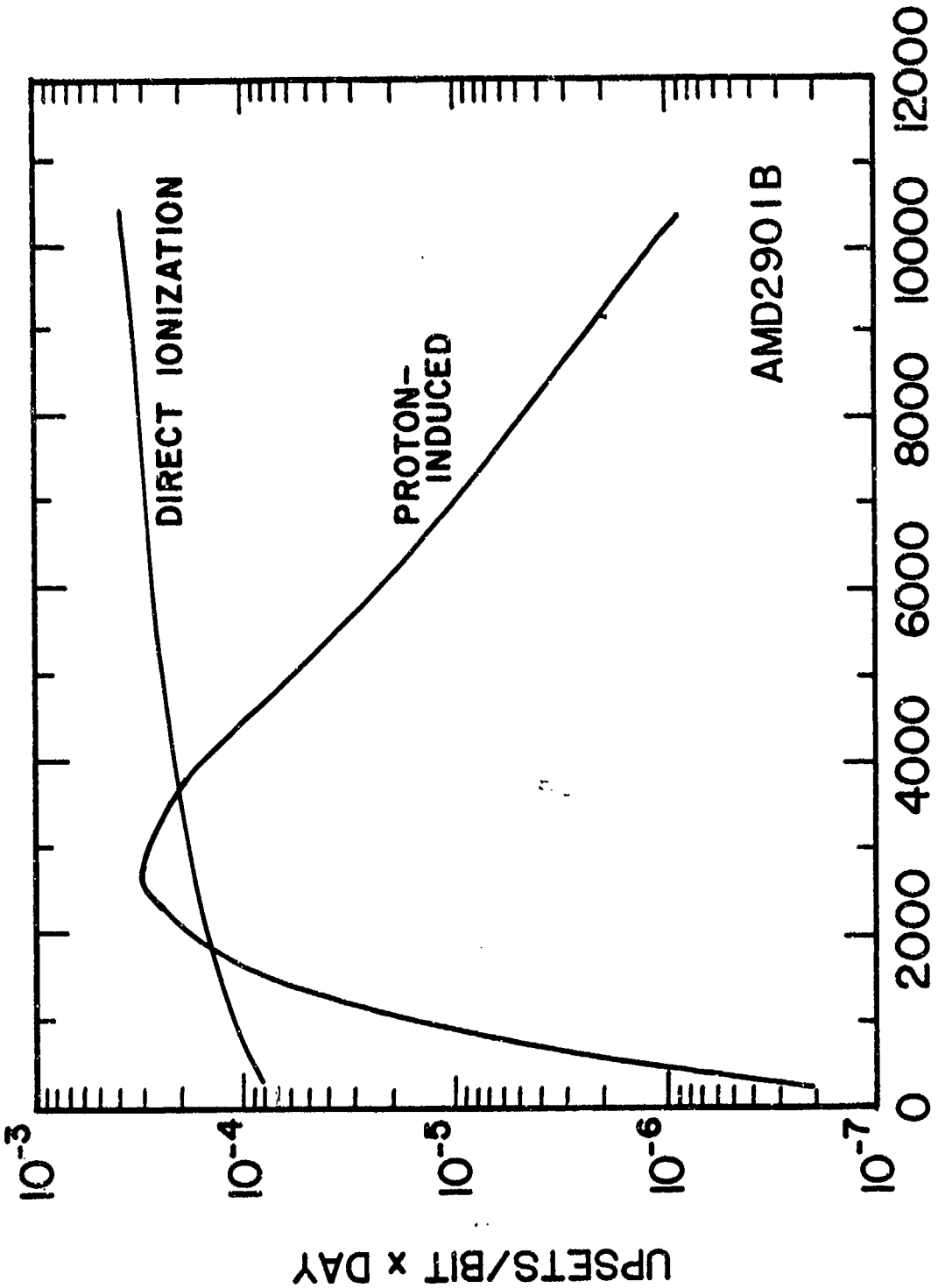

Figure 7: The calculated SEU rates for an AMD2901B. The devices is assumed to be uniformly shielded by 0.1 inches of aluminum and in a 60^{o} inclination circular orbit. The SEU rate is plotted versus orbital altitude, separately, for upsets that result from nuclear reaction caused by protons and upsets that result from the direct ionization of heavy ions.

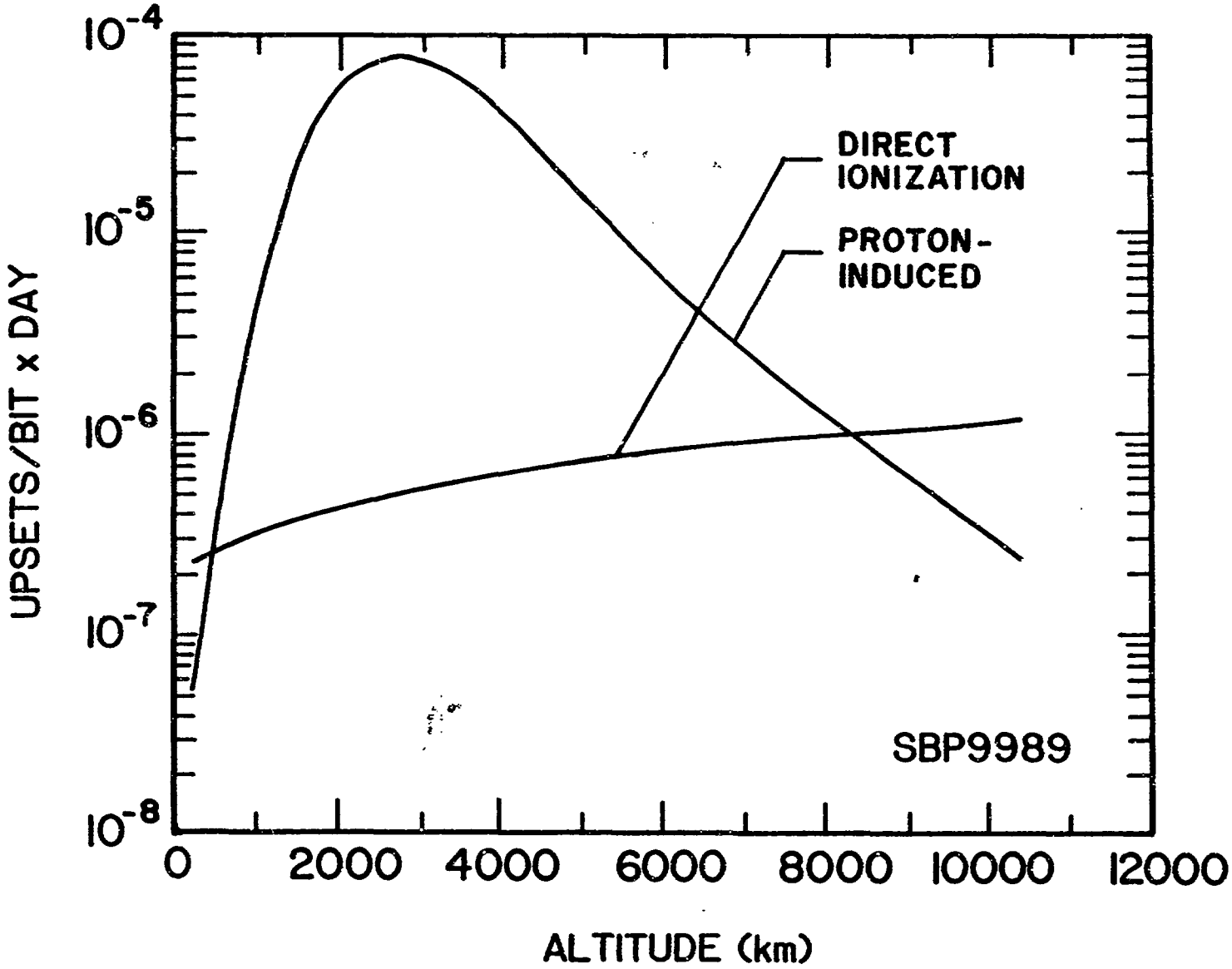

Figure 8: The calculated SEU rates for the SBP9989. The conditions are the same as those in Figure 7 and the labels on the curves have the same meanings.

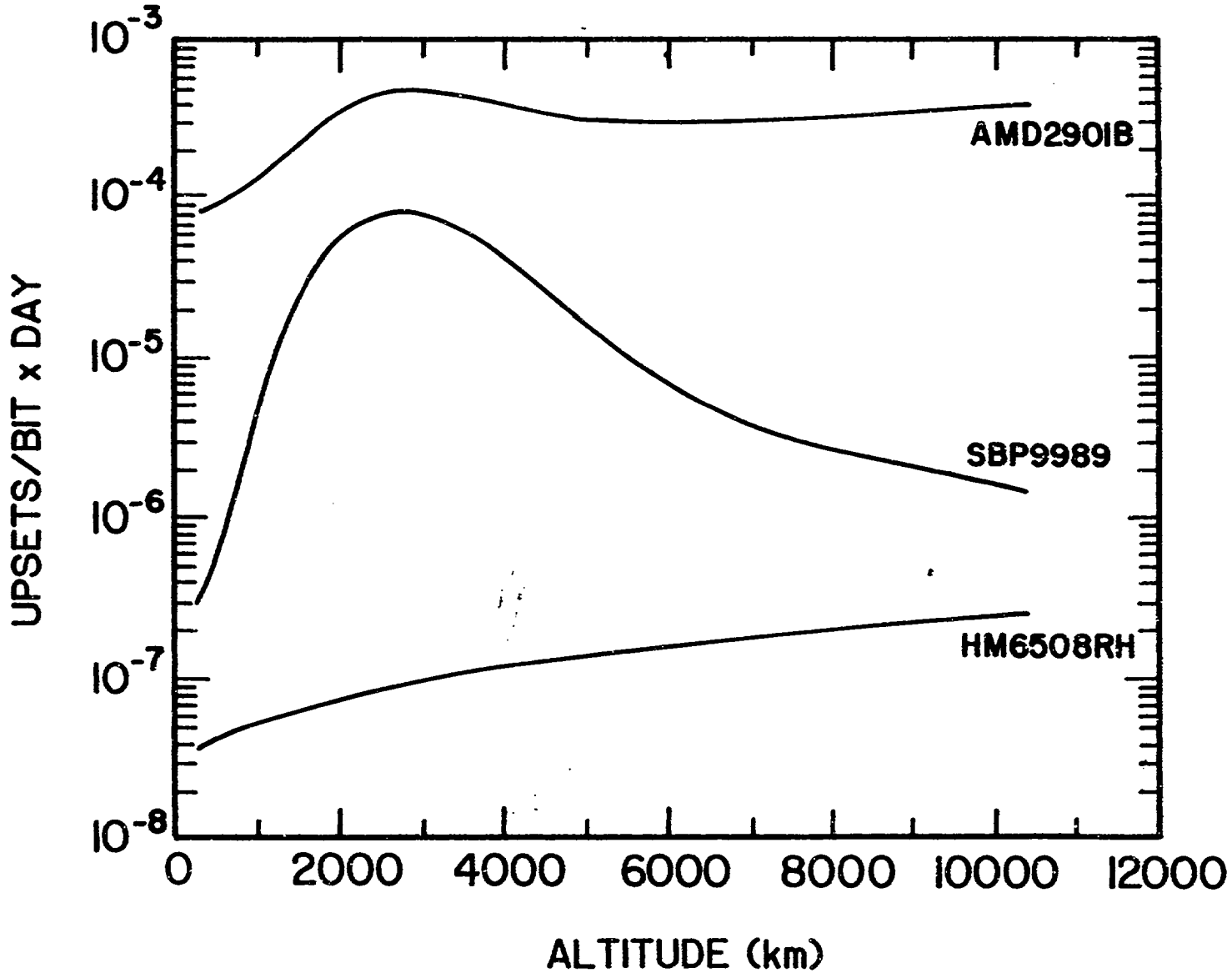

Figure 9: The total SEU rates (proton-induced + direct) for the SBP9989 and the AMD2901B are plotted versus orbital altitude. The conditions are the same as those for Figure 7. This figure also shows the total SEU rate versus altitude for the HM6508RH under the same conditions as the other two devices.

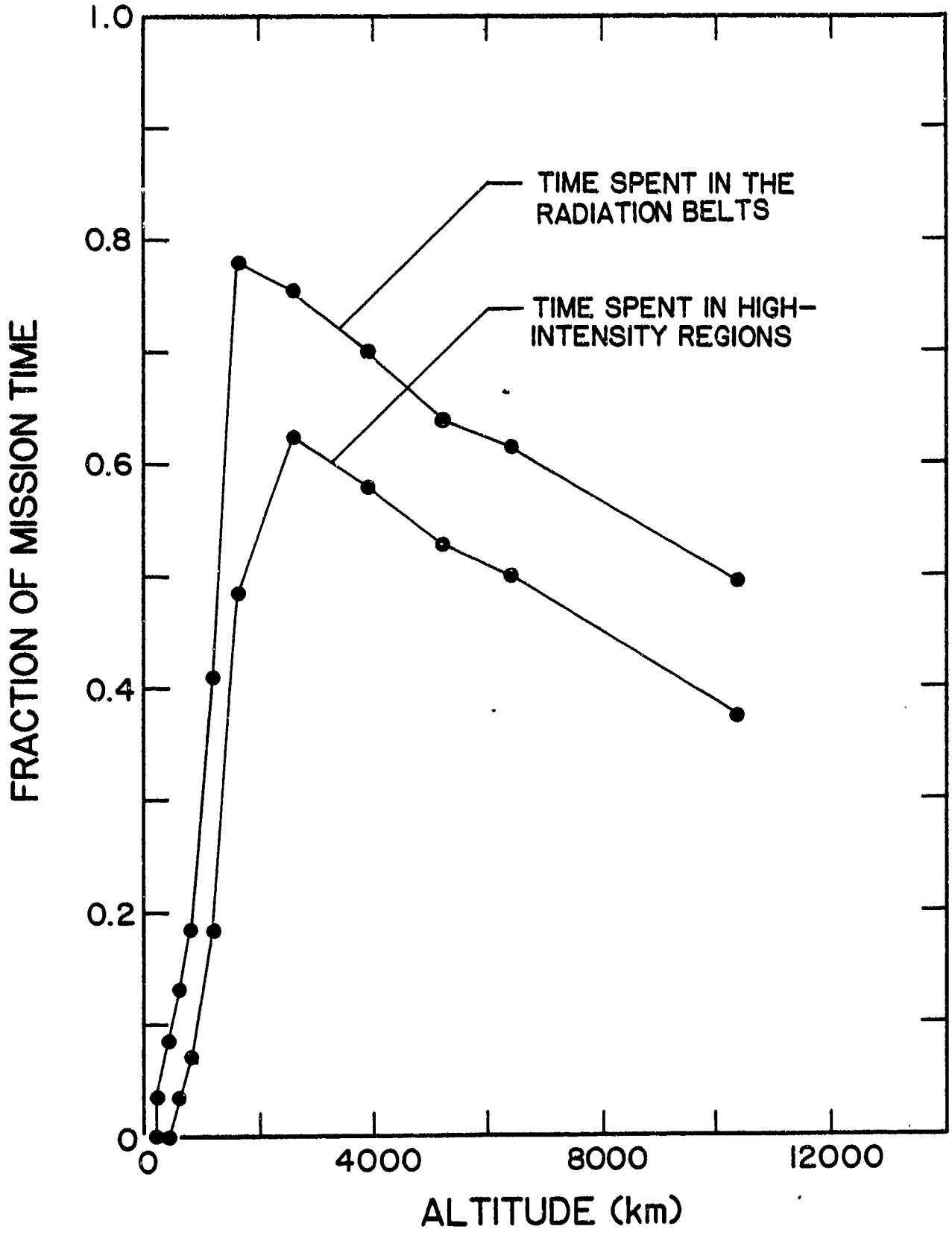

Figure 10: The fraction of mission time that a spacecraft spends in the earth's radiation belts versus orbital altitude. The calculations are for circular orbits at 60° inclination.

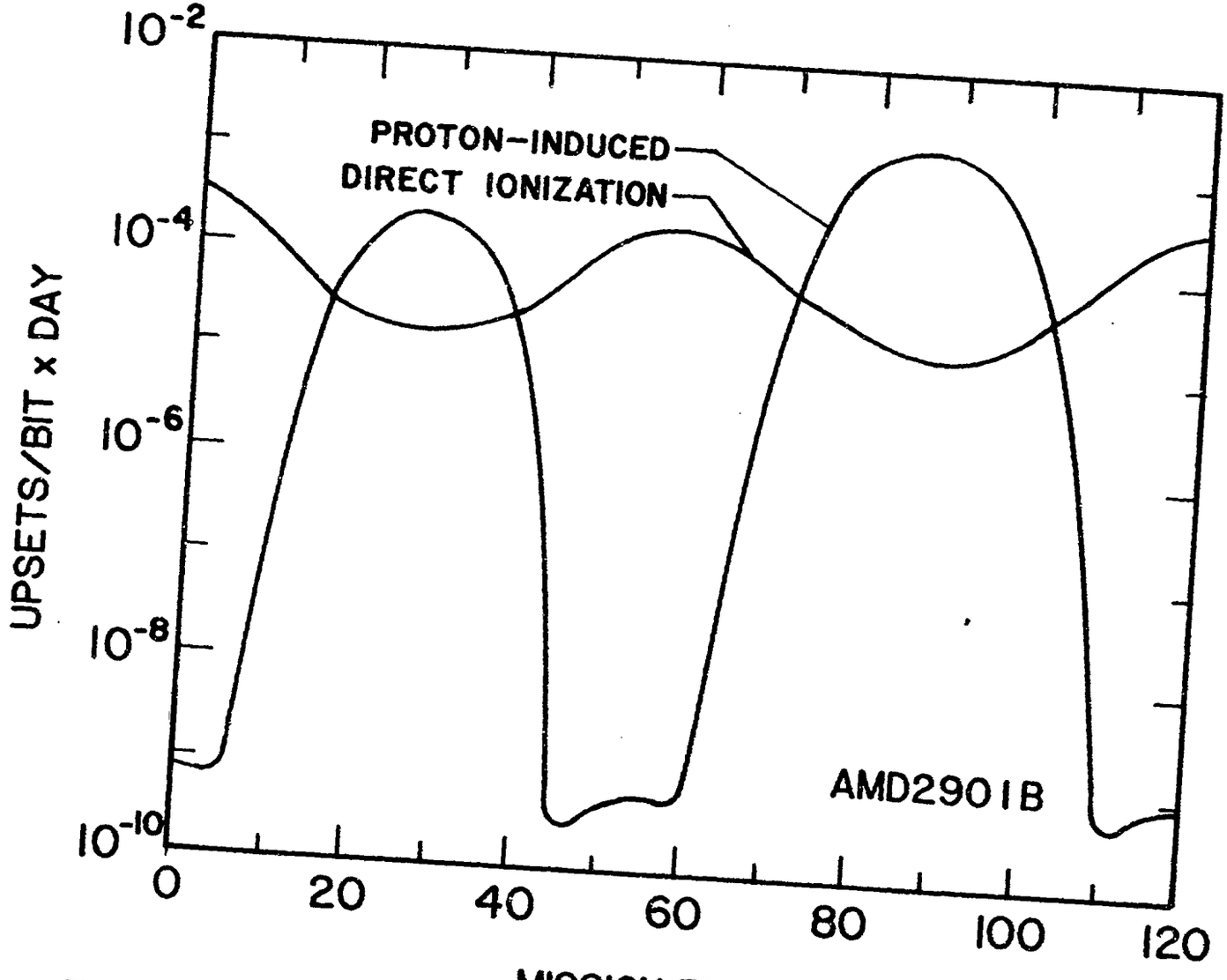

Figure 11: SEU rates versus mission time for the AMD2901B. The component is assumed to be in a circular orbit at 60° inclination and 1667 km altitude. It is uniformly shielded by 0.1 inches of aluminum. The SEU rates for SEU's that result from proton-induced nuclear reactions and from the direct ionization of heavy ions are presented separately.

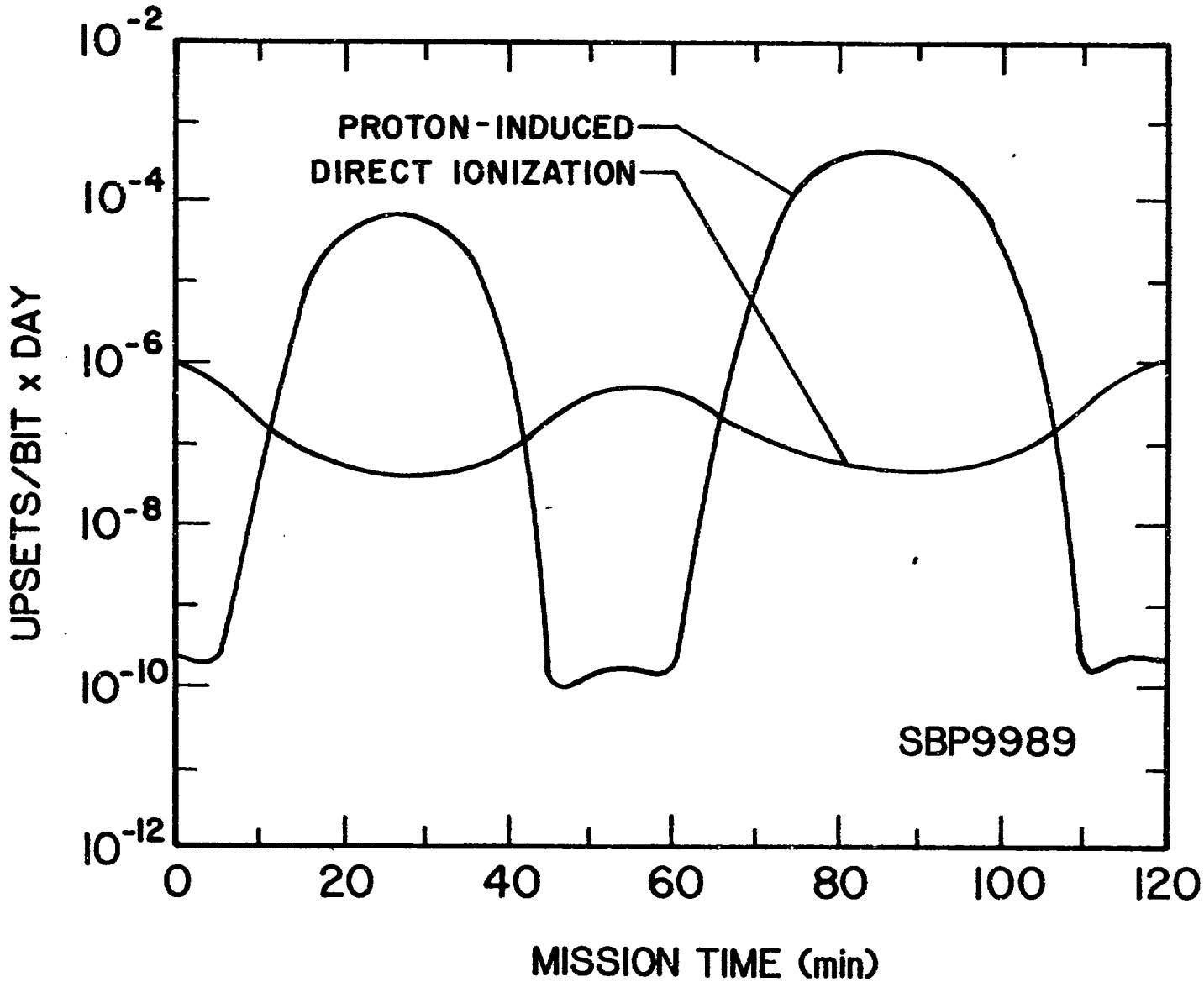

Figure 12: SEU rates versus mission time for the SBP 9989. The orbit and shielding are identical to those for Figure 11. Also the partial upset rates for proton-induced nuclear reactions and the direct ionization of heavy ions are presented separately.

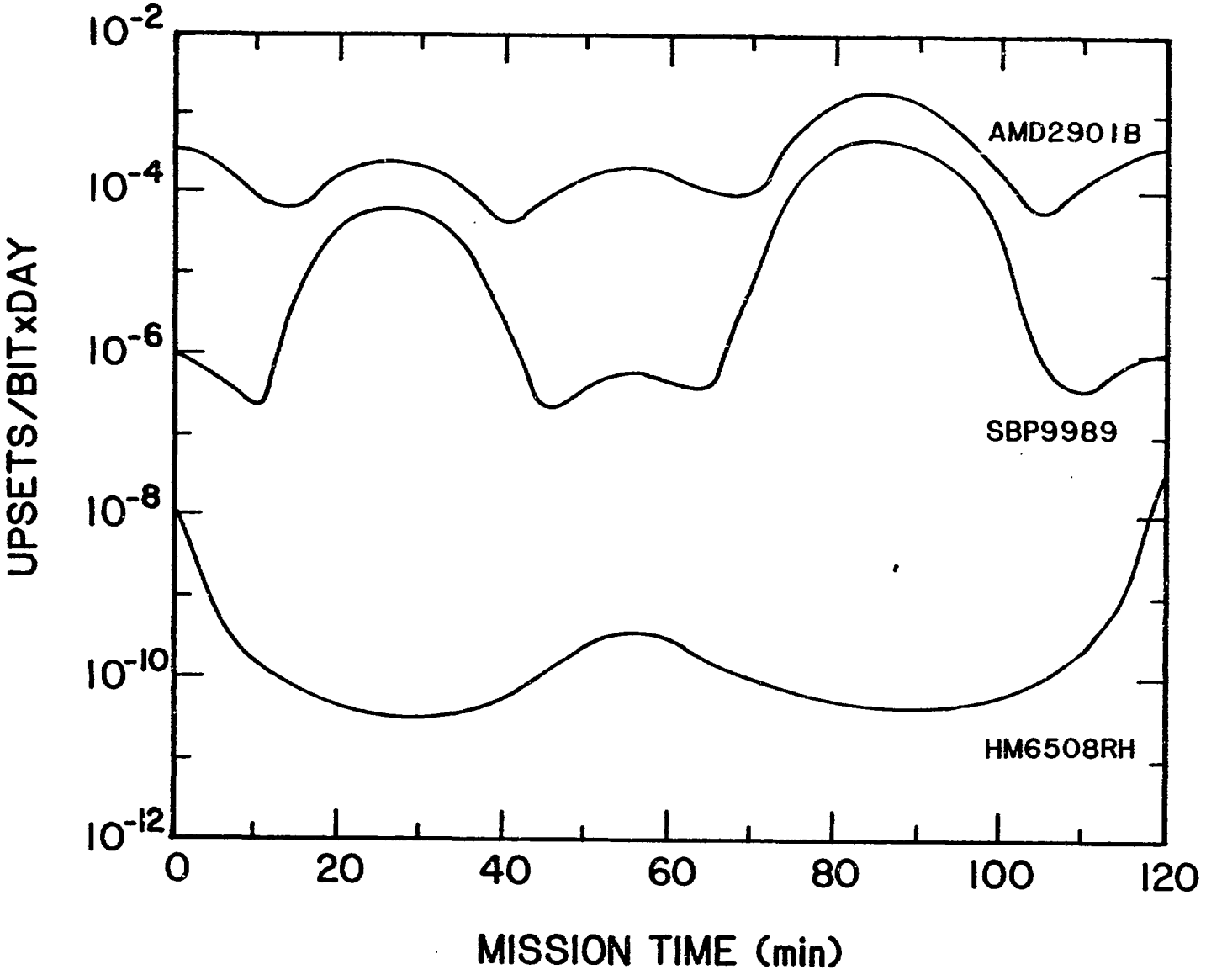

Figure 13: The total SEU rates versus mission time for the AMD2901B, the SBP 9989 and the HM6508RH. The orbit and shielding are the same as those for Figure 11 for all three devices.

APPENDIX 1: THE ANALYTIC MODEL FOR THE CHARGED PARTICLE ENVIRONMENT

Galactic cosmic rays consist of electrons and the nuclei of all the elements in the periodic table; the first 28 elements are the most important for cosmic ray effects on microelectronics. These particles are from outside the solar system and their flux at low energies is anti-correlated with solar activity (i.e. more cosmic rays at solar minimum). The differential energy spectra in particles per square meter - steradian - second - million electron volts per atomic mass unit (i.e. particles/(m^2 .ster.sec.(MeV/u))) are given in the following paragraphs.

The spectra for protons (hydrogen nuclei), α-particle (helium nuclei), and iron nuclei are given below for energies above 10 MeV/u:

$$F(E,t) = A(E) \sin[W(t-t_0)] + B(E), \quad (1)$$

where

$W = 0.576$ radian/year,

$t_0 = 1950.6$ A.D. date,

t = current date in years,

E = particle energy in MeV/nucleon,

$$B(E) = 0.5\,[f_{min}(E) + f_{max}(E)], \quad (2)$$

$$A(E) = 0.5\,[f_{min}(E) - f_{max}(E)]. \quad (3)$$

f_{min} and f_{max} differ only by the choice of constants in the equation

$$f(E) = 10^m (E/E_0)^a, \quad (4)$$

where

$$a = a_0\,(1 - \exp[-X_1\,(\log_{10} E)^b]) \quad (5)$$

and

$$m = C_1\,\exp[-X_2\,(\log_{10} E)^2] - C_2. \quad (6)$$

The values of the constants a_0, E_0, b, X_1, X_2, C_1, and C_2 are given in Table 1 for each of the elements hydrogen (H), helium (He), and iron (Fe) for the conditions of solar maximum and solar minimum.

TABLE 1. Constants Used in Eqs. 5 and 6 to Compute the Differential Energy Spectra of H, He, and Fe at Solar Maximum and Solar Minimum

Element	a_0	E_0	b	X_1	X_2	C_1	C_2
H-min	-2.20	1.1775×10^5	2.685	0.117	0.80	6.52	4.00
H-max	-2.20	1.1775×10^5	2.685	0.079	0.80	6.52	4.00
He-min	-2.35	8.2700×10^4	2.070	0.241	0.83	4.75	5.10
He-max	-2.35	8.2700×10^4	2.070	0.180	0.83	4.75	5.10
Fe-min	-2.14	1.1750×10^5	2.640	0.140	0.65	6.63	7.69
Fe-max	-2.14	1.1750×10^5	2.640	0.102	0.65	6.63	7.69

The differential energy spectra for carbon (C), oxygen (O), fluorine (F), neon (Ne), sodium (Na), aluminum (Al), and phosphorus (P) are obtained by multiplying the helium spectrum (from Eq. (1)) by the scaling factors listed in Table 2.

TABLE 2. The Ratios of the Abundances of Various Nuclei to Helium

Element	Ratio	Element	Ratio
C	3.04×10^{-2}	Na	1.02×10^{-3}
O	2.84×10^{-2}	Al	1.07×10^{-3}
F	6.06×10^{-4}	P	2.34×10^{-4}
Ne	4.63×10^{-3}		

The differential energy spectra for calcium (Ca), cobalt (Co), and nickel (Ni) are obtained by mutliplying the iron spectrum (from Eq. (1)) by the scaling factors listed in Table 3.

TABLE 3. The Ratios of the Abundances of Various Nuclei to Iron

Element	Ratio
Ca	2.1×10^{-1}
Co	3.4×10^{-3}
Ni	5.0×10^{-2}

The spectra of the elements lithium (Li), beryllium (Be), and boron (B) are obtained from the helium spectrum F_{He}, modified by the equation below.

$$F^* = \begin{cases} 0.021\ F_{He}, & E < 3000\ \text{MeV/u} \\ 0.729\ E^{-0.443}\ F_{He}. & E > 3000\ \text{MeV/u} \end{cases} \qquad (7)$$

F^* is the combined spectrum of (Li + Be + B). This value is multiplied by the ratios in Table 4 to obtain the individual element spectra.

TABLE 4. The Relative Fractions of Li, Be, and B in the Combined Total Abundance of Li + Be + B

Element	Ratio
Li	0.330
Be	0.176
B	0.480

The spectrum of the element nitrogen (N) is obtained by modifying the helium spectrum F_{He} as shown:

$$F_N = (8.7 \times 10^{-3}\ \exp[-0.4(\log_{10} E - 3.15^2] + 7.6 \times 10^{-3}\ \exp[-0.9(\log_{10} E - 0.8)^2])\ F_{He}. \qquad (8)$$

The spectra of the elements magnesium (Mg), silicon (Si), and sulfur (S) are obtained by modifying the helium spectrum F_{He} as shown:

$$F^* = \begin{cases} F_{He}, & E > 2200 \\ (1 + 1.56\times10^{-5}\ (E-2200))F_{He}. & E > 2200 \end{cases} \quad (9)$$

The individual spectra for these elements are obtained by multiplying F^* by the ratios of Table 5.

TABLE 5. The Ratios of Mg, Si, and S to an Adjusted Helium Spectrum

Element	Ratio
Mg	6.02×10^{-3}
Si	4.63×10^{-3}
S	9.30×10^{-4}

The spectra for the elements chlorine (Cl), argon (Ar), potassium (K), scandium (Sc), titanium (Ti), vanadium (V), chromium (Cr), and manganese (Mn) are all obtained by modifying the iron spectrum F_{Fe} as shown below:

$$F^* = Q(E)F_{Fe}, \text{ where} \quad (10)$$

$$Q(E) = 16\ [1 - \exp(-0.075E^{0.4})]\ E^{-0.33}. \quad (11)$$

The individual spectra for these elements are obtained by multiplying F^* by the ratios of Table 6.

TABLE 6. The Fractional Abundance of Each Element in the Sub-Iron Group

Element	Ratio	Element	Ratio
Cl	0.070	Ti	0.147
Ar	0.130	V	0.070
K	0.090	Cr	0.140
Sc	0.042	Mn	0.100

The differential energy spectra for elements from copper to uranium are obtained by multiplying the iron spectrum (from Eq. (1)) by the scaling factors listed in Table 7.

TABLE 7. The Ratio of the Abundances of Various Nuclei to Iron

Element	Ratio	Element	Ratio
Cu	6.8×10^{-4}	Pm	1.9×10^{-7}
Zn	8.8×10^{-5}	Sm	8.7×10^{-7}
Ga	6.5×10^{-4}	Eu	1.5×10^{-7}
Ge	1.4×10^{-6}	Gd	7.0×10^{-7}
As	9.9×10^{-5}	Tb	1.7×10^{-7}
Se	5.8×10^{-6}	Dy	7.0×10^{-7}
Br	8.3×10^{-6}	Ho	2.6×10^{-7}

Kr	2.3×10^{-5}	Er	4.3×10^{-7}
Rb	1.1×10^{-5}	Tm	8.9×10^{-8}
Sr	3.6×10^{-5}	Yb	4.4×10^{-7}
Y	6.8×10^{-6}	Lu	6.4×10^{-8}
Zr	1.7×10^{-5}	Hf	4.0×10^{-7}
Nb	2.6×10^{-6}	Ta	3.6×10^{-8}
Mo	7.1×10^{-6}	W	3.8×10^{-7}
Tc	1.6×10^{-6}	Re	1.3×10^{-7}
Ru	5.3×10^{-6}	Os	5.6×10^{-7}
Rh	1.5×10^{-6}	Ir	3.7×10^{-7}
Pd	4.5×10^{-6}	Pt	7.2×10^{-7}
Ag	1.3×10^{-6}	Au	1.3×10^{-7}
Cd	3.6×10^{-6}	Hg	2.3×10^{-7}
In	1.4×10^{-6}	Tl	1.8×10^{-7}
Sn	7.5×10^{-6}	Pb	1.7×10^{-6}
Sb	9.9×10^{-7}	Bi	9.0×10^{-8}
Te	5.7×10^{-6}	Po	0
I	1.5×10^{-6}	At	0
Xe	3.5×10^{-7}	Rn	0
Cs	5.8×10^{-6}	Fr	0
Ba	6.0×10^{-7}	Ra	0
La	5.3×10^{-7}	Ac	0
Ce	1.6×10^{-6}	Th	9.0×10^{-8}
Pr	3.0×10^{-7}	Pa	0
Nd	1.1×10^{-6}	U	5.4×10^{-8}

The recipe given above is correct for quiet periods in the interplanetary medium when only the galactic cosmic rays are present. These conditions are often disturbed, especially at low energies, by small solar flares, co-rotating events, etc. To allow for typical disturbed conditions, we recommend that a worst-case spectrum be used. With 90 per cent confidence, the instantaneous particle flux should never be more intense than described by this case at any energy.

To construct the worst-case spectrum for protons, compute the "H-min" spectrum (using Eq. 4) and then compute $F_{H\text{-worst}}$ as shown below:

$$F_{H\text{-worst}} = [1897e^{-E/9.66} + 1.64]F_{H\text{-min}}. \quad (12)$$

This applies for E < 100 MeV/u.

In like manner, the solar minimum case helium and iron spectra (also from Eq. (4)) are multiplied by:

$$28.4e^{-E/13.84} + 1.64 \quad (13)$$

for E < 100 MeV/u.

The worst-case spectra of H, He, and Fe for any element for E > 100 MeV/u are approximated by a multiple of the solar minimum spectra:

$$F_{worst} = 1.64\, F_{min}. \quad (14)$$

The resulting spectra are used as described above to obtain the other elemental spectra, i.e. in the same way as F_{He} and F_{Fe} were used.

In addition to galactic cosmic rays, some particles are believed to be accelerated in the interplanetary medium. The most important of these are called the anomalous component. Its greatest contribution is to the helium spectrum. We recommend that, for the period 1982-1990, the cosmic ray helium spectrum be modified as follows:

1. Determine the maximum values of the helium spectra from Eq. (4) using the He-max and He-min constants from Table 1.

2. Modify Eq. (4) so that each maximum value applies to all energies below the energy at which the maximum occurs; i.e., for solar minimum:

$$f^*_{\text{He-min}} = \begin{cases} 0.33, & E < 200 \text{ MeV/u} \\ f_{\text{He-min}} \text{ (from Eq. (4))}. & E > 200 \text{ MeV/u} \end{cases} \quad (15)$$

3. Make the same kind of modification, $f^*_{\text{He-max}}$, for solar maximum:

$$f^*_{\text{He-max}} = \begin{cases} 0.079, & E < 300 \text{ MeV/u} \\ f_{\text{He-max}} \text{ (from Eq. (4))}. & E > 300 \text{ MeV/u} \end{cases} \quad (16)$$

4. Combine the resulting spectra as before using Eqs. (1-3).

NOTE: This applies only to He; use the regular He spectra of Eqs. (1-6) to get the spectra of the other elements.

The anomalous component contributes to the spectra of oxygen and nitrogen, as well as helium, at low energies. For the years 1982-1990, the following contributions may be added to the galactic cosmic ray oxygen and nitrogen spectra.

For oxygen, use:

$$f(E) = 6\times10^{-2} \exp[-(\ln(E)-1.79)^2/0.70] \text{ particles/(m}^2\text{ .ster.sec.MeV/u)}. \quad (17)$$

This spectrum crosses the galactic spectrum near 30 MeV/u. The two should be matched at that point with Eq. (17) replacing the galactic spectrum at lower energies. Similarly, for nitrogen:

$$f(E) = 1.54\times10^{-2} \exp[-(\ln(E)-1.79)^2/0.70] \text{ in particles/(m}^2\text{ .ster.sec.MeV/u)}. \quad (18)$$

Again, this crosses the galactic cosmic ray spectrum near 30 MeV/u and should replace it below this energy.

The spectra of the remaining elements are unaffected or affected at too low an energy to matter.

There is a possibility that the anomalous component is singly ionized. If this is so, it will have an extraordinary ability to penetrate the earth's magnetosphere. In this case, the differential energy spectra shown below are assumed for the helium, carbon, nitrogen, oxygen, neon, magnesium, silicon, argon, and iron spectra of the anomalous component. There probably are anomalous components in the spectra of the nuclei heavier than iron, but there are no data on them at this time.

For singly-ionized helium,

$$F = \begin{cases} .4, & E < 195 \\ 1.54 \times 10^{4}\ E^{-2}\ . & E > 195 \end{cases} \tag{19}$$

For singly-ionized carbon,

$$F = \begin{cases} 4.00 \times 10^{3}\ \exp[-(\ln E - 1.79)^{2}\ /0.7], & E < 10 \\ 0.27\ E^{-2}\ . & E > 10 \end{cases} \tag{20}$$

For singly-ionized nitrogen,

$$F = \begin{cases} 1.54 \times 10^{-2}\ \exp[-(\ln E - 1.79)^{2}\ /0.7], & E < 20 \\ 0.773\ E^{-2}\ . & E > 20 \end{cases} \tag{21}$$

For singly-ionized oxygen,

$$F = \begin{cases} 6.00 \times 10^{-2}\ \exp[-(\ln E - 1.79)^{2}\ /0.7], & E < 30 \\ 1.32\ E^{-2}\ . & E > 30 \end{cases} \tag{22}$$

For singly-ionized neon,

$$F = \begin{cases} 8.00 \times 10^{-3}\ \exp[-(\ln E - 1.79)^{2}\ /0.7], & E < 20 \\ 0.40\ E^{-2}\ . & E > 20 \end{cases} \tag{23}$$

For singly-ionized magnesium,

$$F = \begin{cases} 8.00 \times 10^{-4}\ \exp[-(\ln E - 2.30)^{2}\ /0.7], & E < 20 \\ 0.16\ E^{-2}\ . & E > 20 \end{cases} \tag{24}$$

For singly-ionized silicon,

$$F = \begin{cases} 1.00 \times 10^{-3}\ \exp[-(\ln E - 2.20)^{2}\ /0.4], & E < 10 \\ 0.10\ E^{-2}\ . & E > 10 \end{cases} \tag{25}$$

For singly-ionized argon,

$$5.40 \times 10^{-4}\ \exp[-(\ln E - 1.79)^{2}\ /0.7], \qquad E < 20$$

$$F = \begin{cases} 6.00 \times 10^{-4} \exp[-(\ln E - 2.48)^2 / 2.0], & E < 30 \\ 0.35\ E^{-2}. & E > 30 \end{cases} \quad (27)$$

Since these anomalous component particles are assumed to be singly-ionized, they will have a higher magnetic rigidity than galactic cosmic rays of the same energy. The magnetic rigidity of galactic cosmic rays is

$$R = (A/Z)\ (E^2 + 1862.324\ E)^{1/2} / 1000, \quad (28)$$

in GeV/ec. The rigidity of singly ionized nuclei is

$$R = A\ (E^2 + 1862.324\ E)^{1/2} / 1000. \quad (29)$$

To add the singly-ionized anomalous component, it is necessary to modulate both the galactic cosmic ray spectra and the anomalous component spectra given above using the geomagnetic cutoff transmission function. The method for calculating this function is discussed in Adams et. al. (1983) and in Appendix 2 of this report. The resulting modulated spectra are then added together.

Solar flare particle events are sporadic occurrences lasting 1-5 days. When these events occur they can be the dominant cause of SEU's. For statistical treatment, they are broken down into two classes: ordinary (OR) and anomalously large (AL). The probability of having more than a number n of events in a time t is given by:

$$P(n,t,N,T) = 1 - \sum_{i=0}^{n} (i+N)!(t/T)^i / [i!N!(1+t/T)^{1+i+N}], \quad (30)$$

where T and t are in years, and N is the number of flares that have occurred in T years.

For ordinary events, Eq. (30) becomes:

$$\begin{aligned} P_{OR} &= P(n,t,24,7) \text{ for } 1981\text{-}1983 \\ \text{and} \quad P_{OR} &= P(n,t,6,8) \text{ for } 1984\text{-}1988, \end{aligned} \quad (31)$$

where there is a probability P_{OR} of having more than n ordinary events in t years. Similarly, for anomalously large events:

$$P_{AL} = P(n,t,1,7). \quad (32)$$

If there is an unacceptable risk of an AL event then it will be the worst-case flare for the mission.

The peak proton flux differential energy spectrum for ordinary events is, typically

$$F_{OR} = 2.45\times10^{4}\ (e^{-E/27.5} + 173e^{-E/4})\ \text{protons/m}^2\ \text{.ster.sec.MeV.} \quad (33)$$

and no worse than

$$F_{WOR} = 2.06\times10^{5}\ (e^{-E/24.5} + 63.6e^{-E/4})\ \text{protons/m}^2\ \text{.ster.sec.MeV,} \quad (34)$$

with a confidence of about 90 per cent.

Using the August 1972 flare as a model A1 event, the peak proton flux differential energy spectrum is

$$f_{AL} = \begin{cases} 9.3\times10^{9}\ (dP/dE)\ \exp(-P/0.10), & E < 150\ \text{MeV} \\ 1.76\times10^{5}\ (dP/dE)\ P^{-9}, & E > 150\ \text{MeV} \end{cases} \quad (35)$$

in protons/m^2 .ster.sec.MeV, where

$$P = [(E/1000)^2 + 1.86\times10^{-3}\ E]^{1/2}. \quad (36)$$

To model the worst flare that is ever likely to occur, we use the composite of the two worst flares ever recorded: the August, 1972, flare and the February, 1956, flare. The composite worst-case flare proton spectrum is taken to be the peak of the 1972 spectrum, as given by Eq. (35), and the 1956 peak spectrum, given below.

$$f_{1956} = 1.116\times10^{8}\ (E^{-1.248})(0.248 + 2.5\times10^{5}\ \text{x}1.7\text{xEPOW})\ \text{EXPOW}$$
$$+ 4.7\times10^{19}\ (E^{-5.3})(4.3\text{x}(1-\text{EXPOW}) - 6.32\times10^{-15}\ \text{x}4.7\text{xEPOWxEXPOW}), \quad (37)$$

where

$$\text{EPOW} = E^{1.7}$$

and

$$\text{EXPOW} = \exp(-2.5\times10^{-5}\ \text{EPOW}).$$

The composition of flare particles also varies greatly from flare to flare. Table 8 gives the composition relative to hydrogen of the elements through nickel. Both mean and (90 percent confidence level) worst-cases are given. Multiply the abundance ratio from Table 8 by the appropriate flare proton spectrum to get the flare spectrum of any element in the table.

TABLE 8. Mean and Worst-Case Flare Compositions

	Mean Case	Worst Case		Mean Case	Worst Case
H	1	1	P	2.3×10^{-7}	1.1×10^{-6}
He	1.0×10^{-2}	3.3×10^{-2}	S	8.0×10^{-6}	5.0×10^{-5}
Li	0	0	Cl	1.7×10^{-7}	8.0×10^{-7}
Be	0	0	Ar	3.3×10^{-6}	1.8×10^{-5}
B	0	0	K	1.3×10^{-7}	6.0×10^{-7}
C	1.6×10^{-4}	4.0×10^{-4}	Ca	3.2×10^{-6}	2.0×10^{-5}
N	3.8×10^{-5}	1.1×10^{-4}	Sc	0	0
O	3.2×10^{-4}	1.0×10^{-3}	Ti	1.0×10^{-7}	5.0×10^{-7}

F	0	0	V	0	0
Ne	5.1×10^{-5}	1.9×10^{-4}	Cr	5.7×10^{-7}	4.0×10^{-6}
Na	3.2×10^{-6}	1.3×10^{-5}	Mn	4.2×10^{-7}	2.3×10^{-6}
Mg	6.4×10^{-5}	2.5×10^{-4}	Fe	4.1×10^{-5}	4.0×10^{-4}
Al	3.5×10^{-6}	1.4×10^{-5}	Co	1.0×10^{-7}	5.5×10^{-7}
Si	5.8×10^{-5}	1.9×10^{-4}	Ni	2.2×10^{-6}	2.0×10^{-5}

The mean case compositions for the elements from copper to uranium are taken from Cameron (1980). The ratios of these abundances to hydrogen are given in Table 9.

TABLE 9. Mean Flare Compositions

Cu	2.0×10^{-8}	Pm	0
Zn	6.0×10^{-8}	Sm	1.0×10^{-11}
Ga	2.0×10^{-9}	Eu	4.0×10^{-12}
Ge	5.0×10^{-9}	Gd	2.0×10^{-11}
As	3.0×10^{-10}	Tb	3.0×10^{-12}
Se	3.0×10^{-9}	Dy	2.0×10^{-11}
Br	4.0×10^{-10}	Ho	4.0×10^{-12}
Kr	2.0×10^{-9}	Er	1.0×10^{-11}
Rb	3.0×10^{-10}	Tm	2.0×10^{-12}
Sr	1.0×10^{-9}	Yb	9.0×10^{-12}
Y	2.0×10^{-10}	Lu	2.0×10^{-12}
Zr	5.0×10^{-10}	Hf	8.0×10^{-12}
Nb	4.0×10^{-11}	Ta	9.0×10^{-13}
Mo	2.0×10^{-10}	W	1.0×10^{-11}
Tc	0	Re	2.0×10^{-12}
Ru	9.0×10^{-11}	Os	3.0×10^{-11}
Rh	2.0×10^{-11}	Ir	3.0×10^{-11}
Pd	6.0×10^{-11}	Pt	6.0×10^{-11}
Ag	2.0×10^{-11}	Au	1.0×10^{-11}
Cd	7.0×10^{-12}	Hg	1.0×10^{-12}
In	9.0×10^{-10}	Tl	9.0×10^{-10}
Sn	2.0×10^{-11}	Pb	1.0×10^{-12}
Sb	1.4×10^{-11}	Bi	6.0×10^{-12}
Te	3.0×10^{-10}	Po	0
I	6.0×10^{-11}	At	0
Xe	2.7×10^{-10}	Rn	0
Cs	2.0×10^{-11}	Fr	0
Ba	2.0×10^{-10}	Ra	0
La	2.0×10^{-11}	Ac	0
Ce	5.0×10^{-11}	Th	2.0×10^{-12}
Pr	8.0×10^{-12}	Pa	0
Nd	4.0×10^{-11}	U	1.2×10^{-12}

The worst-case compositions of the elements from copper to uranium are obtained by multiplying the abundance ratios of Table 9 by:

$$(C_w(O)/C_t(O))0.48\ \exp(Z^{0.78}/6.89), \tag{38}$$

where $C_w(O)$ and $C_t(O)$ are the worst-case and mean abundance coefficients for oxygen in Table 8.

There are several good mathematical models for the trapped proton environment. We recommend "AP-8 Trapped Proton Environment for Solar Maximum and Solar Minimum," Donald M. Sawyer and James I. Vette, Report No. NSSCS/WDC-A-R and S 76-06, Dec., 1976, NASA-Goddard, Greenbelt, Md.

The environment of trapped α particles and heavier nuclei is very poorly known. The reader is referred to Adams and Partridge (1982) for a discussion of the data base on trapped ions heavier than protons.

The modulation of cosmic ray spectra by the earth's magnetic field is discussed in Adams et. al. (1983) in Appendix 2 of this report. Briefly, the geomagnetic cutoff is a value of magnetic rigidity below which cosmic rays will not reach a specified point in the magnetosphere from a specified direction. The magnetic rigidity P in GeV/ec may be computed from a particle's energy by:

$$P = (A/Z)[(E/1000)^2 + 1.86 \times 10^{-3} E]^{1/2} , \quad (39)$$

where A and Z are the atomic mass and charge of the nucleus in question.

The cutoff at any point for particles arriving from the zenith is most simply computed with:

$$P_c = 15.96/L^{2.005} \text{ GeV/ec}, \quad (40)$$

where L is McIlwain's L parameter (i.e. the radial distance, in earth radii, from the center of the earth to the point in the geomagnetic equitorial plane where it is crossed by the magnetic field line that also passes through the point of observation).

Detailed calculations of the cutoff are available from Shea and Smart (1975). Transmission functions for satellite orbits may be computed using the techniques described in Adams et. al. (1983) and Appendix 2.

The transmission functions are useful in modulating the cosmic ray spectra. Some thought must be given to their use on solar flare spectra because: (1) the flare particle intensity changes on a time scale comparable to or shorter than an orbital period; (2) there is no certain proof that solar flare particles are fully ionized; (3) the geomagnetic cutoff is suppressed to some extent during a flare. We recommend that the geomagnetic cutoff during a flare, P_F, be computed from the "quiet time" cutoff P_o using:

$$\Delta P/P_o = 0.54 \exp(-P_o/2.9) \quad (41)$$

and

$$P_F = P_o - \Delta P, \quad (42)$$

where P_F, P_o, and ΔP are in GeV/ec.

APPENDIX 2: THE GEOMAGNETIC CUTOFF TRANSMISSION FUNCTION

The geomagnetic cutoff transmission function is calculated using the method described in Adams et. al. (1983). Here we will describe how this method has been extended to elliptical orbits.

Section 4.0 of Adams et. al. (1983) describes the procedure for finding the geographic position of satellites in circular orbits. For spacecraft in elliptical orbits, the offset dipole coordinates of the position must be calculated in three steps. First, the position of the satellite along its orbit must be calculated versus time. Second, the geographic latitude and longitude of the sub-satellite point must be found. Third, the geographic coordinates must be transformed into the offset and the tilted dipole coordinates required by the Störmer approximation.

Numerous celestial mechanic texts describe elliptical orbits of satellites constrained by Newton's laws. For convenience, this description will follow the notation of Sterne (1960). Elliptical positions are described by an angle Ω called the "true anomaly" and the distance r from the satellite to the earth's center. These in turn are formulated in terms of the "mean anomaly" M, the "eccentric anomaly" E, the orbit's period P, eccentricity e, and semi-major axis a.

The period is:

$$P = 2\pi \left(a^3 / GM_e\right)^{1/2},$$

where G is the gravitational constant and M_e is the earth's mass. The mean anomaly is given by:

$$M = (2\pi/P)\, t,$$

where t is the time since perihelion. The eccentric anomaly is then found by iteratively solving the equation:

$$M = E - e \sin E.$$

The values r and Ω are calculated from E:

$$r = a (1 - e \cos E),$$

$$\tan (\Omega/2) = ((1+e)/(1-e))^{1/2} \tan (E/2).$$

This last equation is solved uniquely with the added condition that $\Omega/2$ and E/2 be in the same quadrant. For purposes of calculating geographic coordinates, the displacement of the perigee from the ascending node is added to this to obtain a final value of Ω.

The spacecraft's geographic latitude θ and longitude ϕ are calculated from the above r and Ω, and the parameters of the orbit: the orbital inclination θ_0; the initial longitude, ϕ_0, of the ascending node, and the angular velocity, ω, of the earth. The latitude is simply:

$$\theta = \pi/2 - \cos^{-1} (\sin\theta_0 \sin\Omega).$$

The longitude is:

$$\phi = \phi_0 - \pi/2 - \omega t + \tan^{-1} S_1 + \tan^{-1} S_2$$

where

$$S_1 = \frac{\sin[1/2(\pi/2-\theta_0)]\cos[1/2(\pi/2-\Omega)]}{\sin[1/2(\pi/2+\theta_0)]\sin[1/2(\pi/2-\Omega)]},$$

and

$$S_2 = \frac{\cos[1/2(\pi/2-\theta_0)]\cos[1/2(\pi/2-\Omega)]}{\cos[1/2(\pi/2+\theta_0)]\sin[1/2(\pi/2-\Omega)]}.$$

The final step--transforming to offset-tilted dipole coordinates--is done using the method of Smart and Shea (1977).

Appendix B of Adams et. al. (1983) contained some typographical errors. This appendix is presented in its correct form as Appendix 6 of this report.

APPENDIX 3
PARTICLE RANGE VS. ENERGY FOR VARIOUS IONS IN ALUMINUM

Preceding Page Blank

RANGE
IN
ALUMINUM

ATOMIC NUMBER	ATOMIC MASS	PARTIAL DENSITY:G/CC	IADJ: EV
13.	26.9815	2.6980	164.00

ENERGY MEV/AMU	H	HE	C	O	AR	FE	KR	XE	U
	RANGE IN G/CMSQ								
0.010	3.325E-05	6.679E-05	1.209E-04	1.103E-04	8.955E-05	7.072E-05	6.119E-05	4.713E-05	3.355E-05
0.012	3.967E-05	7.958E-05	1.445E-04	1.321E-04	1.081E-04	8.565E-05	7.423E-05	5.722E-05	4.074E-05
0.015	4.861E-05	9.700E-05	1.776E-04	1.636E-04	1.381E-04	1.109E-04	9.691E-05	7.503E-05	5.344E-05
0.020	6.220E-05	1.227E-04	2.261E-04	2.112E-04	1.897E-04	1.576E-04	1.411E-04	1.110E-04	7.936E-05
0.025	7.470E-05	1.457E-04	2.674E-04	2.525E-04	2.399E-04	2.068E-04	1.907E-04	1.534E-04	1.108E-04
0.030	8.649E-05	1.668E-04	3.031E-04	2.887E-04	2.870E-04	2.557E-04	2.429E-04	2.008E-04	1.473E-04
0.040	1.088E-04	2.057E-04	3.633E-04	3.499E-04	3.707E-04	3.476E-04	3.482E-04	3.045E-04	2.327E-04
0.050	1.303E-04	2.418E-04	4.136E-04	4.011E-04	4.426E-04	4.298E-04	4.481E-04	4.121E-04	3.304E-04
0.060	1.516E-04	2.761E-04	4.579E-04	4.460E-04	5.057E-04	5.032E-04	5.403E-04	5.180E-04	4.353E-04
0.070	1.729E-04	3.094E-04	4.981E-04	4.867E-04	5.625E-04	5.695E-04	6.251E-04	6.194E-04	5.435E-04
0.080	1.945E-04	3.418E-04	5.355E-04	5.244E-04	6.145E-04	6.302E-04	7.032E-04	7.155E-04	6.522E-04
0.100	2.390E-04	4.052E-04	6.043E-04	5.933E-04	7.081E-04	7.388E-04	8.437E-04	8.921E-04	8.644E-04
0.120	2.853E-04	4.674E-04	6.679E-04	6.565E-04	7.918E-04	8.351E-04	9.679E-04	1.050E-03	1.065E-03
0.150	3.584E-04	5.603E-04	7.569E-04	7.440E-04	9.047E-04	9.634E-04	1.132E-03	1.260E-03	1.340E-03
0.200	4.896E-04	7.166E-04	8.946E-04	8.778E-04	1.071E-03	1.148E-03	1.366E-03	1.557E-03	1.739E-03
0.250	6.319E-04	8.778E-04	1.025E-03	1.002E-03	1.219E-03	1.310E-03	1.568E-03	1.810E-03	2.080E-03
0.300	7.849E-04	1.046E-03	1.150E-03	1.121E-03	1.356E-03	1.458E-03	1.748E-03	2.034E-03	2.380E-03
0.400	1.121E-03	1.404E-03	1.395E-03	1.350E-03	1.607E-03	1.723E-03	2.068E-03	2.424E-03	2.897E-03
0.500	1.497E-03	1.796E-03	1.639E-03	1.573E-03	1.842E-03	1.964E-03	2.354E-03	2.766E-03	3.343E-03
0.600	1.912E-03	2.222E-03	1.885E-03	1.795E-03	2.066E-03	2.192E-03	2.620E-03	3.078E-03	3.743E-03
0.700	2.364E-03	2.683E-03	2.136E-03	2.020E-03	2.285E-03	2.410E-03	2.871E-03	3.370E-03	4.112E-03
0.800	2.853E-03	3.179E-03	2.394E-03	2.247E-03	2.500E-03	2.622E-03	3.112E-03	3.647E-03	4.457E-03
1.000	3.941E-03	4.275E-03	2.930E-03	2.716E-03	2.927E-03	3.034E-03	3.576E-03	4.170E-03	5.100E-03
1.200	5.169E-03	5.508E-03	3.498E-03	3.205E-03	3.353E-03	3.439E-03	4.023E-03	4.666E-03	5.698E-03
1.500	7.270E-03	7.609E-03	4.414E-03	3.982E-03	4.002E-03	4.041E-03	4.678E-03	5.380E-03	6.541E-03
2.000	1.144E-02	1.176E-02	6.115E-03	5.399E-03	5.120E-03	5.054E-03	5.756E-03	6.526E-03	7.861E-03
2.500	1.641E-02	1.670E-02	8.035E-03	6.975E-03	6.298E-03	6.093E-03	6.837E-03	7.649E-03	9.122E-03
3.000	2.216E-02	2.241E-02	1.018E-02	8.711E-03	7.542E-03	7.168E-03	7.936E-03	8.768E-03	1.035E-02
4.000	3.598E-02	3.610E-02	1.512E-02	1.266E-02	1.024E-02	9.439E-03	1.021E-02	1.102E-02	1.276E-02
5.000	5.263E-02	5.259E-02	2.092E-02	1.723E-02	1.321E-02	1.188E-02	1.260E-02	1.333E-02	1.515E-02
6.000	7.195E-02	7.171E-02	2.755E-02	2.240E-02	1.646E-02	1.450E-02	1.511E-02	1.571E-02	1.756E-02
7.000	9.396E-02	9.349E-02	3.503E-02	2.818E-02	1.999E-02	1.729E-02	1.775E-02	1.817E-02	1.999E-02
8.000	1.186E-01	1.178E-01	4.333E-02	3.456E-02	2.379E-02	2.027E-02	2.053E-02	2.071E-02	2.247E-02

RANGE
IN
ALUMINUM

ATOMIC NUMBER	ATOMIC MASS	PARTIAL DENSITY:G/CC	IADJ: EV
13.	26.9815	2.6980	164.00

ENERGY MEV/AMU	H	HE	C	O	AR	FE	KR	XE	U
					RANGE IN G/CMSQ				
10.00	1.754E-01	1.740E-01	6.239E-02	4.911E-02	3.222E-02	2.675E-02	2.649E-02	2.606E-02	2.754E-02
12.00	2.418E-01	2.397E-01	8.463E-02	6.599E-02	4.171E-02	3.393E-02	3.299E-02	3.176E-02	3.280E-02
15.00	3.582E-01	3.550E-01	1.236E-01	9.553E-02	5.790E-02	4.600E-02	4.373E-02	4.099E-02	4.108E-02
20.00	5.929E-01	5.880E-01	2.025E-01	1.552E-01	8.990E-02	6.945E-02	6.424E-02	5.818E-02	5.598E-02
25.00	8.757E-01	8.688E-01	2.972E-01	2.268E-01	1.278E-01	9.685E-02	8.790E-02	7.759E-02	7.229E-02
30.00	1.205E+00	1.196E+00	4.068E-01	3.094E-01	1.712E-01	1.279E-01	1.145E-01	9.918E-02	9.007E-02
40.00	2.002E+00	1.986E+00	6.705E-01	5.074E-01	2.729E-01	2.001E-01	1.758E-01	1.485E-01	1.301E-01
50.00	2.972E+00	2.949E+00	9.912E-01	7.480E-01	3.940E-01	2.845E-01	2.465E-01	2.051E-01	1.762E-01
60.00	4.106E+00	4.074E+00	1.366E+00	1.029E+00	5.344E-01	3.809E-01	3.259E-01	2.678E-01	2.282E-01
70.00	5.395E+00	5.353E+00	1.792E+00	1.348E+00	6.933E-01	4.893E-01	4.137E-01	3.357E-01	2.855E-01
80.00	6.832E+00	6.778E+00	2.267E+00	1.704E+00	8.698E-01	6.092E-01	5.102E-01	4.085E-01	3.469E-01
100.00	1.012E+01	1.004E+01	3.354E+00	2.519E+00	1.273E+00	8.819E-01	7.278E-01	5.690E-01	4.784E-01
120.00	1.393E+01	1.382E+01	4.613E+00	3.461E+00	1.739E+00	1.196E+00	9.765E-01	7.492E-01	6.171E-01
150.00	2.054E+01	2.038E+01	6.794E+00	5.094E+00	2.544E+00	1.737E+00	1.403E+00	1.054E+00	8.370E-01
200.00	3.365E+01	3.338E+01	1.112E+01	8.334E+00	4.138E+00	2.805E+00	2.241E+00	1.645E+00	1.238E+00
250.00	4.902E+01	4.863E+01	1.619E+01	1.213E+01	6.004E+00	4.053E+00	3.217E+00	2.327E+00	1.680E+00
300.00	6.632E+01	6.579E+01	2.190E+01	1.640E+01	8.101E+00	5.453E+00	4.310E+00	3.085E+00	2.158E+00
400.00	1.056E+02	1.048E+02	3.487E+01	2.611E+01	1.286E+01	8.630E+00	6.784E+00	4.792E+00	3.208E+00
500.00	1.499E+02	1.487E+02	4.948E+01	3.704E+01	1.822E+01	1.220E+01	9.561E+00	6.700E+00	4.359E+00
600.00	1.980E+02	1.964E+02	6.533E+01	4.890E+01	2.403E+01	1.607E+01	1.257E+01	8.761E+00	5.588E+00
700.00	2.490E+02	2.470E+02	8.214E+01	6.148E+01	3.019E+01	2.017E+01	1.575E+01	1.094E+01	6.877E+00
800.00	3.022E+02	2.998E+02	9.970E+01	7.461E+01	3.661E+01	2.446E+01	1.908E+01	1.321E+01	8.214E+00
1000.00	4.138E+02	4.105E+02	1.365E+02	1.021E+02	5.009E+01	3.343E+01	2.604E+01	1.796E+01	1.100E+01
1200.00	5.304E+02	5.261E+02	1.749E+02	1.309E+02	6.416E+01	4.279E+01	3.330E+01	2.292E+01	1.389E+01
1500.00	7.109E+02	7.052E+02	2.344E+02	1.754E+02	8.594E+01	5.729E+01	4.454E+01	3.058E+01	1.834E+01
2000.00	1.020E+03	1.011E+03	3.362E+02	2.516E+02	1.232E+02	8.208E+01	6.376E+01	4.368E+01	2.595E+01
2500.00	1.332E+03	1.321E+03	4.392E+02	3.286E+02	1.609E+02	1.072E+02	8.320E+01	5.693E+01	3.363E+01
3000.00	1.644E+03	1.631E+03	5.423E+02	4.057E+02	1.986E+02	1.323E+02	1.027E+02	7.020E+01	4.133E+01
4000.00	2.266E+03	2.247E+03	7.471E+02	5.589E+02	2.736E+02	1.822E+02	1.413E+02	9.657E+01	5.664E+01
5000.00	2.879E+03	2.856E+03	9.492E+02	7.102E+02	3.476E+02	2.314E+02	1.796E+02	1.226E+02	7.178E+01
6000.00	3.483E+03	3.455E+03	1.149E+03	8.593E+02	4.206E+02	2.800E+02	2.172E+02	1.483E+02	8.674E+01
7000.00	4.080E+03	4.047E+03	1.345E+03	1.007E+03	4.927E+02	3.280E+02	2.545E+02	1.737E+02	1.015E+02
8000.00	4.668E+03	4.631E+03	1.540E+03	1.152E+03	5.638E+02	3.754E+02	2.912E+02	1.988E+02	1.161E+02

APPENDIX 4
PARTICLE STOPPING POWER VS. ENERGY IN ALUMINUM

DE/DX
IN
ALUMINUM

ATOMIC NUMBER	ATOMIC MASS	PARTIAL DENSITY:G/CC	IADJ: EV
13.	26.9815	2.6980	164.00

STOPPING IN MEV/(GM/CM2)

ENERGY MEV/AMU	H	HE	C	O	AR	FE	KR	XE	U
0.010	3.032E+02	5.993E+02	9.939E+02	1.451E+03	4.461E+03	7.897E+03	1.370E+04	2.786E+04	7.094E+04
0.012	3.243E+02	6.528E+02	1.040E+03	1.479E+03	4.137E+03	7.062E+03	1.200E+04	2.418E+04	6.161E+04
0.015	3.518E+02	7.259E+02	1.141E+03	1.575E+03	3.908E+03	6.305E+03	1.035E+04	2.041E+04	5.176E+04
0.020	3.887E+02	8.292E+02	1.347E+03	1.807E+03	3.888E+03	5.753E+03	8.843E+03	1.664E+04	4.137E+04
0.025	4.166E+02	9.119E+02	1.571E+03	2.076E+03	4.096E+03	5.659E+03	8.164E+03	1.452E+04	3.495E+04
0.030	4.374E+02	9.781E+02	1.793E+03	2.354E+03	4.412E+03	5.799E+03	7.922E+03	1.330E+04	3.070E+04
0.040	4.628E+02	1.075E+03	2.206E+03	2.886E+03	5.173E+03	6.418E+03	8.112E+03	1.228E+04	2.575E+04
0.050	4.731E+02	1.140E+03	2.562E+03	3.357E+03	5.957E+03	7.209E+03	8.720E+03	1.223E+04	2.332E+04
0.060	4.741E+02	1.187E+03	2.860E+03	3.759E+03	6.696E+03	8.029E+03	9.488E+03	1.264E+04	2.222E+04
0.070	4.697E+02	1.221E+03	3.108E+03	4.102E+03	7.373E+03	8.826E+03	1.031E+04	1.329E+04	2.188E+04
0.080	4.623E+02	1.246E+03	3.317E+03	4.395E+03	7.990E+03	9.583E+03	1.114E+04	1.406E+04	2.199E+04
0.100	4.444E+02	1.277E+03	3.647E+03	4.873E+03	9.074E+03	1.098E+04	1.274E+04	1.575E+04	2.301E+04
0.120	4.263E+02	1.291E+03	3.895E+03	5.251E+03	1.001E+04	1.223E+04	1.426E+04	1.750E+04	2.459E+04
0.150	4.018E+02	1.292E+03	4.186E+03	5.697E+03	1.121E+04	1.389E+04	1.636E+04	2.009E+04	2.741E+04
0.200	3.682E+02	1.264E+03	4.511E+03	6.233E+03	1.282E+04	1.625E+04	1.945E+04	2.413E+04	3.245E+04
0.250	3.413E+02	1.218E+03	4.715E+03	6.599E+03	1.409E+04	1.818E+04	2.208E+04	2.775E+04	3.738E+04
0.300	3.188E+02	1.168E+03	4.838E+03	6.847E+03	1.510E+04	1.978E+04	2.433E+04	3.094E+04	4.198E+04
0.400	2.828E+02	1.068E+03	4.933E+03	7.113E+03	1.654E+04	2.221E+04	2.790E+04	3.624E+04	5.002E+04
0.500	2.549E+02	9.789E+02	4.913E+03	7.193E+03	1.747E+04	2.392E+04	3.055E+04	4.039E+04	5.668E+04
0.600	2.325E+02	9.021E+02	4.835E+03	7.169E+03	1.806E+04	2.514E+04	3.255E+04	4.368E+04	6.222E+04
0.700	2.141E+02	8.362E+02	4.727E+03	7.087E+03	1.843E+04	2.602E+04	3.409E+04	4.633E+04	6.687E+04
0.800	1.986E+02	7.795E+02	4.606E+03	6.971E+03	1.864E+04	2.665E+04	3.528E+04	4.848E+04	7.082E+04
1.000	1.740E+02	6.872E+02	4.352E+03	6.692E+03	1.877E+04	2.741E+04	3.693E+04	5.173E+04	7.713E+04
1.200	1.553E+02	6.156E+02	4.107E+03	6.397E+03	1.866E+04	2.774E+04	3.793E+04	5.399E+04	8.189E+04
1.500	1.342E+02	5.339E+02	3.775E+03	5.969E+03	1.828E+04	2.779E+04	3.870E+04	5.620E+04	8.712E+04
2.000	1.102E+02	4.398E+02	3.317E+03	5.345E+03	1.742E+04	2.727E+04	3.891E+04	5.805E+04	9.257E+04
2.500	9.396E+01	3.756E+02	2.957E+03	4.831E+03	1.650E+04	2.644E+04	3.848E+04	5.867E+04	9.591E+04
3.000	8.211E+01	3.287E+02	2.667E+03	4.407E+03	1.563E+04	2.553E+04	3.776E+04	5.864E+04	9.780E+04
4.000	6.577E+01	2.639E+02	2.229E+03	3.747E+03	1.408E+04	2.371E+04	3.600E+04	5.761E+04	9.934E+04
5.000	5.614E+01	2.251E+02	1.935E+03	3.289E+03	1.284E+04	2.209E+04	3.421E+04	5.604E+04	9.928E+04
6.000	4.874E+01	1.956E+02	1.703E+03	2.922E+03	1.178E+04	2.063E+04	3.249E+04	5.429E+04	9.841E+04
7.000	4.320E+01	1.734E+02	1.522E+03	2.631E+03	1.090E+04	1.935E+04	3.090E+04	5.252E+04	9.711E+04
8.000	3.891E+01	1.562E+02	1.378E+03	2.395E+03	1.014E+04	1.823E+04	2.945E+04	5.078E+04	9.557E+04

DE/DX
IN
ALUMINUM

ATOMIC NUMBER	ATOMIC MASS	PARTIAL DENSITY:G/CC	IADJ: EV
13.	26.9815	2.6980	164.00

ENERGY MEV/AMU	H	HE	C	O	AR	FE	KR	XE	U
	STOPPING IN MEV/(GM/CM2)								
10.00	3.267E+01	1.312E+02	1.162E+03	2.035E+03	8.917E+03	1.634E+04	2.691E+04	4.754E+04	9.221E+04
12.00	2.839E+01	1.139E+02	1.010E+03	1.775E+03	7.974E+03	1.483E+04	2.478E+04	4.464E+04	8.876E+04
15.00	2.401E+01	9.616E+01	8.525E+02	1.501E+03	6.911E+03	1.306E+04	2.218E+04	4.088E+04	8.378E+04
20.00	1.946E+01	7.780E+01	6.902E+02	1.215E+03	5.701E+03	1.097E+04	1.895E+04	3.586E+04	7.629E+04
25.00	1.645E+01	6.582E+01	5.878E+02	1.037E+03	4.906E+03	9.530E+03	1.665E+04	3.200E+04	6.984E+04
30.00	1.427E+01	5.712E+01	5.130E+02	9.080E+02	4.349E+03	8.502E+03	1.494E+04	2.899E+04	6.427E+04
40.00	1.139E+01	4.557E+01	4.102E+02	7.284E+02	3.586E+03	7.125E+03	1.265E+04	2.470E+04	5.525E+04
50.00	9.568E+00	3.830E+01	3.449E+02	6.127E+02	3.053E+03	6.179E+03	1.116E+04	2.194E+04	4.846E+04
60.00	8.312E+00	3.327E+01	2.997E+02	5.326E+02	2.667E+03	5.452E+03	1.003E+04	2.008E+04	4.347E+04
70.00	7.390E+00	2.958E+01	2.665E+02	4.737E+02	2.380E+03	4.889E+03	9.093E+03	1.867E+04	3.997E+04
80.00	6.682E+00	2.674E+01	2.410E+02	4.285E+02	2.157E+03	4.448E+03	8.325E+03	1.745E+04	3.764E+04
100.00	5.666E+00	2.268E+01	2.044E+02	3.635E+02	1.836E+03	3.802E+03	7.176E+03	1.540E+04	3.514E+04
120.00	4.969E+00	1.989E+01	1.793E+02	3.189E+02	1.614E+03	3.352E+03	6.360E+03	1.384E+04	3.361E+04
150.00	4.256E+00	1.703E+01	1.536E+02	2.732E+02	1.385E+03	2.885E+03	5.502E+03	1.213E+04	3.138E+04
200.00	3.524E+00	1.410E+01	1.272E+02	2.264E+02	1.150E+03	2.401E+03	4.600E+03	1.028E+04	2.820E+04
250.00	3.076E+00	1.231E+01	1.111E+02	1.977E+02	1.005E+03	2.102E+03	4.039E+03	9.095E+03	2.582E+04
300.00	2.775E+00	1.111E+01	1.002E+02	1.784E+02	9.075E+02	1.900E+03	3.657E+03	8.276E+03	2.402E+04
400.00	2.398E+00	9.599E+00	8.663E+01	1.542E+02	7.854E+02	1.646E+03	3.175E+03	7.227E+03	2.155E+04
500.00	2.175E+00	8.707E+00	7.859E+01	1.399E+02	7.130E+02	1.496E+03	2.888E+03	6.594E+03	1.996E+04
600.00	2.031E+00	8.128E+00	7.337E+01	1.306E+02	6.660E+02	1.398E+03	2.700E+03	6.178E+03	1.887E+04
700.00	1.931E+00	7.730E+00	6.978E+01	1.242E+02	6.336E+02	1.330E+03	2.571E+03	5.890E+03	1.810E+04
800.00	1.860E+00	7.446E+00	6.721E+01	1.197E+02	6.104E+02	1.282E+03	2.478E+03	5.683E+03	1.754E+04
1000.00	1.762E+00	7.052E+00	6.367E+01	1.134E+02	5.784E+02	1.215E+03	2.350E+03	5.395E+03	1.674E+04
1200.00	1.703E+00	6.817E+00	6.154E+01	1.096E+02	5.592E+02	1.175E+03	2.273E+03	5.222E+03	1.625E+04
1500.00	1.653E+00	6.618E+00	5.975E+01	1.064E+02	5.430E+02	1.141E+03	2.208E+03	5.074E+03	1.583E+04
2000.00	1.619E+00	6.482E+00	5.852E+01	1.042E+02	5.318E+02	1.117E+03	2.163E+03	4.972E+03	1.554E+04
2500.00	1.611E+00	6.451E+00	5.824E+01	1.037E+02	5.292E+02	1.112E+03	2.152E+03	4.947E+03	1.546E+04
3000.00	1.615E+00	6.463E+00	5.835E+01	1.039E+02	5.301E+02	1.114E+03	2.155E+03	4.955E+03	1.548E+04
4000.00	1.633E+00	6.537E+00	5.901E+01	1.051E+02	5.360E+02	1.126E+03	2.179E+03	5.007E+03	1.563E+04
5000.00	1.656E+00	6.629E+00	5.983E+01	1.065E+02	5.434E+02	1.141E+03	2.208E+03	5.073E+03	1.582E+04
6000.00	1.679E+00	6.720E+00	6.066E+01	1.080E+02	5.508E+02	1.157E+03	2.238E+03	5.139E+03	1.601E+04
7000.00	1.700E+00	6.806E+00	6.143E+01	1.094E+02	5.578E+02	1.171E+03	2.266E+03	5.201E+03	1.619E+04
8000.00	1.720E+00	6.886E+00	6.215E+01	1.106E+02	5.642E+02	1.185E+03	2.291E+03	5.259E+03	1.635E+04

APPENDIX 5
PARTICLE STOPPING POWER VS. ENERGY IN SILICON

DE/DX
IN
SILICON

ATOMIC NUMBER	ATOMIC MASS	PARTIAL DENSITY:G/CC	IADJ: EV
14.	28.0855	2.3210	169.00

ENERGY MEV/AMU	H	HE	C	O	AR	FE	KR	XE	U
				STOPPING IN MEV/(GM/CM2)					
0.010	2.920E+02	5.452E+02	9.982E+02	1.470E+03	4.651E+03	8.312E+03	1.448E+04	2.952E+04	7.515E+04
0.012	3.130E+02	5.975E+02	1.038E+03	1.488E+03	4.291E+03	7.412E+03	1.268E+04	2.562E+04	6.530E+04
0.015	3.409E+02	6.727E+02	1.133E+03	1.574E+03	4.024E+03	6.586E+03	1.090E+04	2.162E+04	5.489E+04
0.020	3.802E+02	7.882E+02	1.337E+03	1.801E+03	3.971E+03	5.965E+03	9.274E+03	1.760E+04	4.388E+04
0.025	4.123E+02	8.924E+02	1.567E+03	2.079E+03	4.173E+03	5.842E+03	8.527E+03	1.532E+04	3.706E+04
0.030	4.387E+02	9.862E+02	1.807E+03	2.377E+03	4.509E+03	5.986E+03	8.260E+03	1.400E+04	3.254E+04
0.040	4.783E+02	1.146E+03	2.284E+03	2.988E+03	5.378E+03	6.697E+03	8.503E+03	1.294E+04	2.728E+04
0.050	5.039E+02	1.272E+03	2.729E+03	3.574E+03	6.342E+03	7.673E+03	9.279E+03	1.301E+04	2.479E+04
0.060	5.188E+02	1.370E+03	3.127E+03	4.109E+03	7.303E+03	8.737E+03	1.029E+04	1.364E+04	2.380E+04
0.070	5.257E+02	1.442E+03	3.475E+03	4.584E+03	8.215E+03	9.802E+03	1.140E+04	1.457E+04	2.367E+04
0.080	5.264E+02	1.493E+03	3.772E+03	4.997E+03	9.054E+03	1.082E+04	1.251E+04	1.564E+04	2.406E+04
0.100	5.159E+02	1.547E+03	4.229E+03	5.649E+03	1.049E+04	1.264E+04	1.461E+04	1.789E+04	2.567E+04
0.120	4.967E+02	1.557E+03	4.539E+03	6.110E+03	1.162E+04	1.416E+04	1.646E+04	2.004E+04	2.772E+04
0.150	4.628E+02	1.529E+03	4.819E+03	6.557E+03	1.288E+04	1.595E+04	1.874E+04	2.290E+04	3.091E+04
0.200	4.103E+02	1.441E+03	5.025E+03	6.943E+03	1.427E+04	1.808E+04	2.162E+04	2.678E+04	3.586E+04
0.250	3.687E+02	1.348E+03	5.093E+03	7.128E+03	1.522E+04	1.950E+04	2.384E+04	2.995E+04	4.030E+04
0.300	3.365E+02	1.265E+03	5.107E+03	7.228E+03	1.594E+04	2.058E+04	2.569E+04	3.268E+04	4.435E+04
0.400	2.906E+02	1.128E+03	5.068E+03	7.308E+03	1.700E+04	2.208E+04	2.868E+04	3.728E+04	5.151E+04
0.500	2.587E+02	1.020E+03	4.987E+03	7.301E+03	1.774E+04	2.329E+04	3.103E+04	4.104E+04	5.766E+04
0.600	2.348E+02	9.335E+02	4.883E+03	7.241E+03	1.824E+04	2.540E+04	3.289E+04	4.415E+04	6.296E+04
0.700	2.158E+02	8.618E+02	4.767E+03	7.146E+03	1.859E+04	2.625E+04	3.439E+04	4.675E+04	6.754E+04
0.800	2.003E+02	8.013E+02	4.645E+03	7.031E+03	1.880E+04	2.689E+04	3.559E+04	4.893E+04	7.152E+04
1.000	1.759E+02	7.046E+02	4.401E+03	6.768E+03	1.898E+04	2.773E+04	3.735E+04	5.234E+04	7.806E+04
1.200	1.576E+02	6.305E+02	4.168E+03	6.492E+03	1.894E+04	2.816E+04	3.850E+04	5.481E+04	8.316E+04
1.500	1.369E+02	5.466E+02	3.851E+03	6.089E+03	1.865E+04	2.835E+04	3.948E+04	5.734E+04	8.891E+04
2.000	1.133E+02	4.502E+02	3.409E+03	5.493E+03	1.790E+04	2.802E+04	3.999E+04	5.966E+04	9.525E+04
2.500	9.710E+01	3.846E+02	3.056E+03	4.993E+03	1.706E+04	2.733E+04	3.977E+04	6.064E+04	9.913E+04
3.000	8.524E+01	3.356E+02	2.769E+03	4.575E+03	1.623E+04	2.650E+04	3.920E+04	6.088E+04	1.015E+05
4.000	6.873E+01	2.704E+02	2.330E+03	3.916E+03	1.472E+04	2.477E+04	3.762E+04	6.021E+04	1.038E+05
5.000	5.892E+01	2.308E+02	2.032E+03	3.453E+03	1.348E+04	2.319E+04	3.592E+04	5.885E+04	1.043E+05
6.000	5.131E+01	2.006E+02	1.794E+03	3.078E+03	1.242E+04	2.174E+04	3.424E+04	5.722E+04	1.037E+05
7.000	4.558E+01	1.780E+02	1.607E+03	2.779E+03	1.151E+04	2.046E+04	3.266E+04	5.551E+04	1.026E+05
8.000	4.110E+01	1.604E+02	1.457E+03	2.534E+03	1.074E+04	1.931E+04	3.120E+04	5.381E+04	1.013E+05

DE/DX
IN
SILICON

ATOMIC NUMBER	ATOMIC MASS	PARTIAL DENSITY:G/CC	IADJ: EV
14.	28.0855	2.3210	169.00

ENERGY MEV/AMU	H	HE	C	O	AR	FE	KR	XE	U
	STOPPING IN MEV/(GM/CM2)								
10.00	3.452E+01	1.347E+02	1.232E+03	2.158E+03	9.473E+03	1.737E+04	2.861E+04	5.056E+04	9.807E+04
12.00	2.992E+01	1.170E+02	1.070E+03	1.883E+03	8.487E+03	1.580E+04	2.641E+04	4.760E+04	9.467E+04
15.00	2.514E+01	9.888E+01	9.000E+02	1.588E+03	7.361E+03	1.393E+04	2.371E+04	4.372E+04	8.964E+04
20.00	2.014E+01	8.006E+01	7.209E+02	1.274E+03	6.051E+03	1.170E+04	2.028E+04	3.846E+04	8.194E+04
25.00	1.695E+01	6.775E+01	6.082E+02	1.076E+03	5.169E+03	1.012E+04	1.779E+04	3.436E+04	7.519E+04
30.00	1.469E+01	5.880E+01	5.287E+02	9.370E+02	4.542E+03	8.969E+03	1.590E+04	3.110E+04	6.930E+04
40.00	1.172E+01	4.693E+01	4.225E+02	7.502E+02	3.703E+03	7.408E+03	1.329E+04	2.633E+04	5.963E+04
50.00	9.854E+00	3.944E+01	3.552E+02	6.310E+02	3.146E+03	6.377E+03	1.159E+04	2.315E+04	5.219E+04
60.00	8.561E+00	3.426E+01	3.087E+02	5.486E+02	2.748E+03	5.618E+03	1.035E+04	2.096E+04	4.658E+04
70.00	7.612E+00	3.046E+01	2.745E+02	4.879E+02	2.452E+03	5.038E+03	9.371E+03	1.934E+04	4.250E+04
80.00	6.883E+00	2.755E+01	2.483E+02	4.414E+02	2.223E+03	4.583E+03	8.579E+03	1.801E+04	3.968E+04
100.00	5.837E+00	2.336E+01	2.106E+02	3.745E+02	1.891E+03	3.918E+03	7.394E+03	1.587E+04	3.651E+04
120.00	5.120E+00	2.049E+01	1.847E+02	3.286E+02	1.663E+03	3.455E+03	6.554E+03	1.426E+04	3.470E+04
150.00	4.385E+00	1.755E+01	1.583E+02	2.816E+02	1.427E+03	2.974E+03	5.671E+03	1.251E+04	3.235E+04
200.00	3.631E+00	1.453E+01	1.311E+02	2.333E+02	1.185E+03	2.475E+03	4.742E+03	1.060E+04	2.907E+04
250.00	3.170E+00	1.269E+01	1.145E+02	2.037E+02	1.036E+03	2.167E+03	4.163E+03	9.376E+03	2.662E+04
300.00	2.860E+00	1.145E+01	1.033E+02	1.838E+02	9.355E+02	1.959E+03	3.770E+03	8.532E+03	2.477E+04
400.00	2.472E+00	9.895E+00	8.930E+01	1.590E+02	8.097E+02	1.697E+03	3.273E+03	7.451E+03	2.222E+04
500.00	2.242E+00	8.976E+00	8.102E+01	1.442E+02	7.351E+02	1.542E+03	2.977E+03	6.799E+03	2.058E+04
600.00	2.094E+00	8.380E+00	7.565E+01	1.347E+02	6.867E+02	1.441E+03	2.784E+03	6.371E+03	1.946E+04
700.00	1.991E+00	7.971E+00	7.195E+01	1.281E+02	6.533E+02	1.371E+03	2.651E+03	6.075E+03	1.867E+04
800.00	1.918E+00	7.677E+00	6.931E+01	1.234E+02	6.294E+02	1.322E+03	2.556E+03	5.861E+03	1.809E+04
1000.00	1.818E+00	7.277E+00	6.569E+01	1.170E+02	5.968E+02	1.253E+03	2.425E+03	5.568E+03	1.728E+04
1200.00	1.758E+00	7.038E+00	6.354E+01	1.131E+02	5.773E+02	1.213E+03	2.347E+03	5.391E+03	1.678E+04
1500.00	1.708E+00	6.837E+00	6.173E+01	1.099E+02	5.609E+02	1.178E+03	2.281E+03	5.243E+03	1.636E+04
2000.00	1.674E+00	6.702E+00	6.051E+01	1.077E+02	5.498E+02	1.155E+03	2.236E+03	5.141E+03	1.606E+04
2500.00	1.667E+00	6.673E+00	6.025E+01	1.073E+02	5.474E+02	1.150E+03	2.226E+03	5.118E+03	1.599E+04
3000.00	1.671E+00	6.689E+00	6.039E+01	1.075E+02	5.487E+02	1.153E+03	2.231E+03	5.128E+03	1.602E+04
4000.00	1.691E+00	6.770E+00	6.111E+01	1.088E+02	5.551E+02	1.166E+03	2.256E+03	5.185E+03	1.618E+04
5000.00	1.716E+00	6.868E+00	6.199E+01	1.104E+02	5.630E+02	1.182E+03	2.288E+03	5.255E+03	1.639E+04
6000.00	1.740E+00	6.965E+00	6.286E+01	1.119E+02	5.709E+02	1.199E+03	2.319E+03	5.326E+03	1.659E+04
7000.00	1.763E+00	7.055E+00	6.368E+01	1.134E+02	5.782E+02	1.214E+03	2.349E+03	5.391E+03	1.678E+04
8000.00	1.784E+00	7.139E+00	6.444E+01	1.147E+02	5.850E+02	1.228E+03	2.376E+03	5.452E+03	1.695E+04

APPENDIX 6: THE WORLDWIDE VERTICAL GEOMAGNETIC CUTOFF AT 20KM ALTITUDE

LATITUDE	LONGITUDE	RIGIDITY (GeV/ec)	LATITUDE	LONGITUDE	RIGIDITY (GeV/ec)
80.00	0.00	0.02	70.00	0.00	0.26
80.00	15.00	0.04	70.00	15.00	0.34
80.00	30.00	0.06	70.00	30.00	0.41
80.00	45.00	0.09	70.00	45.00	0.47
80.00	60.00	0.09	70.00	60.00	0.49
80.00	75.00	0.10	70.00	75.00	0.51
80.00	90.00	0.10	70.00	90.00	0.52
80.00	105.00	0.11	70.00	105.00	0.55
80.00	120.00	0.11	70.00	120.00	0.59
80.00	135.00	0.11	70.00	135.00	0.60
80.00	150.00	0.08	70.00	150.00	0.62
80.00	165.00	0.06	70.00	165.00	0.56
80.00	180.00	0.04	70.00	180.00	0.47
80.00	195.00	0.00	70.00	195.00	0.36
80.00	210.00	0.00	70.00	210.00	0.23
80.00	225.00	0.00	70.00	225.00	0.13
80.00	240.00	0.00	70.00	240.00	0.06
80.00	255.00	0.00	70.00	255.00	0.00
80.00	270.00	0.00	70.00	270.00	0.00
80.00	285.00	0.00	70.00	285.00	0.00
80.00	300.00	0.00	70.00	300.00	0.00
80.00	315.00	0.00	70.00	315.00	0.05
80.00	330.00	0.00	70.00	330.00	0.11
80.00	345.00	0.00	70.00	345.00	0.18
75.00	0.00	0.10	65.00	0.00	0.58
75.00	15.00	0.14	65.00	15.00	0.72
75.00	30.00	0.18	65.00	30.00	0.80
75.00	45.00	0.20	65.00	45.00	0.89
75.00	60.00	0.23	65.00	60.00	0.93
75.00	75.00	0.25	65.00	75.00	0.97
75.00	90.00	0.25	65.00	90.00	1.01
75.00	105.00	0.26	65.00	105.00	1.03
75.00	120.00	0.27	65.00	120.00	1.12
75.00	135.00	0.28	65.00	135.00	1.19
75.00	150.00	0.26	65.00	150.00	1.20
75.00	165.00	0.24	65.00	165.00	1.13
75.00	180.00	0.20	65.00	180.00	0.95
75.00	195.00	0.14	65.00	195.00	0.74
75.00	210.00	0.09	65.00	210.00	0.53
75.00	225.00	0.03	65.00	225.00	0.32
75.00	240.00	0.00	65.00	240.00	0.17
75.00	255.00	0.00	65.00	255.00	0.09
75.00	270.00	0.00	65.00	270.00	0.05
75.00	285.00	0.00	65.00	285.00	0.04
75.00	300.00	0.00	65.00	300.00	0.08
75.00	315.00	0.00	65.00	315.00	0.16
75.00	330.00	0.02	65.00	330.00	0.28
75.00	345.00	0.07	65.00	345.00	0.42

LATITUDE	LONGITUDE	RIGIDITY (GeV/ec)	LATITUDE	LONGITUDE	RIGIDITY (GeV/ec)
60.00	0.00	1.14	50.00	0.00	3.21
60.00	15.00	1.34	50.00	15.00	3.54
60.00	30.00	1.46	50.00	30.00	3.81
60.00	45.00	1.57	50.00	45.00	3.97
60.00	60.00	1.61	50.00	60.00	4.14
60.00	75.00	1.67	50.00	75.00	4.27
60.00	90.00	1.73	50.00	90.00	4.36
60.00	105.00	1.82	50.00	105.00	4.37
60.00	120.00	1.95	50.00	120.00	4.68
60.00	135.00	2.05	50.00	135.00	4.93
60.00	150.00	2.05	50.00	150.00	4.92
60.00	165.00	1.99	50.00	165.00	4.67
60.00	180.00	1.75	50.00	180.00	4.27
60.00	195.00	1.40	50.00	195.00	3.38
60.00	210.00	1.00	50.00	210.00	2.81
60.00	225.00	0.65	50.00	225.00	2.03
60.00	240.00	0.40	50.00	240.00	1.41
60.00	255.00	0.22	50.00	255.00	0.95
60.00	270.00	0.16	50.00	270.00	0.73
60.00	285.00	0.14	50.00	285.00	0.69
60.00	300.00	0.21	50.00	300.00	0.89
60.00	315.00	0.38	50.00	315.00	1.34
60.00	330.00	0.59	50.00	330.00	1.98
60.00	345.00	0.86	50.00	345.00	2.65
55.00	0.00	1.94	45.00	0.00	4.77
55.00	15.00	2.28	45.00	15.00	5.12
55.00	30.00	2.47	45.00	30.00	5.36
55.00	45.00	2.61	45.00	45.00	5.51
55.00	60.00	2.68	45.00	60.00	5.73
55.00	75.00	2.78	45.00	75.00	5.90
55.00	90.00	2.85	45.00	90.00	6.11
55.00	105.00	2.92	45.00	105.00	6.29
55.00	120.00	3.12	45.00	120.00	6.57
55.00	135.00	3.31	45.00	135.00	6.86
55.00	150.00	3.35	45.00	150.00	6.86
55.00	165.00	3.15	45.00	165.00	6.33
55.00	180.00	2.88	45.00	180.00	5.59
55.00	195.00	2.22	45.00	195.00	4.85
55.00	210.00	1.75	45.00	210.00	4.08
55.00	225.00	1.23	45.00	225.00	3.16
55.00	240.00	0.78	45.00	240.00	2.37
55.00	255.00	0.50	45.00	255.00	1.74
55.00	270.00	0.36	45.00	270.00	1.32
55.00	285.00	0.36	45.00	285.00	1.22
55.00	300.00	0.46	45.00	300.00	1.49
55.00	315.00	0.75	45.00	315.00	2.21
55.00	330.00	1.13	45.00	330.00	3.16
55.00	345.00	1.59	45.00	345.00	4.20

LATITUDE	LONGITUDE	RIGIDITY (GeV/ec)	LATITUDE	LONGITUDE	RIGIDITY (GeV/ec)
40.00	0.00	6.75	30.00	0.00	11.30
40.00	15.00	7.27	30.00	15.00	11.71
40.00	30.00	7.48	30.00	30.00	12.13
40.00	45.00	7.70	30.00	45.00	12.67
40.00	60.00	8.19	30.00	60.00	13.34
40.00	75.00	8.73	30.00	75.00	14.07
40.00	90.00	9.14	30.00	90.00	14.37
40.00	105.00	9.29	30.00	105.00	14.40
40.00	120.00	9.49	30.00	120.00	14.26
40.00	135.00	9.89	30.00	135.00	13.95
40.00	150.00	9.74	30.00	150.00	13.44
40.00	165.00	8.95	30.00	165.00	12.72
40.00	180.00	7.86	30.00	180.00	11.65
40.00	195.00	6.46	30.00	195.00	10.48
40.00	210.00	5.41	30.00	210.00	9.63
40.00	225.00	4.55	30.00	225.00	8.78
40.00	240.00	3.61	30.00	240.00	7.00
40.00	255.00	2.76	30.00	255.00	5.60
40.00	270.00	2.07	30.00	270.00	4.44
40.00	285.00	1.93	30.00	285.00	4.07
40.00	300.00	2.42	30.00	300.00	4.87
40.00	315.00	3.41	30.00	315.00	6.98
40.00	330.00	4.82	30.00	330.00	9.67
40.00	345.00	5.92	30.00	345.00	10.60
35.00	0.00	9.54	25.00	0.00	13.10
35.00	15.00	9.89	25.00	15.00	13.64
35.00	30.00	10.10	25.00	30.00	14.10
35.00	45.00	10.53	25.00	45.00	14.53
35.00	60.00	11.15	25.00	60.00	15.06
35.00	75.00	11.44	25.00	75.00	15.58
35.00	90.00	11.52	25.00	90.00	15.85
35.00	105.00	11.71	25.00	105.00	15.79
35.00	120.00	11.93	25.00	120.00	15.49
35.00	135.00	12.04	25.00	135.00	15.03
35.00	150.00	11.55	25.00	150.00	14.44
35.00	165.00	10.60	25.00	165.00	13.76
35.00	180.00	9.49	25.00	180.00	13.07
35.00	195.00	8.97	25.00	195.00	12.43
35.00	210.00	7.65	25.00	210.00	11.81
35.00	225.00	6.12	25.00	225.00	10.98
35.00	240.00	5.21	25.00	240.00	9.74
35.00	255.00	4.25	25.00	255.00	7.89
35.00	270.00	3.19	25.00	270.00	6.08
35.00	285.00	2.89	25.00	285.00	5.44
35.00	300.00	3.58	25.00	300.00	6.56
35.00	315.00	4.98	25.00	315.00	9.65
35.00	330.00	6.80	25.00	330.00	11.47
35.00	345.00	8.70	25.00	345.00	12.46

LATITUDE	LONGITUDE	RIGIDITY (GeV/ec)	LATITUDE	LONGITUDE	RIGIDITY (GeV/ec)
20.00	0.00	14.11	10.00	0.00	14.73
20.00	15.00	14.62	10.00	15.00	15.26
20.00	30.00	15.09	10.00	30.00	15.80
20.00	45.00	15.57	10.00	45.00	16.34
20.00	60.00	16.12	10.00	60.00	16.94
20.00	75.00	16.63	10.00	75.00	17.44
20.00	90.00	16.87	10.00	90.00	17.67
20.00	105.00	16.75	10.00	105.00	17.56
20.00	120.00	16.37	10.00	120.00	17.18
20.00	135.00	15.83	10.00	135.00	16.65
20.00	150.00	15.20	10.00	150.00	16.10
20.00	165.00	14.55	10.00	165.00	15.61
20.00	180.00	13.93	10.00	180.00	15.16
20.00	195.00	13.40	10.00	195.00	14.75
20.00	210.00	12.91	10.00	210.00	14.39
20.00	225.00	12.33	10.00	225.00	14.00
20.00	240.00	11.47	10.00	240.00	13.44
20.00	255.00	9.69	10.00	255.00	12.55
20.00	270.00	7.82	10.00	270.00	11.50
20.00	285.00	6.84	10.00	285.00	11.07
20.00	300.00	8.65	10.00	300.00	12.16
20.00	315.00	11.45	10.00	315.00	13.09
20.00	330.00	12.76	10.00	330.00	13.76
20.00	345.00	13.54	10.00	345.00	14.25
15.00	0.00	14.61	5.00	0.00	14.50
15.00	15.00	15.14	5.00	15.00	14.99
15.00	30.00	15.65	5.00	30.00	15.52
15.00	45.00	16.17	5.00	45.00	16.10
15.00	60.00	16.74	5.00	60.00	16.71
15.00	75.00	17.25	5.00	75.00	17.22
15.00	90.00	17.47	5.00	90.00	17.47
15.00	105.00	17.34	5.00	105.00	17.42
15.00	120.00	16.93	5.00	120.00	17.11
15.00	135.00	16.37	5.00	135.00	16.66
15.00	150.00	15.76	5.00	150.00	16.21
15.00	165.00	15.17	5.00	165.00	15.83
15.00	180.00	14.63	5.00	180.00	15.49
15.00	195.00	14.16	5.00	195.00	15.15
15.00	210.00	13.76	5.00	210.00	14.82
15.00	225.00	13.30	5.00	225.00	14.47
15.00	240.00	12.62	5.00	240.00	14.03
15.00	255.00	11.27	5.00	255.00	13.41
15.00	270.00	9.49	5.00	270.00	12.67
15.00	285.00	8.46	5.00	285.00	12.40
15.00	300.00	10.71	5.00	300.00	12.78
15.00	315.00	12.52	5.00	315.00	13.36
15.00	330.00	13.43	5.00	330.00	13.80
15.00	345.00	14.07	5.00	345.00	14.11

LATITUDE	LONGITUDE	RIGIDITY (GeV/ec)	LATITUDE	LONGITUDE	RIGIDITY (GeV/ec)
0.00	0.00	13.94	-10.00	0.00	12.11
0.00	15.00	14.37	-10.00	15.00	12.31
0.00	30.00	14.87	-10.00	30.00	12.71
0.00	45.00	15.46	-10.00	45.00	13.29
0.00	60.00	16.10	-10.00	60.00	13.89
0.00	75.00	16.62	-10.00	75.00	14.35
0.00	90.00	16.90	-10.00	90.00	14.68
0.00	105.00	16.94	-10.00	105.00	14.90
0.00	120.00	16.73	-10.00	120.00	14.91
0.00	135.00	16.38	-10.00	135.00	14.80
0.00	150.00	16.05	-10.00	150.00	14.74
0.00	165.00	15.81	-10.00	165.00	14.84
0.00	180.00	15.59	-10.00	180.00	14.94
0.00	195.00	15.32	-10.00	195.00	14.90
0.00	210.00	15.03	-10.00	210.00	14.76
0.00	225.00	14.71	-10.00	225.00	14.55
0.00	240.00	14.33	-10.00	240.00	14.29
0.00	255.00	13.06	-10.00	255.00	13.94
0.00	270.00	13.32	-10.00	270.00	13.51
0.00	285.00	12.95	-10.00	285.00	13.10
0.00	300.00	13.05	-10.00	300.00	12.92
0.00	315.00	13.38	-10.00	315.00	12.82
0.00	330.00	13.58	-10.00	330.00	12.55
0.00	345.00	13.69	-10.00	345.00	12.20
-5.00	0.00	13.13	-15.00	0.00	10.75
-5.00	15.00	13.45	-15.00	15.00	10.91
-5.00	30.00	13.91	-15.00	30.00	11.23
-5.00	45.00	14.50	-15.00	45.00	11.69
-5.00	60.00	15.14	-15.00	60.00	12.18
-5.00	75.00	15.65	-15.00	75.00	12.70
-5.00	90.00	15.97	-15.00	90.00	13.00
-5.00	105.00	16.10	-15.00	105.00	13.25
-5.00	120.00	16.00	-15.00	120.00	13.25
-5.00	135.00	15.77	-15.00	135.00	13.32
-5.00	150.00	15.58	-15.00	150.00	13.48
-5.00	165.00	15.50	-15.00	165.00	13.78
-5.00	180.00	15.42	-15.00	180.00	14.09
-5.00	195.00	15.25	-15.00	195.00	14.24
-5.00	210.00	15.02	-15.00	210.00	14.24
-5.00	225.00	14.74	-15.00	225.00	14.15
-5.00	240.00	14.41	-15.00	240.00	13.97
-5.00	255.00	14.01	-15.00	255.00	13.69
-5.00	270.00	13.53	-15.00	270.00	13.30
-5.00	285.00	13.14	-15.00	285.00	12.89
-5.00	300.00	13.08	-15.00	300.00	12.59
-5.00	315.00	13.19	-15.00	315.00	12.31
-5.00	330.00	13.15	-15.00	330.00	11.76
-5.00	345.00	13.04	-15.00	345.00	11.15

LATITUDE	LONGITUDE	RIGIDITY (GeV/ec)	LATITUDE	LONGITUDE	RIGIDITY (GeV/ec)
-20.00	0.00	9.21	-30.00	0.00	6.36
-20.00	15.00	9.06	-30.00	15.00	6.02
-20.00	30.00	9.29	-30.00	30.00	5.86
-20.00	45.00	9.70	-30.00	45.00	5.79
-20.00	60.00	10.21	-30.00	60.00	5.42
-20.00	75.00	10.25	-30.00	75.00	5.23
-20.00	90.00	10.41	-30.00	90.00	5.10
-20.00	105.00	10.65	-30.00	105.00	5.16
-20.00	120.00	10.84	-30.00	120.00	5.19
-20.00	135.00	10.62	-30.00	135.00	5.39
-20.00	150.00	10.74	-30.00	150.00	5.89
-20.00	165.00	11.93	-30.00	165.00	6.58
-20.00	180.00	12.78	-30.00	180.00	7.99
-20.00	195.00	13.19	-30.00	195.00	9.45
-20.00	210.00	13.44	-30.00	210.00	9.43
-20.00	225.00	13.51	-30.00	225.00	10.64
-20.00	240.00	13.46	-30.00	240.00	11.85
-20.00	255.00	13.28	-30.00	255.00	12.00
-20.00	270.00	12.94	-30.00	270.00	11.88
-20.00	285.00	12.53	-30.00	285.00	11.43
-20.00	300.00	12.14	-30.00	300.00	10.75
-20.00	315.00	11.65	-30.00	315.00	9.83
-20.00	330.00	10.73	-30.00	330.00	8.39
-20.00	345.00	9.78	-30.00	345.00	7.09
-25.00	0.00	7.55	-35.00	0.00	5.24
-25.00	15.00	7.50	-35.00	15.00	4.59
-25.00	30.00	7.72	-35.00	30.00	4.45
-25.00	45.00	7.88	-35.00	45.00	4.31
-25.00	60.00	7.86	-35.00	60.00	4.07
-25.00	75.00	7.37	-35.00	75.00	3.72
-25.00	90.00	7.08	-35.00	90.00	3.35
-25.00	105.00	7.24	-35.00	105.00	3.32
-25.00	120.00	7.43	-35.00	120.00	3.37
-25.00	135.00	7.71	-35.00	135.00	3.65
-25.00	150.00	8.47	-35.00	150.00	4.10
-25.00	165.00	9.55	-35.00	165.00	4.90
-25.00	180.00	10.22	-35.00	180.00	5.65
-25.00	195.00	11.22	-35.00	195.00	6.54
-25.00	210.00	12.01	-35.00	210.00	7.88
-25.00	225.00	12.63	-35.00	225.00	9.11
-25.00	240.00	12.76	-35.00	240.00	9.58
-25.00	255.00	12.72	-35.00	255.00	11.12
-25.00	270.00	12.46	-35.00	270.00	11.16
-25.00	285.00	12.04	-35.00	285.00	10.67
-25.00	300.00	11.53	-35.00	300.00	9.90
-25.00	315.00	10.74	-35.00	315.00	8.72
-25.00	330.00	9.63	-35.00	330.00	7.16
-25.00	345.00	8.36	-35.00	345.00	6.18

LATITUDE	LONGITUDE	RIGIDITY (GeV/ec)	LATITUDE	LONGITUDE	RIGIDITY (GeV/ec)
-40.00	0.00	4.29	-50.00	0.00	2.87
-40.00	15.00	3.74	-50.00	15.00	2.37
-40.00	30.00	3.40	-50.00	30.00	1.95
-40.00	45.00	3.21	-50.00	45.00	1.60
-40.00	60.00	2.83	-50.00	60.00	1.27
-40.00	75.00	2.43	-50.00	75.00	0.94
-40.00	90.00	2.08	-50.00	90.00	0.66
-40.00	105.00	2.00	-50.00	105.00	0.54
-40.00	120.00	2.01	-50.00	120.00	0.53
-40.00	135.00	2.21	-50.00	135.00	0.60
-40.00	150.00	2.65	-50.00	150.00	0.84
-40.00	165.00	3.24	-50.00	165.00	1.15
-40.00	180.00	4.11	-50.00	180.00	1.63
-40.00	195.00	4.76	-50.00	195.00	2.24
-40.00	210.00	5.56	-50.00	210.00	2.94
-40.00	225.00	6.65	-50.00	225.00	3.76
-40.00	240.00	8.20	-50.00	240.00	4.48
-40.00	255.00	9.75	-50.00	255.00	5.57
-40.00	270.00	10.18	-50.00	270.00	7.02
-40.00	285.00	9.77	-50.00	285.00	7.57
-40.00	300.00	8.98	-50.00	300.00	6.98
-40.00	315.00	7.61	-50.00	315.00	5.68
-40.00	330.00	6.42	-50.00	330.00	4.51
-40.00	345.00	5.31	-50.00	345.00	3.50
-45.00	0.00	3.46	-55.00	0.00	2.23
-45.00	15.00	2.96	-55.00	15.00	1.79
-45.00	30.00	2.53	-55.00	30.00	1.42
-45.00	45.00	2.30	-55.00	45.00	1.12
-45.00	60.00	1.93	-55.00	60.00	0.87
-45.00	75.00	1.53	-55.00	75.00	0.53
-45.00	90.00	1.28	-55.00	90.00	0.34
-45.00	105.00	1.12	-55.00	105.00	0.23
-45.00	120.00	1.11	-55.00	120.00	0.21
-45.00	135.00	1.25	-55.00	135.00	0.26
-45.00	150.00	1.51	-55.00	150.00	0.38
-45.00	165.00	2.04	-55.00	165.00	0.59
-45.00	180.00	2.72	-55.00	180.00	0.90
-45.00	195.00	3.33	-55.00	195.00	1.38
-45.00	210.00	4.24	-55.00	210.00	1.88
-45.00	225.00	4.93	-55.00	225.00	2.64
-45.00	240.00	5.91	-55.00	240.00	3.38
-45.00	255.00	7.83	-55.00	255.00	4.20
-45.00	270.00	9.00	-55.00	270.00	4.96
-45.00	285.00	8.76	-55.00	285.00	5.19
-45.00	300.00	7.84	-55.00	300.00	5.02
-45.00	315.00	6.91	-55.00	315.00	4.45
-45.00	330.00	5.63	-55.00	330.00	3.67
-45.00	345.00	4.32	-55.00	345.00	2.93

LATITUDE	LONGITUDE	RIGIDITY (GeV/ec)	LATITUDE	LONGITUDE	RIGIDITY (GeV/ec)
-60.00	0.00	1.78	-70.00	0.00	0.89
-60.00	15.00	1.32	-70.00	15.00	0.64
-60.00	30.00	1.03	-70.00	30.00	0.47
-60.00	45.00	0.75	-70.00	45.00	0.31
-60.00	60.00	0.49	-70.00	60.00	0.18
-60.00	75.00	0.30	-70.00	75.00	0.08
-60.00	90.00	0.15	-70.00	90.00	0.00
-60.00	105.00	0.08	-70.00	105.00	0.00
-60.00	120.00	0.06	-70.00	120.00	0.00
-60.00	135.00	0.08	-70.00	135.00	0.00
-60.00	150.00	0.14	-70.00	150.00	0.00
-60.00	165.00	0.27	-70.00	165.00	0.03
-60.00	180.00	0.48	-70.00	180.00	0.10
-60.00	195.00	0.79	-70.00	195.00	0.22
-60.00	210.00	1.18	-70.00	210.00	0.41
-60.00	225.00	1.62	-70.00	225.00	0.64
-60.00	240.00	2.23	-70.00	240.00	0.96
-60.00	255.00	3.00	-70.00	255.00	1.28
-60.00	270.00	3.77	-70.00	270.00	1.58
-60.00	285.00	3.95	-70.00	285.00	1.75
-60.00	300.00	3.97	-70.00	300.00	1.80
-60.00	315.00	3.52	-70.00	315.00	1.67
-60.00	330.00	2.88	-70.00	330.00	1.39
-60.00	345.00	2.27	-70.00	345.00	1.14
-65.00	0.00	1.30	-75.00	0.00	0.59
-65.00	15.00	0.98	-75.00	15.00	0.43
-65.00	30.00	0.72	-75.00	30.00	0.30
-65.00	45.00	0.50	-75.00	45.00	0.19
-65.00	60.00	0.30	-75.00	60.00	0.10
-65.00	75.00	0.15	-75.00	75.00	0.04
-65.00	90.00	0.06	-75.00	90.00	0.00
-65.00	105.00	0.00	-75.00	105.00	0.00
-65.00	120.00	0.00	-75.00	120.00	0.00
-65.00	135.00	0.00	-75.00	135.00	0.00
-65.00	150.00	0.03	-75.00	150.00	0.00
-65.00	165.00	0.11	-75.00	165.00	0.00
-65.00	180.00	0.23	-75.00	180.00	0.05
-65.00	195.00	0.43	-75.00	195.00	0.12
-65.00	210.00	0.71	-75.00	210.00	0.23
-65.00	225.00	1.06	-75.00	225.00	0.36
-65.00	240.00	1.51	-75.00	240.00	0.54
-65.00	255.00	1.98	-75.00	255.00	0.72
-65.00	270.00	2.53	-75.00	270.00	0.91
-65.00	285.00	2.71	-75.00	285.00	1.02
-65.00	300.00	2.72	-75.00	300.00	1.03
-65.00	315.00	2.50	-75.00	315.00	1.05
-65.00	330.00	2.10	-75.00	330.00	0.88
-65.00	345.00	1.61	-75.00	345.00	0.76

LATITUDE	LONGITUDE	RIGIDITY (GeV/ec)
-80.00	0.00	0.37
-80.00	15.00	0.28
-80.00	30.00	0.19
-80.00	45.00	0.13
-80.00	60.00	0.07
-80.00	75.00	0.03
-80.00	90.00	0.00
-80.00	105.00	0.00
-80.00	120.00	0.00
-80.00	135.00	0.00
-80.00	150.00	0.00
-80.00	165.00	0.00
-80.00	180.00	0.03
-80.00	195.00	0.08
-80.00	210.00	0.13
-80.00	225.00	0.21
-80.00	240.00	0.30
-80.00	255.00	0.40
-80.00	270.00	0.48
-80.00	285.00	0.55
-80.00	300.00	0.56
-80.00	315.00	0.54
-80.00	330.00	0.49
-80.00	345.00	0.42

APPENDIX 7: SOURCE CODES OF THE CREME PROGRAMS

```
      PROGRAM STASS
C
C     THIS PROGRAM PREPARES ORBIT-AVERAGED TRAPPED PROTON DATA
C     FILES FOR THE LET PROGRAM.
C     THE TRAPPED PROTON DATA CAN BE OBTAINED
C     FROM REPORTS PUBLISHED BY THE NATIONAL SPACE SCIENCE DATA
C     CENTER AT GODDARD SPACE FLIGHT CENTER. THE
C     PROGRAM IS SET UP TO TAKE THE TABULAR DATA UNDER
C     'AVERAGED DIFFER. FLUX' IN THE 'COMPOSITE ORBIT
C     SPECTRUM' TABLE OF ONE OF THESE REPORTS.  CARE SHOULD BE
C     TAKEN TO BE SURE CONTRIBUTIONS FROM SOLAR FLARE PROTONS
C     HAVE NOT BEEN INCLUDED IN THIS TABLE.
C     THE DATA SHOULD BE ENTERED IN PAIRS OF POINTS (I.E. THE
C     PROTON ENERGY FOLLOWED BY THE CORRESPONDING FLUX).
C     THE ENERGY SHOULD BE IN MEV AND THE FLUX SHOULD BE IN
C     #/CM**2/SEC/KEV.  DATA BELOW 10 MEV NEED NOT BE ENTERED.
C     ENTER A PAIR OF ZERO VALUES TO CLOSE THE FILE AFTER ALL
C     THE DATA HAS BEEN ENTERED.  THIS FILE MAY BE EDITED
C     AFTERWARDS TO CORRECT ANY ERRORS IN THE DATA YOU ENTERED.
C
      CHARACTER*12 ALPHA
      WRITE(6,100)
  100 FORMAT(' ENTER THE NAME OF THE FILE TO CONTAIN THE PROTON DATA
     1:  ',$)
      READ(5,200)ALPHA
C
C     NOTE:  THIS FILE MUST BE RENAMED TO STASS.DAT BEFORE IT
C            CAN BE USED IN THE LET PROGRAM.
C
  200 FORMAT(A12)
      OPEN(UNIT=1,STATUS='NEW',FILE=ALPHA)
      WRITE(6,300)
  300 FORMAT(' ENTER THE DATA POINT PAIRS, STARTING WITH'/
     2 ' 10 MEV AND PROCEEDING MONOTONICALLY TO THE HIGHEST'/
     4 ' ENERGY.  THE PAIRS ARE TO BE TAKEN FROM THE COMPOSITE'/
     5 ' ORBIT SPECTRUM.  THE PAIRS ARE ENERGY LEVEL IN MEV, FOLLOWED'/
     6 ' BY THE AVERAGED DIFFER. FLUX IN #/CM**2/SEC/KEV.'/
     7 ' ENTER A PAIR OF ZERO VALUES WHEN YOU ARE DONE.')
      I=1
  6   CONTINUE
      WRITE(6,500)I
  500 FORMAT(' ENTER PAIR ',I2,':  ',$)
      ACCEPT *,E,F
      IF (E.LE.0.) GOTO 7
      WRITE(1,600)E,F
  600 FORMAT(1X,F6.1,1X,E10.3)
      I=I+1
      GOTO 6
  7   CONTINUE
      END
```

```
      PROGRAM GEOMAG
C     THIS PROGRAM CALCULATES THE 2 DAY ORBIT AVERAGE OF
C     THE GEOMAGNETIC TRANSMISSION FUNCTION FOR CIRCULAR ORBITS.
C     WHEN YOU RUN THIS PROGRAM, ALL INPUT
C     DATA WILL BE REQUESTED IN PROMPTS.  OUTPUT DATA TABULATED IN
C     INTERVALS OF .1 GV ARE STORED IN THE OUTPUT FILE GTRANS.DAT.
C     [EXCEPTION:  THE HIGHEST RIGIDITY VALUE WITH A ZERO
C     TRANSMISSION FUNCTION (I.E., A PARTICLE WITH THAT RIGITITY
C     CANNOT REACH THE SPACECRAFT AT ANY POINT ON THE SPACECRAFT'S
C     ORBIT) MAY BE INTERPOLATED TO GIVE A VALUE NOT DIVISIBLE BY
C     .1 GV.  THE RIGIDITIES WILL BE IN INCREASING ORDER IN ANY CASE.]
C     AN INPUT FILE CALLED "CUTOFF.DAT" CONTAINS THE TABULATION
C     OF WORLDWIDE VERTICAL GEOMAGNETIC CUTOFFS AT 20KM ALTITUDE,
C     TAKEN FROM M. A. SHEA AND D. F. SMART, REPORT NO.
C     AFCRL-TR-75-0185, HANSCOM AFB, MASS., 1975.
C     AZ IS THE AZMUTH ANGLE OF THE PARTICLE WRT THE SPACECRAFT.
C     ZE IS THE ZENITH ANGLE OF THE PARTICLE WRT THE SPACECRAFT.
C     THESE ANGLES ARE BOTH IN DEGREES AND ARE DATAED IN AS ZERO.
C     THEY CAN BE RESET TO ANY OTHER ARRIVAL DIRECTION.
C
      DIMENSION MAT(200),CUTOFF(33,24),T(201),CF(201)
      DATA (MAT(J),J=1,200)/200*0/
      DATA AZ/0./,ZE/0./,AZG/0./,ZEG/0./
      OPEN(UNIT=15,READONLY,SHARED,STATUS='OLD',FILE='CUTOFF.DAT')
      OPEN(UNIT=16,FILE='GTRANS.DAT',STATUS='NEW')
C
C     ASK FOR INPUT.
C     IS THE SHADOW OF THE EARTH ON THE SPACECRAFT
C     TO BE ACCOUNTED FOR IN THIS CALCULATION?
C
      WRITE (6,411)
      ACCEPT *, ISHADOW
C
C     IS THE MAGNETOSPHERE QUIET OR STORMY?
C
      WRITE (6,412)
      ACCEPT *, ISTORM
C     ********************************************************************
      CALL ORBIT(1,PERIOD,ZLON,ZLAT,RADIUS)
      WRITE (6,1) PERIOD
 1    FORMAT(' THE ORBITAL PERIOD IS ',E12.5,' SECONDS.')
C     ********************************************************************
C     READ IN THE TABLE OF WORLD WIDE VERTICAL
C     GEOMAGNETIC CUTOFFS AT 20KM ALTITUDE.
C     THESE DATA ARE TABULATED EVERY 5 DEGREES IN LATITUDE
C     AND EVERY 15 DEGREES IN LONGITUDE.
C     THEY ARE TAKEN FROM M. A. SHEA AND D. F. SMART, REPORT NO.
C     AFCRL-TR-75-0185, HANSCOM AFB, MASS, 1975.
C
      DO 20 I=1,33
      II=34-I
```

```
      DO 20 J=1,24
      READ(15,405) CUTOFF(II,J)
C     THIS ACCOUNTS FOR GEOMAGNETIC CUTOFF SUPRESSION DURING
C     LARGE MAGNETIC STORMS (FOLLOWING ADAMS ET AL., 1981).
C
      IF(ISTORM.EQ.1) CUTOFF(II,J)=CUTOFF(II,J)*(1.-.54*EXP(
     1 -CUTOFF(II,J)/2.9))
 20   CONTINUE
C
C     AVERAGE THE CUTOFF AROUND THE 80 DEGREE LATITUDE LINES,
C     NORTH AND SOUTH, TO APPROXIMATE THE CUTOFFS AT 90 DEGREES.
C
      CN=0.
      CS=0.
      DO 30 J=1,24
      CN=CN+CUTOFF(33,J)
 30   CS=CS+CUTOFF(1,J)
      CN=CN/24.
      CS=CS/24.
C
C     COMPUTE THE TOTAL NUMBER OF STEPS IN TWO DAYS IF WE MAKE
C     200 STEPS PER ORBIT.
C
      JMAX=INT(2.*200.*86400./PERIOD + 1.5)
C
C     COMPUTE THE STEP SIZE IN SECONDS.
C
      STEP=PERIOD/200.
C
C     COMPUTE THE VERTICAL CUTOFF AT THE SPACECRAFT
C     POSITION FOR EVERY TIME STEP.
C
      DO 50 J=1,JMAX
      TIME=FLOAT(J-1)*STEP
      CALL ORBIT(2,TIME,ZLON,ZLAT,ALT)
C
C     COMPUTE THE TABULAR POSITION OF THE VERTICAL CUTOFF.
C
      ZI=ZLAT/5.+17.
      ZJ=ZLON/15.+1.
      ILO=INT(ZI)
      IUP=ILO+1
      JLO=INT(ZJ)
      JUP=JLO+1
      IF (JUP.EQ.25) JUP=1
C
C     INTERPOLATE THE VERTICAL CUTOFF TO THE EXACT LOCATION
C     OF THE SPACECRAFT USING STORMER THEORY.
C
      IF(ABS(ZLAT).GE.80.) GO TO 100
      DI=ZI-FLOAT(ILO)
      DJ=ZJ-FLOAT(JLO)
```

```
      XORB=(6371.2+ALT)/6371.2
      RGRD= 6391.2/6371.2
      ZLONLO=(JLO-1)*15.
      ZLONUP=ZLONLO+15.
      ZLATLO=ILO*5.-85.
      ZLATUP=ZLATLO+5.
      SC=STORMER(ZLAT,ZLON,XORB,AZ,ZE)
      SCLL=STORMER(ZLATLO,ZLONLO,RGRD,AZG,ZEG)
      SCUL=STORMER(ZLATUP,ZLONLO,RGRD,AZG,ZEG)
      SCLU=STORMER(ZLATLO,ZLONUP,RGRD,AZG,ZEG)
      SCUU=STORMER(ZLATUP,ZLONUP,RGRD,AZG,ZEG)
      Y1=SC*CUTOFF(ILO,JLO)/SCLL
     Y2= SC*CUTOFF(IUP,JLO)/SCUL
     Y3=  SC*CUTOFF(ILO,JUP)/SCLU
     Y4= SC*CUTOFF(IUP,JUP)/SCUU
      C=(1.-DI)*(1.-DJ)*Y1+(1.-DI)*DJ*Y3+DI*(1.-DJ)*Y2+DI*DJ*Y4
      GO TO 200
C
C     FOR ABS(LATITUDE).GT.80 USE THE CUTOFFS AT THE POLE INSTEAD OF
C     THE CUTOFFS AT FOUR NEARBY LOCATIONS.
C
 100  CONTINUE
      IF(ZLAT.LE.-80.)GO TO 110
      SC=STORMER(90.,0.,XORB,AZ,ZE)
      SCX=STORMER(90.,0.,RGRD,AZG,ZEG)
      C=SC*CN/SCX
      GO TO 200
 110  CONTINUE
      SC=STORMER(-90.,0.,XORB,AZ,ZE)
      SCX=STORMER(-90.,0.,RGRD,AZG,ZEG)
      C=SC*CS/SCX
 200  CONTINUE
C
C     HISTOGRAM THE CUTOFFS.
C
      IDEX=INT(C*10.)+1
      MAT(IDEX)=MAT(IDEX)+1
C*****************************************************************************
C     TO PRINT OUT THE LONGITUDE, LATITUDE, AND CUTOFF AT EACH
C     POINT ARROUND THE SPACECRAFT'S ORBIT, JUST ENABLE THE FOLLOWING
C     STATEMENT BY REMOVING THE COMMENT C.
C*****************************************************************************
C     WRITE(6,435)ZLON,ZLAT,C
 50   CONTINUE
      CMAT=0.
C
C     SAVE THE THRESHOLD.
C
      JSAV=0
      DO 300 J=1,200
C
C     CONVERT THE HISTOGRAM TO TRANSMISSION.
```

```
C
      CMAT=FLOAT(MAT(J))/FLOAT(JMAX)+CMAT
      IF((JSAV.EQ.0).AND.(CMAT.GT.0)) JSAV=J+1
      CF(J+1)=FLOAT(J)/10.
 300  T(J+1)=CMAT
      CF(1)=0.0
      T(1)=0.0
C     INTERPOLATE THE HIGHEST ZERO TRANSMISSION VALUE TO BE
C     JUST AT THE CUTOFF THRESHOLD.
C
      DT=T(JSAV+1)-T(JSAV)
      IF(DT.EQ.0.) GO TO 301
      CFT=CF(JSAV)-T(JSAV)*(CF(JSAV+1)-CF(JSAV))/DT
      CF(JSAV-1)=AMAX1(CFT,CF(JSAV-1))
 301  CONTINUE
C
C     THIS IS A CORRECTION FOR THE EARTH'S SHADOW ON THE SPACECRAFT
C     ACCORDING TO SIMPLE GEOMETRICAL OPTICS.
C
      IF(ISHADOW.NE.1) GO TO 390
      DO 380 J=1,200
      T(J)=T(J)*(1.-0.5*(1.-((6371.2+ALT)**2.-(6371.2)**2.)**.5/
     1 (6371.2+ALT)))
 380  CONTINUE
 390  DO 400 J=1,200
 400  WRITE(16,410)CF(J),T(J)
 405  FORMAT(17X,F6.2)
 410  FORMAT(5X,F6.3,5X,F8.6)
 411  FORMAT(1X,'DO YOU WANT TO INCLUDE THE EFFECT OF THE SHADOW',/,
     1 ' OF THE EARTH?  (1 FOR YES; 0 FOR NO):  ',$)
 412  FORMAT(1X,'ENTER THE MAGNETIC WEATHER CONTITION:  1 FOR STORMY;
     1 0 FOR QUIET:  ',$)
 435  FORMAT(' LONGITUDE = ',F6.2,', LATITUDE = ',F5.2,' CUTOFF = ',
     1 F6.3,'.')
      END
```

```
      FUNCTION STORMER(GCLATD,GCLOND,RGC,AZ,ZE)
C     WE DID NOT WRITE THIS SUBROUTINE.  WE HAVE MADE NO CHANGES IN
C     IT IN 1984. C

      COMMON/KARL/RED,EDLAT,AZM,ZEM,GAMMA

C     THIS FUNCTION TRANSFORMS A GEOGRAPHIC LOCATION AND ARRIVAL
C     DIRECTION INTO OFFSET DIPOLE COORDINATES, THEN COMPUTES THE
C     STORMER CUTOFF IN GV AND RETURNS THE RESULT. THE OFFSET DIPOLE
C     COORDINATES ARE AVAILABLE IN THE COMMON BLOCK /KARL/.


C     GCLATD IS GEOCENTRIC LATITUDE  IN DEGREES
C     GCLONG IS GEOCENTRIC LONGITUDE IN DEGREES
C     RGC    IS RADIAL DISTANCE FROM GEOCENTER IN EARTH RADII
C     AZ     IS GEOGRAPHIC AZIMUTH
C     ZE     IS GEOGRAPHIC ZENITH
C     RED    IS RADIAL DISTANCE FROM OFFSET DIPOLE POSITION IN
                                          EARTH RADII
C     EDLAT IS THE GEOMAGNETIC LATITUDE IN OFFSET DIPOLE COORDINATES
C        AZM    IS GEOMAGNETIC AZIMUTH IN OFFSET DIPOLE COORDINATES
C        ZEM    IS GEOMAGNETIC ZENITH  IN OFFSET DIPOLE COORDINATES
C        GAMMA  IS GAMMA ANGLE MEASURED FROM MAGNETIC EAST
C
      DATA JDATA,NOPT/2*0/,PI,RAD,PIO2,XEDFGC,YEDFGC,ZEDFGC,CP,SP
     1 ,ST,CPCT,CPST,SPCT,SPST,XGMED,YGMED,ZGMED/16*-8000./
      DATA SMALL/1.0E-35/
       DPEC(U)=SIGN(1./SNGL(DSQRT(1D0+DBLE((U/ZEDRTL)**2))),ZRTL*ZEDRTL)
      IF(JDATA.EQ.77)   GO TO 10
        PI = ACOS(-1.0)
        RAD = 180.0/PI
        PIO2 = PI/2.0
        TWOPI = PI*2.0
     DATA ERAD,THETAD,PHID,R1KM,TH1DEG,PH1DEG/6371.2,
     1 11.4354,-290.2392,450.2586,72.8278,148.7753/
      NOPT = 0
      SQRT3 = SQRT(3.0)
C         ENTER GEOMAGNETIC DATA,     IGRF  1975
C           SEE JGR, 81, 5163, 1976
C                                    DT IS NUMBER OF YEARS SINCE 1975
      DT = 5.0
      G01 = -30186.0  +  25.6*DT
      G02 =  -1898.0  -  24.9*DT
      G11 =  -2036.0  +  10.0*DT
      G12 =   2997.0  +   0.7*DT
      H11 =   5735.0  -  10.2*DT
      H12 =  -2124.0  -   3.0*DT
      G22 =   1551.0  +   4.3*DT
      H22 =    -37.0  -  18.9*DT
      IF(NOPT.EQ.1)PRINT 1000, G01, G02, G11, G12, G22, H11, H12, H22
C       COMPUTE POSITION OF OFFSET DIPOLE
```

```
      HO = SQRT( G01*G01+G11*G11+H11*H11)
      HOSQ = HO*HO
      EL0 = 2.0*G01*G02+(G11*G12+H11*H12)*SQRT3
      EL1 = -G11*G02+(G01*G12+G11*G22+H11*H22)*SQRT3
      EL2 = -H11*G02+(G01*H12-H11*G22+G11*H22)*SQRT3
C      E = (EL0*G01+EL1*G11+EL2*H11)*4.0*HOSQ
      E = (EL0*G01+EL1*G11+EL2*H11)/(4.0*HOSQ)
      IF(NOPT.EQ.1)  PRINT 1011, EL0, EL1, EL2, E, HO
 1011 FORMAT(1H , 8E15.5)
C      XEDFGC = ERAD*(EL1-G11*E)/(3.0*HOSQ)
      XEDFGC =      (EL1-G11*E)/(3.0*HOSQ)
C      YEDFGC = ERAD*(EL2-H11*E)/(3.0*HOSQ)
      YEDFGC =      (EL2-H11*E)/(3.0*HOSQ)
C      ZEDFGC = ERAD*(EL0-G01*E)/(3.0*HOSQ)
      ZEDFGC =      (EL0-G01*E)/(3.0*HOSQ)
      REDFGC = SQRT(XEDFGC*XEDFGC+YEDFGC*YEDFGC+ZEDFGC*ZEDFGC)
      IF(NOPT.EQ.1)PRINT 3001, XEDFGC, YEDFGC, ZEDFGC, REDFGC
 3001 FORMAT (1H , 4F10.4,       3X, 'XEDFGC, YEDFGC, ZEDFGC, REDFGC')
 1000 FORMAT (1H , 10F13.5)
 1010 FORMAT(1H0, 8F15.5/1H ,8F15.5)
      THETA = THETAD/RAD
      PHI = PHID/RAD
      CP = COS(PHI)
      SP = SIN(PHI)
      ST = SIN(THETA)
      CT = COS(THETA)
      CPCT   = CP*CT
      CPST   = CP*ST
      SPCT   = SP*CT
      SPST   = SP*ST
      R1ER = R1KM/ERAD
      TH1RAD = TH1DEG/RAD
      PH1RAD = PH1DEG/RAD
      IF(NOPT.EQ.1)PRINT 1000,R1KM,TH1DEG,PH1DEG,R1ER,TH1RAD,PH1RAD
      XGMED = XEDFGC*CPCT -YEDFGC*SPCT -ZEDFGC*ST
      YGMED = XEDFGC*SP   +YEDFGC*CP
      ZGMED = XEDFGC*CPST -YEDFGC*SPST +ZEDFGC*CT
      IF(NOPT.EQ.1)PRINT 3002, XGMED, YGMED, ZGMED
 3002 FORMAT(1H , 3F10.4, 13X, 'XGMED, YGMED, ZGMED')
      IF(NOPT.EQ.1)PRINT 1010, CP, SP, CT, ST, CPCT, CPST, SPCT, SPST
      JDATA = 77
   10 CONTINUE
C        ITERATE TO FIND COORDINATES OF OFFSET NORTH DIPOLE AT ANY
C       LATITUDE
C      FIRST GUESS FIND OFFSET NORTH DIPOLE AT DISTANCE RGC
      ZDEDNP = RGC
  100 XODNP =  XGMED*CPCT + YGMED*SP + ZDEDNP*CPST
      YODNP = -XGMED*SPCT + YGMED*CP - ZDEDNP*SPST
      ZODNP = -XGMED*SP              + ZDEDNP*CT
      DODNP = SQRT(XODNP*XODNP + YODNP*YODNP + ZODNP*ZODNP)
      DIFLA = DODNP - RGC
      IF(ABS(DIFLA) - 1.0E-5)  120, 120, 110
```

```
  110  ZDEDNP = ZDEDNP - DIFLA
 4001  FORMAT (1H , 5X,'ODC 0, 0, 'F7.5, ' = GC X, Y, Z  OF'3F8.5,
     1 '   DODNP ='F9.5,'   DIF OF 'F9.6, '  AT LOND LAT'F10.4, F8.4)
       GO TO 100
  120  CONTINUE
       PHINOF = ATAN2(YODNP,XODNP)*RAD
       IF(PHINOF.LT.0.0)   PHINOF = PHINOF + 360.0
       TNOF = -ACOS(ZODNP/DODNP)*RAD + 90.0
       IF(NOPT.EQ.1)PRINT 4001,ZDEDNP,XODNP,YODNP,ZODNP,DODNP,DIFLA,
     1 PHINOF,TNOF
       SGCLATD = SIN(GCLATD/RAD)
       CGCLATD = COS(GCLATD/RAD)
       SGCLOND = SIN(GCLOND/RAD)
       CGCLOND = COS(GCLOND/RAD)
C         GET GEOCENTRIC X Y Z  COORDINATES
       XGC = RGC*CGCLATD*CGCLOND
       YGC = RGC*CGCLATD*SGCLOND
       ZGC = RGC*SGCLATD
       GCT = (90.0 - GCLATD)/RAD
       SGCT = SIN(GCT)
       CGCT = COS(GCT)
C         FIND X Y Z IN LOCAL COORDINATES OF X=0, Y=0, Z
C                  THE LOCAL COORDINATE Z AXIS PASSES THRU P
C                  THE LOCAL COORDINATE X,Z PLANE CONTAINS P
       GCROT = ATAN2(YGC,XGC)
       IF(NOPT.EQ.1)PRINT 2001, XGC, YGC, ZGC, GCROT
 2001  FORMAT(1H , 4F10.4,          3X, 'XGC, YGC, ZGC, GCROT')
       SGCROT = SIN(GCROT)
       CGCROT = COS(GCROT)
       XRL =  XGC*CGCROT*CGCT + YGC*SGCROT*CGCT - ZGC*SGCT
       YRL = -XGC*SGCROT      + YGC*CGCROT
       ZRL =  XGC*CGCROT*SGCT + YGC*SGCROT*SGCT + ZGC*CGCT
 2002  FORMAT(1H , 3F10.4,         13X, 'XRL, YRL, ZRL')
       IF(NOPT.EQ.1)PRINT 2002, XRL, YRL, ZRL
C        DETERMINE LOCATION OF OFFSET DIPOLE CENTER IN THESE SAME
C                                 ROTATED LOCAL COORDINATES
       XEDRL =  XEDFGC*CGCROT*CGCT + YEDFGC*SGCROT*CGCT - ZEDFGC*SGCT
       YEDRL = -XEDFGC*SGCROT      + YEDFGC*CGCROT
       ZEDRL =  XEDFGC*CGCROT*SGCT + YEDFGC*SGCROT*SGCT + ZEDFGC*CGCT
       IF(NOPT.EQ.1)PRINT 3003, XEDRL, YEDRL, ZEDRL
 3003  FORMAT (1H , 3F10.4, 13X, 'XEDRLM YEDRL, ZEDRL')
       XEDRTL = XEDRL
       YEDRTL = YEDRL
       ZEDRTL = ZEDRL - ZRL
       IF(NOPT.EQ.1)PRINT 2303, XEDRTL, YEDRTL, ZEDRTL
 2303  FORMAT (1H , 3F10.4,  13X, 'XEDRTL, YEDRTK, ZEDRTL')
C         TRANSLATE TO LOCAL COORDINATE SYSTEM WITH ORIGIN AT SURFACE
       XRTL = XRL
       YRTL = YRL
       ZRTL =-ZRL
       XEDP = XRTL + XEDRL
       YEDP = YRTL + YEDRL
```

```
      ZEDP = ZRTL + ZEDRL
      RED = SQRT(XEDP*XEDP+YEDP*YEDP+ZEDP*ZEDP)
 2302 FORMAT (1H , 3F10.4,  13X, 'XRTL, YRTL, ZRTL')
      IF(NOPT.EQ.1)PRINT 2302,  XRTL, YRTL, ZRTL
C                               EARTHS SURFACE AT A SPECIFIED ALTITUDE
C       POSITION OF OFFSET NORTH DIPOLE  IN LOCAL COORDINATE SYSTEM
      XODNPR=   XODNP*CGCROT*CGCT +  YODNP*SGCROT*CGCT -  ZODNP*SGCT
      YODNPR= -XODNP*SGCROT       +  YODNP*CGCROT
      ZODNPR=   XODNP*CGCROT*SGCT +  YODNP*SGCROT*SGCT +  ZODNP*CGCT
      XODNPT = XODNPR
      YODNPT = YODNPR
      ZODNPT = ZODNPR - ZRL
      IF(NOPT.EQ.1)PRINT 1103, XODNPT, YODNPT, ZODNPT
 1103 FORMAT(1H ,10X,'XODNPT ='F10.4,2X,'YODNPT ='F10.4,2X,'ZODNPT ='
     1 F10.4,3X, 'OFFSET N DIPOLE IN LQCAL COORDINATES')
      ROTM =  ATAN2(YODNPT, XODNPT) + PI
C                FIND ANGLE FROM GEOGRAPHIC NORTH
C                NEGATIVE - ROTATION FROM GEOGRAPHIC NP CLOCKWISE
C                POSITIVE - ROTATION FROM GEOGRAPHIC NP CCW
      SROTM = SIN(ROTM)
      CROTM = COS(ROTM)
      ROTMD = ROTM*RAD
 2327 FORMAT (1H ,  F15.5, 3X, ' ROTM IN DEGREES MEASURED    CCW SO -X
     1 WILL POINT TOWARD OFFSET NORTH DIPOLE AXIS')
      IF(NOPT.EQ.1)PRINT 2327, ROTMD
C       FIND COMPONENTS OF UNIT VECTOR AT ARBITARY AZIMUTH AND ZENITH
      PLAZ = -AZ/RAD + PI
      TLZE = ZE/RAD
      SPLAZ = SIN(PLAZ)
      CPLAZ = COS(PLAZ)
      STLZE = SIN(TLZE)
      CTLZE = COS(TLZE)
      XLD = STLZE*CPLAZ
      YLD = STLZE*SPLAZ
      ZLD = CTLZE
      IF(NOPT.EQ.1)PRINT 2005, XLD, YLD, ZLD, AZ, ZE
 2005 FORMAT (1H , 5F10.4, 3X, 'UNIT VECTOR COMPOENTS AT AZ & ZE')
C
C        FIND COMPONENTS OF UNIT VECTOR IN DIPOLE RADIAL COORDINATES
C
C       ROTATE AROUND Y AXIS SO -Z AXIS PASSES THROUGH XED, 0, ZED
C       NEW VECTOR IS VA = ZRTL + ZEDRTK + XEDRTL
C       ANGLE BETWEEN VECTOR FROM POINT LOCAL ORIGIN TO GEOCENTER
C        AND VECTOR FROM POINT LOCAL ORIGIN TO XED, 0, ZED
C*************************************************************************
C       JIM LANGWORTHY'S FIX
C*************************************************************************
       CA=DPEC(XEDRTL)
C       CA = ZRTL*ZEDRTL/(ABS(ZRTL)*SQRT(ZEDRTL*ZEDRTL + XEDRTL*XEDRTL))
      A = ACOS(CA)
      IF(XEDRTL.GT.0.0)   A = -A
      SA = SIN(A)
```

```
      ADEG = A*RAD
      IF(NOPT.EQ.1)PRINT 1000, CA, A, SA, ADEG
      XLP = XLD*CA +     ZLD*SA
      YLP =         YLD
      ZLP =-XLD*SA +     ZLD*CA
      IF(NOPT.EQ.1)PRINT 5001, XLP, YLP, ZLP
 5001 FORMAT(1H , 3F10.4, 13X,'XLP,  YLP,  ZLP  ')
C       ROTATE AROUND X PRIME AXIS SO -Z PASSES THROUGH XED, YED, ZED
       CB=DPEC(YEDRTL)
C      CB = ZRTL*ZEDRTL/(ABS(ZRTL)*SQRT(ZEDRTL*ZEDRTL + YEDRTL*YEDRTL))
      B = ACOS(CB)
      IF(YEDRTL.GT.0.0)   B = -B
      SB = SIN(B)
      BDEG = B*RAD
      IF(NOPT.EQ.1)PRINT 1000, CB, B, SB, BDEG
      XLPP = XLP
      YLPP = YLP*CB + ZLP*SB
      ZLPP =-YLP*SB + ZLP*CB
      IF(NOPT.EQ.1)PRINT 5002, XLPP, YLPP, ZLPP
 5002 FORMAT(1H , 3F10.4, 13X,'XLPP, YLPP, ZLPP ')
C       ROTATE AROUND ZPP AXIS SO -X AXIS PASSES THROUGH NORTH
C                                          OFFSET DIPOLE AXIS
      ZLDM = ZLPP
      XLDM = XLPP*CROTM + YLPP*SROTM
      XLDM = XLPP*CROTM  -YLPP*SROTM
      YLDM =-XLPP*SROTM + YLPP*CROTM
      YLDM = XLPP*SROTM + YLPP*CROTM
      IF(NOPT.EQ.1)PRINT 1101, XLD, YLD, ZLD, XLDM, YLDM, ZLDM
 1101 FORMAT (1H , 'UNIT VECTOR IN LOCAL COORDINATES ', 3F8.5,5X,
     1 'UNIT VECTOR IN LOCAL MAGNETIC COORDINATES', 3F10.5)
C        FIND AZUMITH ANGLE OF UNIT VECTOR IN LOCAL DIPOLAR RADIAL COOR
      IF((ABS(YLDM).GT.SMALL).OR.(ABS(XLDM).GT.SMALL)) GO TO 1102
      PAZM=0.0
      GO TO 1104
 1102 PAZM = ATAN2(YLDM,XLDM)
 1104 AZM = (PI - PAZM)*RAD
      IF(AZM.GT.360.0)  AZM = AZM - 360.0
      ZEM = ACOS(ZLDM)*RAD
C        FIND GAMMA ANGLE
      GAMMA = ACOS(YLDM)*RAD
C      TRANSFORM TO OFFSET DIPOLE COORDINATES
       XED1=XGC-XEDFGC
       YED1=YGC-YEDFGC
       ZED1=ZGC-ZEDFGC
C      FIND THE Z COORDINATE IN OFFSET DIPOLE COORDINATES
       ZED2=XED1*CPST-YED1*SPST+ZED1*CT
C      FIND THE GEOMAGNETIC LATITUDE
       EDLAT=RAD*(PIO2-ACOS(ZED2/RED))
       COSLDA=COS(EDLAT/RAD)
     STORMER=60.*COSLDA**4./(RED*RED*(1.+SQRT(1.-COSLDA**3.*YLDM))**2)
      RETURN
      END
```

```
      SUBROUTINE ORBIT(N,TIME,ZLON,ZLAT,RADIUS)
C     ******************************************************************
C     THIS SUBROUTINE ACCEPTS INPUT CONCERNING SATELLITE
C     ORBITS AND CALCULATES THEIR GEOGRAPHICAL LOCATION.
C     N=0:   ACCEPT DATA ON ORBIT (FAST MODE).
C     N=1:   ACCEPT DATA ON ORBIT (COMPLETE MODE).
C     N=2:   CALCULATE ORBIT AS A FUNCTION OF TIME.
C     CLEARLY DATA MUST BE INPUT BEFORE COMPUTATIONS.
C     ON DATA INPUT, TIME RETURNS THE ORBITAL PERIOD.
C     DURING ORBIT CALCULATIONS, TIME IS AN INPUT VARIABLE.
C     ******************************************************************
      DATA PI,ALTA,ALTP,RE,E,A1,A2,A3,XI,W1,RMAJ,W2,FACT
     1,THO,PHO,PSI,XIO /17*-8000./
C
C     THESE VARIABLES HAVE BEEN DATAED IN HERE TO FORCE THE COMPUTER
C     TO CREATE STORAGE LOCATIONS FOR THEM BETWEEN CALLS OF THIS
C     SUBROUTINE.  THE DATAED-IN VALUES ARE NEVER USED BY THE PROGRAM.
C
      PI=355./113.
      IF (N.EQ.2) GO TO 1000
C     ******************************************************************
C     ACCEPT ORBITAL DATA.
C     ******************************************************************
C     ALTA=ORBITAL ALTITUDE AT APOGEE (KILOMETERS).
C     ALTP=ORBITAL ALTITUDE AT PERIGEE (KILOMETERS).
C     RE=RADIUS OF EARTH (KILOMETERS).
C     E=ORBIT ECCENTRICITY.
C     A1=ORBITAL INCLINATION (DEGREES).
C     A2=INITIAL LONGITUDE OF ASCENDING NODE (DEGREES).
C     A3=INITIAL DISPLACEMENT FROM ASCENDING NODE (DEGREES).
C     XI=DISPLACEMENT OF PERIGEE FROM ASCENDING NODE (DEGREES).
C
C     WHAT IS THE ALTITUEDE AT APOGEE?
C
      WRITE(6,420)
      ACCEPT *, ALTA
C
C     WHAT IS THE ALTITUDE AT PERIGEE?
C
      WRITE(6,400)
      ACCEPT *, ALTP
      RE=6371.2
      E=(ALTA-ALTP)/(ALTA+ALTP+2.*RE)
      IF (E.LT..00001) E=0.
C
C     WHAT IS THE ORBITAL INCLINATION?
C
      WRITE(6,405)
      ACCEPT *, A1
      A2=0.
      A3=0.
```

```
      XI=0.
      IF (N.EQ.0) GO TO 100

C     WHAT IS THE INITIAL LONGITUDE OF THE ASCENDING NODE?
C
      WRITE(6,410)
      ACCEPT *, A2
C
C     WHAT IS THE INITIAL DISPLACEMENT FROM THE ASCENDING NODE?
C
      WRITE(6,415)
      ACCEPT *, A3
      IF (E.EQ.0.) GOTO 100
C
C     WHAT IS THE DISPLACEMENT OF THE PERIGEE FROM THE ASCENDING NODE?
C
        WRITE(6,425)
        ACCEPT *, XI
 100  CONTINUE
C
C     W1=ANGULAR VELOCITY OF EARTH (RADIANS/SEC).
C     RMAJ=SEMI-MAJOR AXIS (KILOMETERS).
C     W2=MEAN ORBITAL ANGULAR VELOCITY (RADIANS/SECOND).
C     TIME=ORBITAL PERIOD (SECONDS).
C     FACT=A USEFUL FACTOR.
C
      W1=7.27E-5
      RMAJ=(ALTP+RE)/(1.-E)
      W2=1.24E-3*(RE/RMAJ)**1.5
      TIME=2.*PI/W2
      FACT=SQRT((1.+E)/(1.-E))
C
C     DEFINE MORE USEFUL ANGLES.
C
      THO=PI*A1/180.
      PHO=PI*(A2-90.)/180.
      PSI=PI*A3/180.
      XIO=PI*XI/180.
C
C     FORMAT STATEMENTS.
C
 400  FORMAT(1X,'ENTER ALTITUDE AT PERIGEE (KILOMETERS):  '$)
 405  FORMAT(1X,'ENTER ORBITAL INCLINATION (DEGREES):  '$)
 410  FORMAT(1X,'ENTER INITIAL LONGITUDE OF ASCENDING NODE',
     1  ' (DEGREES):  '$)
 415  FORMAT(1X,'ENTER INITIAL DISPLACEMENT FROM ASCENDING',
     1  ' NODE (DEGREES):  '$)
 420  FORMAT(1X,'ENTER ALTITUDE AT APOGEE (KILOMETERS):  '$)
 425  FORMAT(1X,'ENTER DISPLACEMENT OF PERIGEE FROM',
     1  ' ASCENDING NODE (DEGREES):  '$)
      RETURN
 1000 CONTINUE
```

```
C
C       COMPUTE SATELLITE POSITION.
C
C       QM=MEAN ANOMALY.
C
        IF (E.NE.0.) GOTO 1009
          QM=W2*TIME+PSI
        GOTO 1010
 1009   CONTINUE
          YSS=(PSI-XIO)/2.
          QE0=2.*ATAN2(SIN(YSS),FACT*COS(YSS))
          QM0=QE0-E*SIN(QE0)
          QM=W2*TIME-QM0
 1010   CONTINUE
C
C       QE=ECCENTRIC ANOMALY.
C
        QE=QM
        DEL=1.
 1014   CONTINUE
          QTEMP=QE
          QE=QM+E*SIN(QE)
          DEL=QE-QTEMP
        IF (ABS(DEL).GT..0001) GOTO 1014
C
C       QT=TRUE ANOMALY.
C
        IF (E.NE.0.) GOTO 1019
          QT=QE
        GOTO 1020
 1019   CONTINUE
          QECYC=INT(QE/2./PI)
          QERED=QE-2.*PI*QECYC
          AA1=FACT*SIN(QERED/2.)
          AA2=COS(QERED/2.)
          QTRED=2.*ATAN2(AA1,AA2)
          IF (QTRED.LT.0.) QTRED=QTRED+2.*PI
          QT=QTRED+2.*PI*QECYC+XIO
C
C       NOTE:  ANOMALY COMPUTATIONS ARE DONE FROM PERIGEE
C       WHILE ORBIT COMPUTATIONS BELOW ARE DONE FROM THE
C       ASCENDING NODE.  THE FACTOR OF XIO CORRECTS THIS.
C
 1020   CONTINUE
C
C       ZLAT=LATITUDE.
C
        R1=SIN(THO)*SIN(QT)
        THP=ACOS(R1)
        ZLAT=90.-180.*THP/PI
C
C       ZLON=LONGITUDE.
```

```
C
      RP=.5*(PI/2.+THO)
      RM=.5*(PI/2.-THO)
      RF=.5*(PI/2.-QT)
      IF (SIN(RF).NE.0.) GOTO 1029
        PHP=PI+PHO-W1*TIME
      GOTO 1030
 1029 CONTINUE
        S1=SIN(RM)*COS(RF)/SIN(RP)/SIN(RF)
        S2=COS(RM)*COS(RF)/COS(RP)/SIN(RF)
        SUM=ATAN(S1)+ATAN(S2)
        PHP=PHO-W1*TIME+SUM
 1030 CONTINUE
      IF (PHP.GE.0.) GOTO 1034
        PHP=PHP+2.*PI
      GOTO 1030
 1034 CONTINUE
      IF (PHP.LT.2.*PI) GOTO 1035
        PHP=PHP-2.*PI
      GOTO 1034
 1035 CONTINUE
      ZLON=180.*PHP/PI
C
C     RADIUS=ALTITUDE (KILOMETERS).
C
      RADIUS=RMAJ*(1.-E*COS(QT))-RE
      RETURN
      END
```

```
      PROGRAM LET
C     THIS PROGRAM COMPUTES INTEGRAL AND DIFFERENTIAL LET SPECTRA.
C     THE PARTICLE SPECTRA IN THE INTERPLANETARY MEDIUM ARE IN
C     THE CRF SUBROUTINE.
C     THE GEOMAGNETIC CUTOFF IS APPLIED BY THE CUT SUBROUTINE.
C     PROPAGATION THROUGH SHIELDING IS HANDLED IN THE INSIDE ROUTINE.
C     THE DEDXSI ROUTINE RETURNS LET IN SILICON.
C     THE CONTROL PARAMETERS ARE:
C         Y = YEAR OF THE PARTICLE ENVIRONMENT (1975.144 WAS SOLAR MIN.
C         AND 1980.598 WAS SOLAR MAX.);
C         IT = ORBITAL INDEX (0 = HIGH ORBIT:  NO CUTOFF, NO TRAPPED
C         PROTONS; 1 = LOW ORBIT:  CUTOFF AND TRAPPED PROTONS);
C         MQ = INTERPLANETARY MEDIUM WEATHER INDEX (SEE NOTES IN CRF
C         ROUTINE);
C         THK = SHIELDING THICKNESS (ALUMINUM EQUIVALENT) IN G/CM**2;
C         IDEM = NO. OF LOG STEPS IN ENERGY;
C         IELM = LIGHTEST ELEMENT INCLUDED;
C         JELM = HEAVIEST ELEMENT INCLUDED (JELM MUST NOT EXCEED 92).
C     THE OUTPUTS ARE THE DIFFERENTIAL AND INTEGRAL LET SPECTRA.
C     THE UNITS ARE PARTICLES/((M**2)*STER*SEC*MEV*CM**2/G) AND
C     PARTICLES/((M**2)*STER*SEC) RESPECTIVELY
C     VERSUS MEV*CM**2/G.
C
C     DXMAX AND DXMIN THE MAXIMUM AND MINIMUM LET VALUES CONSIDERED.
C     EMIN IS THE MINIMUM ENERGY CONSIDERED.
C     ABOVE EMAX, LET IS CONSTANT.
C
      REAL N(101),INSIDE
      CHARACTER*12 ALPHA,BETA,GAMMA
      DIMENSION DX(101),F(1000),DEDX(1000)
      DATA DXMAX/1.1E+5/,DXMIN/1.6/,EMIN/.1/,EMAX/20000./
      DATA F/1000*0.0/,GAMMA/'            '/,NDIF/0/,NINT/0/

C     ASK FOR ALL THE CONTROL DATA NEEDED FOR A RUN.
C
      WRITE (6,101)
 101  FORMAT(' ENTER THE NAME OF THE DIFFERENTIAL LET SPECTRUM'/
     1 ' (ENTER NOTHING IF YOU DO NOT WANT ONE):  ',$)
      ACCEPT 102, ALPHA
 102  FORMAT(A12)
      IF(ALPHA.EQ.GAMMA) GO TO 104
      OPEN(UNIT=40,FILE=ALPHA)
      WRITE (6,103)
 103  FORMAT(' ENTER THE NUMBER OF POINTS IN THE TABULATION OF'/
     1 ' THE DIFFERENTIAL LET SPECTRUM (MAXIMUM:  1000):  ',$)
      ACCEPT *,NDIF
 104  WRITE (6,105)
 105  FORMAT(' ENTER THE NAME OF THE INTEGRAL LET SPECTRUM'/
     1 ' (ENTER NOTHING IF YOU DO NOT WANT ONE):  ',$)
      ACCEPT 102, BETA
      IF(BETA.EQ.GAMMA) GO TO 107
      OPEN(UNIT=45,FILE=BETA)
```

```
      WRITE (6,106)
106   FORMAT(' ENTER THE NUMBER OF POINTS IN THE TABULATION OF'/
     1 ' THE INTEGRAL LET SPECTRUM (MAXIMUM:  1000):  ',$)
      ACCEPT *,NINT
107   NPT=MAXO(NDIF,NINT)
      WRITE (6,108)
108   FORMAT(' ENTER THE ATOMIC NUMBER OF THE LIGHTEST ELEMENT'/
     1 ' TO BE INCLUDED IN THE LET SPECTRA:  ',$)
      ACCEPT *,IELM
      WRITE (6,109)
109   FORMAT(' ENTER THE ATOMIC NUMBER (<93) OF THE HEAVIEST ELEMENT'/
     1 ' TO BE INCLUDED IN THE LET SPECTRA:  ',$)
      ACCEPT *,JELM
      IF (JELM.GT.92) JELM=92
      WRITE (6,110)
110   FORMAT(' ENTER THE YEAR FOR WHICH YOU WANT THE SPECTRUM'/
     1 ' (1975.144 FOR SOLAR MIN.; 1980.598 FOR SOLAR MAX.):  ',$)
      ACCEPT *,Y
      WRITE (6,111)
111   FORMAT(' ENTER THE ORBITAL INDEX:  0 FOR NO CUTOFF AND NO ',
     1 'TRAPPED PROTONS;'/' 1 FOR CUTOFF AND TRAPPED PROTONS',
     2' (NOTE:  STASS.DAT AND GTRANS.DAT'/
     3' MUST BE SUPPLIED WHEN 1 IS ENTERED HERE):  ',$)
      ACCEPT *,IT
      WRITE (6,112)
112   FORMAT(' ENTER THE INTERPLANETARY WEATHER INDEX:  ',$)
      ACCEPT *, MQ
      WRITE (6,113)
113   FORMAT(' ENTER THE SHIELDING THICKNESS IN INCHES OF'/
     1 ' ALUMINUM (OR EQUIVALENT):  ',$)
      ACCEPT *,THK
C
C     CONVERT THE THICKNESS TO G/CM**2 (ALUMINUM EQUIVALENT).
C
      THK=THK*6.4528
      WRITE (6,116) IELM,JELM
116   FORMAT(//' THE LET SPECTRA WILL INCLUDE THE CONTRIBUTIONS'/
     1 ' OF THE ELEMENTS ',I2,' THROUGH ',I2,'.')
      IF(NDIF.GT.0) WRITE (6,114) ALPHA,NPT
      IF(NINT.GT.0) WRITE (6,115) BETA,NPT
114   FORMAT(' THE FILE ',A12,' WILL CONTAIN THE DIFFERENTIAL LET'/
     1 ' SPECTRUM, TABULATED IN ',I4,' DATA POINTS.')
115   FORMAT(' THE FILE ',A12,' WILL CONTAIN THE INTEGRAL LET'/
     1 ' SPECTRUM, TABULATED IN ',I4,' DATA POINTS.')
      WRITE (6,117) Y
117   FORMAT(' THESE LET SPECTRA WILL BE FOR THE YEAR ',F8.3,'.')
      IF(IT.EQ.0) WRITE (6,118)
118   FORMAT(' THESE LET SPECTRA WILL BE UNSHIELDED BY THE'/
     1 ' EARTH''S MAGNETIC FIELD, AND THE CONTRIBUTION FROM TRAPPED'/
     2 ' PROTONS WILL NOT BE INCLUDED.')
      IF(IT.EQ.1) WRITE (6,119)
119   FORMAT(' THESE LET SPECTRA WILL INCLUDE THE EFFECTS OF'/
```

```
     1 ' GEOMAGNETIC SHIELDING ACCORDING TO THE GEOMAGNETIC CUTOFF'/
     2 ' TRANSMITTANCE FUNCTION TABULATED IN GTRANS.DAT.  THE'/
     3 ' CONTRIBUTION FROM TRAPPED PROTONS WILL BE INCLUDED'/
     4 ' ACCORDING TO THE ORBIT-AVERAGED TRAPPED PROTON SPECTRA'/
     5 ' TABULATED IN STASS.DAT.')
       WRITE (6,120) MQ
 120   FORMAT(' THE INTERPLANETARY WEATHER INDEX IS ',I2,'.')
       WRITE (6,121) THK
 121   FORMAT(' THE SHIELDING THICKNESS IS ',F7.3,' GM/CM**2
     1 ALUMINUM (OR EQUIVALENT).'//)
       DLL=ALOG(DXMIN)
       DD=(ALOG(DXMAX)-DLL)/NPT
       DLX=DLL
       IDEM=100
       JDEM=IDEM+1
C
C      SET UP LOG ENERGY STEPS.
C
       ELNX=ALOG(EMIN)
       DELN=(ALOG(EMAX)-ELNX)/IDEM
C
C      DO ONE ELEMENT AT A TIME.
C
       DO 41 IZ=IELM,JELM
C
C      SET LOWER BIN BOUNDARIES.
C
       L=1
       E=EMIN
       K=1
       ELN=ELNX
       Z=FLOAT(IZ)
C
C      GET LET.
C
       DX(1)=DEDXSI(Z,E)
C
C      GET INTERNAL FLUX.
C
       FL=INSIDE(Z,E,Y,MQ,IT,THK)
C
C      RETURN TO HERE AFTER FLUX IN EACH BIN HAS BEEN CALCULATED.
C
 10    L=L+1
C
C      RETURN TO HERE IF D(LET)/DE IS SINGULAR TO INCREASE THE BIN
C      WIDTH.
C
 11    K=K+1
C
C      WHEN K EXCEEDS JDEM YOU ARE THROUGH.
C
```

```
      IF(K.GT.JDEM) GO TO 20
C
C     STEP TO UPPER ENERGY BIN BOUNDARY.
C
      ELN=ELN+DELN
C
C     COMPUTE UPPER ENERGY BIN BOUNDARY.
C
      EU=EXP(ELN)
C
C     COMPUTE UPPER LET BIN BOUNDARY.
C
      DU=DEDXSI(Z,EU)
C
C     TEST FOR D(LET)/DE SINGULARITY.
C
      T=ABS(DX(L-1)-DU)/DU
      IF(T.LT.1.0E-6) GO TO 11
C
C     COMPUTE FLUX IN THE BIN.
C
      FU=INSIDE(Z,EU,Y,MQ,IT,THK)
      N(L-1)=0.5*(FU+FL)*(EU-E)
C
C     THE UPPER BIN BOUNDARY BECOMES THE LOWER BOUNDARY OF NEXT BIN.
C
      DX(L)=DU
      E=EU
      FL=FU
C
C     CLOSE THE LOOP.
C
      GO TO 10
C
C     DO THE HIGH ENERGY TAIL IN THE LAST BIN, ASSUMING AN E**(-2.5)
C     POWER LAW FOR HIGH ENERGY COSMIC RAYS.
C
 20   LL=L-2
      N(LL+1)=0.6666*FL*E
C
C     PRESERVE THE LET BIN BOUNDARIES.
C
      DLU=DLL
      DL=DXMIN
C
C     RE-BIN EACH ELEMENT IN A COMMON SET OF LET BINS.
C
      DO 41 KK=1,NPT
C
C     SET UP THE COMMON LET BIN BOUNDARIES.
C
      DLU=DLU+DD
```

```
      DU=EXP(DLU)
C
C     SPIN THROUGH THE ELEMENT BIN SET ADDING FLUX TO THE
C     COMMON BIN.
C
      DO 40 I=1,LL
      DX1=DX(I)
      DX2=DX(I+1)
C
C     SKIP THE LOOP FOR ELEMENT BINS NOT OVERLAPPING THE COMMON BIN.
C
      IF ((DX1.GE.DU).AND.(DX2.GE.DU)) GO TO 40
      IF ((DX1.LE.DL).AND.(DX2.LE.DL)) GO TO 40
      IF(DX1.LT.DX2) GO TO 35
      IF(DX1.GE.DU) GO TO 32
      IF(DX2.LT.DL) GO TO 31
      F(KK)=F(KK)+N(I)
      GO TO 40
 31   F(KK)=F(KK)+N(I)*(DX1-DL)/(DX1-DX2)
      GO TO 40
 32   IF(DX2.GE.DL) GO TO 33
      F(KK)=F(KK)+N(I)*(DU-DL)/(DX1-DX2)
      GO TO 40
 33   F(KK)=F(KK)+N(I)*(DU-DX2)/(DX1-DX2)
      GO TO 40
 35   IF(DX2.GE.DU) GO TO 37
      IF(DX1.LT.DL) GO TO 36
      F(KK)=F(KK)+N(I)
      GO TO 40
 36   F(KK)=F(KK)+N(I)*(DX2-DL)/(DX2-DX1)
      GO TO 40
 37   IF(DX1.GE.DL) GO TO 38
      F(KK)=F(KK)+N(I)*(DU-DL)/(DX2-DX1)
      GO TO 40
 38   F(KK)=F(KK)+N(I)*(DU-DX1)/(DX2-DX1)
 40   CONTINUE
C
C     DO THE INTEGRAL BIN FOR THE HIGH ENERGY TAIL.
C
      IF((DX2.GE.DL).AND.(DX2.LE.DU)) F(KK)=F(KK)+N(LL+1)
C
C     FINISH STEPPING THROUGH THE COMMON LET BINS
C     THEN GO BACK AND DO THE NEXT ELEMENT.
C
 41   DL=DU
C
C     COMPUTE THE DIFFERENTIAL LET SPECTRA.
C
      DL=DXMIN
      DO 50 K=1,NPT
      DLX=DLX+DD
      DU=EXP(DLX)
```

```
      G = F(K)/(DU-DL)
      DEDX(K) = 0.5*(DU+DL)
      IF(NDIF.GT.0) WRITE(40,600) G, DEDX(K)
600   FORMAT(2X,E12.5,2X,E12.5)
50    DL=DU
      SUM=0.0
C
C     INTEGRATE THE LET SPECTRA.
C
      DO 60 I=NPT,1,-1
      SUM=SUM+F(I)
      DL=DEDX(I)
      IF(NINT.GT.0) WRITE(45,600)SUM,DL
60    CONTINUE
      END
```

```
      FUNCTION DEDXSI(Z,E)
C     THIS SUBROUTINE RETURNS THE STOPPING POWER IN SILICON IN
C     MEV*CM**2/G.
C     Z IS THE ION ATOMIC NUMBER.
C     E IS THE ION ENERGY IN MEV/AMU.
C     ZN ARE THE ATOMIC NUMBERS FOR WHICH THE STOPPING POWERS HAVE
C     BEEN TABULATED.
C     KK ASSOCIATES EACH ELEMENT WITH ONE WHOSE STOPPING POWER HAS
C     BEEN TABULATED.
C
      DIMENSION EN(77),RN(9,77),ZN(9),KK(92)
      DATA IST/0/,ZN/1.,2.,6.,8.,18.,26.,36.,54.,92./
      DATA IZS,J/0,3/,KK/1,2*2,3*3,7*4,8*5,9*6
     1 ,14*7,28*8,20*9/
C
C     THE STOPPING POWER TABLES ARE IN THE SILICN.DT1 FILE.
C
C
C     READ THE STOPPING POWER TABLES UPON THE FIRST ENTRY.
C
      IF(IST.NE.0) GO TO 5
        IST=1
      OPEN(UNIT=51,READONLY,SHARED,STATUS='OLD',FILE='SILICN.DT1')
        DO 3 I=1,77
        READ(51,2) EN(I),(RN(J,I),J=1,9)
 2      FORMAT(6X,F9.3,9(3X,E9.3))
 3      CONTINUE
        CLOSE (UNIT=51)
 5      CONTINUE
        IZ=Z+0.5
C
C     COMPUTE THE APPROXIMATE STARTING INDEX FOR TABLE LOOKUP.
C
        IJ=(ALOG(E)+4.065)*4.85567-1.0
        IJ=MAX0(IJ,1)
        IJ=MIN0(IJ,77)
C
C     SEARCH FOR THE ENERGY TABULAR POINT JUST ABOVE E.
C
 10     CONTINUE
        DO 11 I=IJ,77
        IF(EN(I).LT.E) GO TO 11
        J=I
        GO TO 13
 11     CONTINUE
        J=77
C
C     CALCULATE THE INTERPOLATION FACTOR.
C
 13     CONTINUE
        F=(E-EN(J-1))/(EN(J)-EN(J-1))
```

```
      F=AMIN1(F,1.0)
C
C     FIND THE NEAREST TABULATED ELEMENT.
C
 14   CONTINUE
      K=KK(IZ)
C
C     INTERPOLATE THE STOPPING POWER FOR THE TABULATED ELEMENT.
C
      DEDXSI=F*(RN(K,J)-RN(K,J-1))+RN(K,J-1)
      ZNE=ZN(K)
C
C     IF THE ION IS THE ONE TABULATED, YOU ARE DONE.
C
      IF (Z.EQ.ZNE)RETURN
      ZE=Z
      EC=1.+2.*Z
C
C     IF THE ENERGY IS HIGH ENOUGH, THE ION IS FULLY STRIPPED.
C
      IF(E.GT.EC) GO TO 21
C
C     COMPUTE THE EQUILIBRIUM CHARGE STATE.
C
      B=SQRT(1.-(E*.001073927+1)**(-2.))
      ZE=Z*(1.-EXP(-130.*B*(Z**(-.6666))))
      ZNE=ZNE*(1.-EXP(-130.*B*(ZNE**(-.6666))))
C
C     INTERPOLATE TO THE ION IN QUESTION.
C
 21   CONTINUE
      DEDXSI=(ZE*ZE)/(ZNE*ZNE)*DEDXSI
      RETURN
      END
```

```
      FUNCTION INSIDE (Z,E,Y,M,IT,TH)
C
C     TRANSPORTS THE PARTICLE SPECTRA THROUGH THE SPACECRAFT WALL
C     CONSIDERING ENERGY LOSS EFFECTS AND NUCLEAR FRAGMENTATION,
C     BUT DOES NOT KEEP TRACK OF THE FRAGMENTS.
C     Z IS THE ATOMIC NUMBER OF THE ION.
C     E IS THE ENERGY IN MEV/AMU.
C     Y IS THE YEAR OF THE ENVIRONMENT.
C     M IS THE INTERPLANETARY MEDIUM WEATHER INDEX (SEE CRF.FOR).
C     IT IS THE ORBITAL INDEX:  1 FOR LOW ORBITS, 0 FOR HIGH ORBITS.
C     TH IS THE THICKNESS OF ALUMINUM SHIELDING IN G/CM**2.
C     THIS ROUTINE RETURNS THE INTERNAL FLUX IN PARTICLES/((M**2)*
C     STER*SEC*MEV/U).
C
C     AN ARE THE AVERAGE ION MASSES FOR EACH ELEMENT (TAKEN FROM
C     THE HANDBOOK OF CHEMISTRY AND PHYSICS, 59TH EDITION).
C
      REAL INSIDE
      COMMON/MASS/AN(92)
      DATA (AN(I),I=1,92)/1.,4.,6.9,
     1 9.,10.8,12.,14.,16.,19.,20.2,23.,24.3,27.,28.,
     2 31.,32.,35.5,39.9,39.,40.,45.,47.9,50.9,
     3 52.,54.9,55.8,58.9,58.7,63.5,65.4,69.7,72.6,
     4 74.9,79.,79.9,83.8,85.5,87.6,88.9,91.2,92.9,95.9,97.,101.,
     5 102.9,106.4,107.9,112.4,114.8,118.7,121.8,127.6,126.9,131.3,
     6 132.9,137.3,138.9,140.1,140.9,144.2,145.,150.4,152.,157.3,
     7 158.9,162.5,164.9,167.3,168.9,173.,175.,178.5,180.9,183.9,
     8 186.2,190.2,192.2,195.1,197.,200.6,204.4,207.2,209.,209.,
     9 210.,222.,223.,226.,227.,232.,231.,238./
      IZ=Z+.5
      A=AN(IZ)
C
C     COMPUTE THE TOTAL INELASTIC CROSS SECTION USING C.H.
C     TSAO'S VERSION OF THE BRANDT-PETERS FORMULA.
C     USE A SIMPLER FORMULA FOR PROTONS.
C
      IF (Z.NE.1.) COEF=((6.02E+23)*(5.0E-26)
     1 *(A**(1./3.)+AN(13)**(1./3.)-0.4)**2)/AN(13)
      IF (Z.EQ.1.) COEF=0.
C
C     FIND THE RESIDUAL RANGE OF THE ION INSIDE THE SPACECRAFT.
C
      R=RAL(Z,A,E)
C
C     FIND THE RESIDUAL RANGE OF THE SAME ION OUTSIDE THE SPACECRAFT.
C
      R=R+TH
C
C     FIND THE CORRESPONDING ENERGY OUTSIDE.
C
```

```
      ES=EAL(Z,A,R)
C
C     FIND THE STOPPING POWER INSIDE AND OUTSIDE.
C
      SS=DEDXAL(Z,ES)
      S=DEDXAL(Z,E)
C
C     GET THE FLUX OUTSIDE AND COMPUTE IT INSIDE.
C
C     IT=0 FOR AN ORBIT SO HIGH THAT CUTOFF IS INSIGNIFICANT
C     AND TRAPPED PROTONS ARE INSIGNFICANT.
C
C     IT=1 FOR LOWER ORBITS:  INCLUDE CUTOFF AND TRAPPED PROTONS.
C
      IF (IT.EQ.0) INSIDE=CRF(Z,ES,Y,M)*(SS/S)*EXP(-COEF*TH)
      IF (IT.GT.0) INSIDE=CUT(Z,ES,Y,M)*(SS/S)*EXP(-COEF*TH)
      RETURN
      END
```

```
      FUNCTION DEDXAL(Z,E)
C
C       THIS SUBROUTINE RETURNS THE STOPPING POWER IN ALUMINUM IN
C       MEV*CM**2/G.
C       Z IS THE ION ATOMIC NUMBER.
C       E IS THE ION ENERGY IN MEV/AMU.
C
C       ZN ARE THE ATOMIC NUMBERS FOR WHICH THE STOPPING POWER HAS BEEN
C       TABULATED.
C       KK ASSOCIATES EACH ELEMENT WITH ONE WHOSE STOPPING POWER
C       HAS BEEN TABULATED.
C
      DIMENSION EN(66),RN(9,66),ZN(9),KK(92)
      DATA IST/0/,ZN/1.,2.,6.,8.,18.,26.,36.,54.,92/
      DATA IZS,J/0,3/,KK/1,2*2,3*3,7*4,8*5,9*6
     1 ,14*7,28*8,20*9/
C
C       THE STOPPING POWER TABLES ARE ON THE ALUMNM.DT1 FILE.
C
C
C       READ THE STOPPING POWER TABLES UPON THE FIRST ENTRY.
C
      IF(IST.NE.0) GO TO 5
        IST=1
      OPEN(UNIT=50,READONLY,SHARED,STATUS='OLD',FILE='ALUMNM.DT1')
        DO 3 I=1,66
        READ(50,2) EN(I),(RN(J,I),J=1,9)
 2       FORMAT(6X,F9.3,9(3X,E9.3))
 3       CONTINUE
 5      CONTINUE
         IZ=Z+0.5
C
C       COMPUTE THE APPROXIMATE STARTING INDEX FOR TABLE LOOKUP.
C
        IJ=(ALOG(E)+4.605)*4.85567-1.0
        IJ=MAXO(IJ,1)
        IJ=MINO(IJ,66)
C
C       SEARCH FOR THE ENERGY TABULAR POINT JUST ABOVE E.
C
 10     CONTINUE
        DO 11 I=IJ,66
        IF(EN(I).LT.E) GO TO 11
        J=I
        GO TO 13
 11      CONTINUE
        J=66
C
C       CALCULATE THE INTERPOLATION FACTOR.
C
 13     CONTINUE
```

```
      F=(E-EN(J-1))/(EN(J)-EN(J-1))
      F=AMIN1(F,1.0)
C
C     FIND THE NEAREST TABULATED ELEMENT.
C
 14   CONTINUE
       K=KK(IZ)
C
C     INTERPOLATE THE STOPPING POWER FOR THE TABULATED ELEMENT.
C
 20   CONTINUE
       DEDXAL=F* (RN(K,J)-RN(K,J-1))+RN(K,J-1)
      ZNE=ZN(K)
C
C     IF THE ION IS THE ONE TABULATED, YOU ARE DONE.
C
      IF (Z.EQ.ZNE) RETURN
      ZE=Z
      EC=1.+2.*Z
C
C     IF THE ENERGY IS HIGH ENOUGH, THE ION IS FULLY STRIPPED.
C
      IF(E.GT.EC) GO TO 21
C
C     COMPUTE THE EQUILIBRUM CHARGE STATE.
C
      B=SQRT(1.-(E*.001073927+1)**(-2.))
      ZE=Z*(1.-EXP(-130.*B*(Z**(-.6666))))
      ZNE=ZNE*(1.-EXP(-130.*B*(ZNE**(-.6666))))
C
C     INTERPOLATE TO THE ION IN QUESTION.
C
 21   CONTINUE
      DEDXAL=(ZE*ZE)/(ZNE*ZNE)*DEDXAL
      RETURN
      END
```

```
      FUNCTION RAL(Z,A,E)

C     THIS ROUTINE RETURNS THE RESIDUAL RANGE IN ALUMINUM IN G/CM**2.
C     Z IS THE ION ATOMIC NUMBER.
C     E IS THE ION ENERGY IN MEV/AMU.
C     A IS THE ION ATOMIC MASS.

C     ZN ARE THE ATOMIC NUMBERS OF THE TABULATED ELEMENTS.
C     KK ASSOCIATES EACH ELEMENT WITH A TABULATED ELEMENT.
C     AN ARE THE MEAN ATOMIC MASSES OF THE TABULATED ELEMENTS.
C     DEDX ARE STOPPING POWER DATA IN (MEV/AMU)/(G/CM**2).
C
      DIMENSION EN(66),RN(9,66),ZN(9),AN(9),KK(92),DEDX(9)
      DATA IST/0/,ZN/1.,2.,6.,8.,18.,26.,36.,54.,92/
      DATA IZS,J/0,3/,KK/1,2*2,3*3,7*4,8*5,9*6
     1 ,14*7,28*8,20*9/
      DATA AN/1.008,4.0026,12.01115,15.99994,39.948,55.847
     1 ,83.8,131.3,238.03/
        DATA DEDX/1.706,1.720,5.174,6.913,14.12,21.22,27.34
     1 ,40.05,68.69/
C
C       SET ENTRY FLAG FOR RANGE.
C
        NTRY=0
C
C       READ IN THE TABLES UPON THE FIRST ENTRY.
C
      IF(IST.NE.0) GO TO 5
C
C       FILE ALUMNM.DT2 CONTAINS THE RANGE-ENERGY TABLES.
C
 1      CONTINUE
        OPEN(UNIT=60,READONLY,SHARED,STATUS='OLD',FILE='ALUMNM.DT2')
        IST=1
        DO 3 I=1,66
        READ(60,2) EN(I),(RN(J,I),J=1,9)
 2      FORMAT(6X,F9.3,9(3X,E9.3))
 3      CONTINUE
C
C       IF ENERGY FLAG SET, RETURN TO ENERGY PART.
C
        IF(NTRY.EQ.1) GO TO 100
 5      CONTINUE
        IZ=Z+.5
C
C       FIND THE NEAREST TABULATED ION.
C
        K=KK(IZ)
C
C       COMPUTE THE APPROXIMATE INDEX IN THE TABLE.
C
```

```
      IJ=66
      IF(E.GT.8000.) GO TO 10
      IJ=(ALOG(E)+4.605)*4.85567-1.0
      IJ=MAX0(IJ,1)
      IJ=MIN0(IJ,66)
C
C     FIND THE TABULATED ENERGY JUST ABOVE E.
C
 10   CONTINUE
      DO 11 I=IJ,66
      IF(EN(I).LT.E) GO TO 11
      J=I
      GO TO 13
 11   CONTINUE
C
C     EXTRAPOLATE THE RANGE ACCORDING TO THE PLATEAU
C     VALUE OF THE STOPPING POWER.
C
      RNK=RN(K,66)+(E-EN(66))/DEDX(K)
      GO TO 14
C
C     COMPUTE THE INTERPOLATION FACTOR.
C
 13   CONTINUE
      F=(E-EN(J-1))/(EN(J)-EN(J-1))
      F=AMIN1(F,1.0)
C
C     INTERPOLATE RANGE IN THE TABLE.
C
      RNK=F*(RN(K,J)-RN(K,J-1))+RN(K,J-1)
C
C     INTERPOLATE TO THE ION IN QUESTION.
C
 14   CONTINUE
      RAL=(A/(Z*Z))*(ZN(K)*ZN(K)/AN(K))*RNK
      RETURN
      ENTRY EAL(Z,A,R)
C
C     THIS ENTRY RETURNS THE ENERGY (IN MEV/AMU) OF AN ION HAVING
C     A RESIDUAL RANGE R, IN G/CM**SQ.
C     Z IS THE ION ATOMIC NUMBER.
C     A IS THE ION ATOMIC MASS.
C
C     SET ENTRY FLAG FOR ENERGY.
C
      IZ=Z+.5
      NTRY=1
C
C     IF THIS IS THE FIRST CALL, READ IN THE TABLES.
C
      IF(IST.EQ.0) GO TO 1
C
```

```
C       FIND THE NEAREST TABULATED ION.
C
 100    CONTINUE
        K=KK(IZ)
C
C       COMPUTE THE ION INTERPOLATION FACTOR.
C
 110    CONTINUE
        FK=(A/(Z*Z))*(ZN(K)*ZN(K)/AN(K))
C
C       FIND THE TABULATED RANGE JUST ABOVE R.
C
        DO 120 I=1,66
        RT=FK*RN(K,I)
        IF(RT.LT.R) GO TO 120
        J=I
        GO TO 130
 120    CONTINUE
C
C       EXTRAPOLATE THE ENERGY.
C
        RAT=DEDX(K)/FK
        EAL=EN(66)+RAT*(R-FK*RN(K,66))
        RETURN
C
C       INTERPOLATE THE ENERGY.
C
 130    CONTINUE
        F=(R-FK*RN(K,J-1))/(RT-FK*RN(K,J-1))
        EAL=F*(EN(J)-EN(J-1))+EN(J-1)
        RETURN
        END
```

```
      FUNCTION CUT (Z,E,Y,M)
C
C     THIS ROUTINE OBTAINS DIFFERENTIAL PARTICLE FLUXES FROM CRF,
C     APPLIES THE GEOMAGNETIC CUTOFF TRANSMISSION FUNCTION
C     IN THE GTRANS.DAT FILE, AND RETURNS
C     THE RESULTING FLUX, MODULATED TO THE ORBIT-AVERAGE CUTOFF.
C     THIS ROUTINE ALSO ADDS SINGLY-IONIZED ANOMALOUS COMPONENT NUCLEI
C     TO THE COSMIC RAY SPECTRA (WHEN M=4).
C     Z = ION ATOMIC NUMBER.
C     E = ION ENERGY IN MEV/AMU.
C     Y = YEAR (1975.144 = SOLAR MIN.; 1980.598 = SOLAR MAX.).
C     M = INTERPLANETARY MEDIUM WEATHER INDEX.
C
      COMMON/MASS/A(92)
      DIMENSION R(200),T(200)
      DATA ITS/-1/
      IF(ITS.EQ.1) GO TO 6
      OPEN(UNIT=15,READONLY,SHARED,STATUS='OLD',FILE='GTRANS.DAT')
      ITS=1
      DO 5 I=1,200
      READ(15,1) R(I),T(I)
    1 FORMAT(5X,F6.3,5X,F8.6)
    5 CONTINUE
      SHADOW=T(200)
    6 IZ=Z+.5
      CUT=0.0
      ES=E
C
C     DON'T CALL CRF WITH ENERGIES BELOW 10 MEV/U.
C
      IF(E.LT.10.) ES=10.
      MK=M
      MQ=M
C
C     M=4 MEANS A SINGLY-IONIZED ANOMALOUS COMPONENT + GALACTIC COSMIC
C     RAYS.
C     GET THE GALACTIC COSMIC RAYS HERE, THE ANOMALOUS COMPONENT WILL
C     BE ADDED BELOW.
C
      IF(M.EQ.4) MQ=1
C
C     GET THE DIFFERENTIAL FLUX.
C
      F=CRF(Z,ES,Y,MQ)
C
C     COMPUTE THE MAGNETIC RIGIDITY.
C
      P=(A(IZ)/Z)*(ES*ES+1862.324*ES)**.5/1000
C
C     LOOK UP THE TABULATED MAGNETIC RIGIDITY JUST ABOVE P.
C
```

```
 4      DO 2 I=2,200
        IF(P.GT.R(I))GOTO 2
        ISAV=I
        GOTO 3
 2      CONTINUE
        TR=SHADOW
        GO TO 10
C
C       INTERPOLATE THE TRANSMISSION FACTOR (AVERAGED FOR THE ORBIT).
C
 3      TR=(T(ISAV)-T(ISAV-1))*(P-R(ISAV-1))/(R(ISAV)-R(ISAV-1))
     1 +T(ISAV-1)
C
C       APPLY THE TRANSMISSION FACTOR TO MODULATE THE FLUX.
C
 10     CUT=CUT+F*TR
C
C       ADD IN THE DIRECT CONTRIBUTION FROM THE TRAPPED PROTONS.
C
        IF(IZ.EQ.1) CUT=CUT+PROTON(ES)
C
C       UNLESS A SINGLY-IONIZED ANOMALOUS COMPONENT MUST BE ADDED, RETURN.
C
        IF(MK.NE.4) GO TO 12
C
C       ADD SINGLY-IONIZED HELIUM.
C
        IF(IZ.NE.2) GO TO 40
        F=(1.54E+4)*ES**(-2)
        IF(ES.LT.195.) F=.4
        P=4.*(ES*ES+1862.324*ES)**.5/1000
        MK=1
        GO TO 4
C
C       ADD SINGLY-IONIZED CARBON.
C
 40     IF(IZ.NE.6) GO TO 45
        IF(ES.LT.10.) GO TO 43
        F=0.27*ES**(-2)
        GO TO 44
 43     F=(4.0E-3)*EXP(-(ALOG(ES)-1.79)**2/.7)
        IF(F.LT.0.) F=0.
 44     P=12.*(ES*ES+1862.324*ES)**.5/1000.
        MK=1
        GO TO 4
C
C       ADD SINGLY-IONIZED NITROGEN.
C
 45     IF(IZ.NE.7) GO TO 50
        IF(ES.LT.20.) GO TO 41
        F=.773*ES**(-2)
        GO TO 42
```

```
 41     F=(1.54E-2)*EXP(-(ALOG(ES)-1.79)**2/.7)
        IF(F.LT.0.) F=0.
 42     P=14.*(ES*ES+1862.324*ES)**.5/1000.
        MK=1
        GO TO 4
C
C       ADD SINGLY-IONIZED OXYGEN.
C
 50     IF(IZ.NE.8) GO TO 60
        IF(ES.LT.30.) GO TO 51
        F=1.32*ES**(-2.)
        GO TO 52
 51     F=(6.0E-2)*EXP(-(ALOG(ES)-1.79)**2/.7)
        IF(F.LT.0.) F=0.
 52     P=16*(ES*ES+1862.324*ES)**.5/1000.
        MK=1
        GO TO 4
C
C       ADD SINGLY-IONIZED NEON.
C
 60     IF(IZ.NE.10.) GO TO 70
        IF(ES.LT.20.) GO TO 61
        F=0.4*ES**(-2)
        GO TO 62
 61     F=(8.0E-3)*EXP(-(ALOG(ES)-1.79)**2/.7)
        IF(F.LT.0.) F=0.
 62     P=20*(ES*ES+1862.324*ES)**.5/1000.
        MK=1
        GO TO 4
C
C       ADD SINGLY-IONIZED MAGNESIUM.
C
 70     IF(IZ.NE.12) GO TO 80
        IF(ES.LT.20.) GO TO 71
        F=0.16*ES**(-2)
        GO TO 72
 71     F=(8.0E-4)*EXP(-(ALOG(ES)-2.3)**2/.7)
        IF(F.LT.0.) F=0.
 72     P=24.3*(ES*ES+1862.324*ES)**.5/1000.
        MK=1
        GO TO 4
C
C       ADD SINGLY-IONIZED SILICON.
C
 80     IF(IZ.NE.14) GO TO 85
        IF(ES.LT.10.) GO TO 81
        F=0.1*ES**(-2)
        GO TO 82
 81     F=(1.0E-3)*EXP(-(ALOG(ES)-2.2)**2/0.4)
        IF(F.LT.0.) F=0.
 82     P=28.*(ES*ES+1862.324*ES)**.5/1000.
        MK=1
```

```
      GO TO 4
C
C     ADD SINGLY-IONIZED ARGON.
C
 85   IF(IZ.NE.18) GO TO 90
      IF(ES.LT.20.) GO TO 86
      F=0.028*ES**(-2)
      GO TO 87
 86   F=(5.4E-4)*EXP(-(ALOG(ES)-1.79)**2/.7)
      IF(F.LT.0.) F=0.
 87   P=40.*(ES*ES+1862.324*ES)**.5/1000.
      MK=1
      GO TO 4
C
C     ADD SINGLY-IONIZED IRON.
C
 90   IF(IZ.NE.26) GO TO 12
      IF(ES.LT.30.) GO TO 91
      F=0.35*ES**(-2)
      GO TO 92
 91   F=(6.0E-4)*EXP(-(ALOG(ES)-2.48)**2/2.)
      IF(F.LT.0.) F=0.
 92   P=56.*(ES*ES+1862.324*ES)**.5/1000.
      MK=1
      GO TO 4
C
C     THERE PROBABLY ARE ANOMALOUS COMPONENTS IN THE SPECTRA OF
C     THE NUCLEI HEAVIER THAN IRON, BUT THERE ARE NO DATA ON THEM
C     AT THIS TIME, SO THEY CANNOT BE INCLUDED IN THE MODEL.
C
 12   RETURN
      END
```

```
      PROGRAM BENDEL
C
C     THIS PROGRAM USES BENDEL'S FORMULA ("Proton Upsets in Orbit", by
C     W. L. Bendel and E. L. Petersen, IEEE Trans in Nucl. Sci., Vol. NS-30,
C     p. 4481-5, 1983) TO CALCULATE THE UPSET RATE CAUSED BY PROTONS.  THE
C     PARAMETER A MUST BE INPUT.  THIS PROGRAM WAS CREATED BY MODIFYING THE
C     SPEC PROGRAM.  SUBROUTINES:  INSIDE, CUT, CRF, DEDXAL, RAL.
C
      REAL INSIDE
      Z=1.
      WRITE (6,103)
  103 FORMAT(' ENTER THE NUMBER OF ENERGY STEPS USED IN THE'/
     1' CALCULATION (MAXIMUM:  1000):  ',$)
      ACCEPT *,NDIF
      WRITE (6,110)
  110 FORMAT(' ENTER THE YEAR FOR WHICH YOU WANT THE PROTON-INDUCED '/
     1' UPSET RATE (1975.144 FOR SOLAR MIN.; 1980.598 FOR SOLAR MAX.)',
     2':  ',$)
      ACCEPT *,Y
      WRITE (6,111)
  111 FORMAT(' ENTER THE ORBITAL INDEX:  0 FOR NO CUTOFF AND NO ',
     1 'TRAPPED PROTONS;'/' 1 FOR CUTOFF AND TRAPPED PROTONS',
     2' (NOTE:  STASS.DAT AND GTRANS.DAT'/
     3' MUST BE SUPPLIED WHEN 1 IS ENTERED HERE):  ',$)
      ACCEPT *,IT
      WRITE (6,112)
  112 FORMAT( ' ENTER THE INTERPLANETARY WEATHER INDEX:  ',$)
      ACCEPT *,M
      WRITE (6,113)
  113 FORMAT(' ENTER THE SHIELDING THICKNESS IN INCHES OF '/
     1' ALUMINUM (OR EQUIVALENT):  ',$)
      ACCEPT *,THK
      WRITE (6,114)
  114 FORMAT(' ENTER THE PARAMETER A (MEV).  (ENTER 0'/
     1' IF YOU DON''T KNOW IT):  ',$)
      ACCEPT *,A
      IF (A.GT.0.) GOTO 150
C
C     IF NOTHING WAS ENTERED, FIGURE OUT THE VALUE OF "A" FROM
C     EXPERIMENTAL DATA.
C
      WRITE (6,115)
  115 FORMAT(' ENTER AN EXPERIMENTALLY MEASURED UPSET CROSS-SECTION'/
     1' IN UNITS OF (UPSETS/BIT)/(PROTON/CM**2):  ',$)
      ACCEPT *,XSECT
      WRITE (6,116)
  116 FORMAT(' ENTER THE ENERGY (MEV) AT WHICH THIS CROSS-SECTION'/
     1' MEASUREMENT WAS MADE:  ',$)
      ACCEPT *, ENERGY
      ALOW = 1.
      AHIGH = 200.
```

```
      XSECT = 1.E12*XSECT
      DO 130 J=1,16
          A = .5*(AHIGH+ALOW)
          X = SIGMA(A,ENERGY)
C
C     SIGMA IS A DECREASING FUNCTION OF A.
C
          IF (X.GT.XSECT) ALOW=A
          IF (X.LE.XSECT) AHIGH=A
 130  CONTINUE
 150  CONTINUE
C
C     CONVERT THE THICKNESS TO G/CM**2 (ALUMINUM EQUIVALENT).
C
      TH=THK*6.8528
C
C     TYPE OUT THE INPUTTED DATA.
C
      WRITE (6,117) Y
 117  FORMAT(//' THE UPSET RATE WILL BE FOR THE YEAR ',F8.3,'.')
      IF(IT.EQ.0) WRITE (6,118)
 118  FORMAT(' THE COSMIC RAYS WILL BE UNSHIELDED BY THE',/,
     1 ' EARTH''S MAGNETIC FIELD, AND THE CONTRIBUTION FROM TRAPPED',/,
     2 ' PROTONS WILL NOT BE INCLUDED.')
      IF(IT.EQ.1) WRITE (6,119)
 119  FORMAT(' THE UPSET RATE WILL INCLUDE THE EFFECTS OF',/,
     1 ' GEOMAGNETIC SHIELDING ACCORDING TO THE GEOMAGNETIC CUTOFF',/,
     2 ' TRANSMITTANCE FUNCTION TABULATED IN GTRANS.DAT.  THE',/,
     3 ' CONTRIBUTION FROM TRAPPED PROTONS WILL BE INCLUDED',/,
     4 ' ACCORDING TO THE ORBIT-AVERAGED TRAPPED PROTON SPECTRA',/,
     5 ' TABULATED IN STASS.DAT.')
      WRITE (6,120) M
 120  FORMAT(' THE INTERPLANETARY WEATHER INDEX IS ',I2,'.')
      WRITE (6,121) TH
 121  FORMAT(' THE SHIELDING THICKNESS IS ',F7.3,' GM/CM**2
     1 ALUMINUM (OR EQUIVALENT).')
      WRITE (6,122) A
 122  FORMAT(' THE UPSET THRESHOLD PARAMETER IS ',F6.2,' MEV.')
C
C     SET UP THE ENERGY RANGE AND DIVIDE IT INTO EQUAL LOGARITHMIC STEPS.
C
      EMAX=32000.
      EMIN=10.
      ELNX=ALOG(EMIN)
      DELN=(ALOG(EMAX)-ELNX)/NDIF
      UPSETS=0.
C
C     COMPUTE THE DIFFERENTIAL FLUX AT EACH ENERGY.  THE SUBPROGRAMS RETURN
C     FLUX IN PARTICLES/((M**2)*STER*SEC)/(MEV/(G/CM**2)).
C
      DO 200 I=1,NDIF
      EN=EXP(ELNX)
```

```
      ELNX=ELNX+DELN
      F=INSIDE(Z,EN,Y,M,IT,TH)
C
C     COMPUTE BENDEL'S FLUX.  E AND A ARE IN MEV, Y IS DIMENSIONLESS,
C     SIGMA IS IN 1E-12 (UPSETS/BIT)/(PROTON/CM**2), UPSETS IS IN
C     UPSETS/BIT*DAY.
C
C     THE FACTORS IN THE CONVERSION CONSTANT ARE:
C         1E-12 FROM THE DEFINITION OF SIGMA;
C         86400 TO CONVERT FROM SECONDS TO DAYS;
C         .01**2 TO CONVERT FROM M**2 TO CM**2;
C         4*PI TO GET RID OF THE STERADIANS.
C
      CONST=1.E-12*(.01**2.)*(4.*3.1416)
      UPSETS = UPSETS + CONST*SIGMA(A,EN)*F*(EXP(ELNX)-EN)
 200  CONTINUE
      WRITE(6,14)UPSETS
 14   FORMAT(' ERROR RATE = ',1PE12.5,' IN UPSETS/BIT*SEC.')
      UPSETS=UPSETS*86400.
      WRITE(6,15)UPSETS
 15   FORMAT(' ERROR RATE = ',1PE12.5,' IN UPSETS/BIT*DAY.')
      END
```

```
      FUNCTION SIGMA (A,E)
C
C     THIS IS THE SIGMA FROM PAGE 4484 OF THE BENDEL PAPER.
C
      Y = (SQRT(18./A))*(E-A)
      IF (Y.LT.0.) Y=0.
      SIGMA = ((24./A)**14.)*((1.-EXP(-.18*SQRT(Y)))**4.)
      RETURN
      END
```

```
      PROGRAM SPEC

C     THIS PROGRAM USES THE SUBPROGRAMS INSIDE, CUT, CRF, DEDXAL,
C     AND RAL TO TABULATE THE DIFFERENTIAL AND INTEGRAL ENERGY SPECTRA OF
C     COSMIC RAYS OF A SPECIFIED CHARGE.
C
      REAL INSIDE
      COMMON /MASS/AMSTAB(92)
      CHARACTER*12 ALPHA,BETA,GAMMA
      DIMENSION F(1000),E(1001)
      DATA NDIF/0/,NINT/0/,GAMMA/'            '/
      WRITE (6,101)
 101  FORMAT(' ENTER THE NAME OF THE DIFFERENTIAL ENERGY SPECTRUM',/,
     1' (ENTER NOTHING IF YOU DO NOT WANT ONE):  ',$)
      ACCEPT 102,ALPHA
 102  FORMAT(A12)
      IF(ALPHA.EQ.GAMMA) GO TO 104
      OPEN(UNIT=40,FILE=ALPHA)
      WRITE (6,103)
 103  FORMAT(' ENTER THE NUMBER OF POINTS IN THE TABULATION OF',/,
     1' THE DIFFERENTIAL ENERGY SPECTRUM (MAXIMUM:  1000):  ',$)
      ACCEPT *,NDIF
 104  WRITE (6,105)
 105  FORMAT(' ENTER THE NAME OF THE INTEGRAL ENERGY SPECTRUM',/,
     1' (ENTER NOTHING IF YOU DO NOT WANT ONE):  ',$)
      ACCEPT 102,BETA
      IF(BETA.EQ.GAMMA) GO TO 107
      OPEN(UNIT=45,FILE=BETA)
      WRITE (6,106)
 106  FORMAT(' ENTER THE NUMBER OF POINTS IN THE TABULATION OF',/,
     1' THE INTEGRAL ENERGY SPECTRUM (MAXIMUM:  1000):  ',$)
      ACCEPT *,NINT
 107  NPT=MAX0(NDIF,NINT)
      WRITE (6,108)
 108  FORMAT(' ENTER THE ATOMIC NUMBER OF THE ELEMENT FOR WHICH',/,
     1' YOU WANT THE ENERGY SPECTRUM:  ',$)
      ACCEPT *,IELM
      Z=IELM
      WRITE (6,110)
 110  FORMAT(' ENTER THE YEAR FOR WHICH YOU WANT THE SPECTRUM',/,
     1' (1975.144 FOR SOLAR MIN.; 1980.598 FOR SOLAR MAX.):  ',$)
      ACCEPT *,Y
      WRITE (6,111)
 111  FORMAT(' ENTER THE ORBITAL INDEX:  0 FOR NO CUTOFF AND NO ',
     1 'TRAPPED PROTONS;'/' 1 FOR CUTOFF AND TRAPPED PROTONS',
     2' (NOTE:  STASS.DAT AND GTRANS.DAT'/
     3' MUST BE SUPPLIED WHEN 1 IS ENTERED HERE):  ',$)
      ACCEPT *,IT
      WRITE (6,112)
 112  FORMAT(' ENTER THE INTERPLANETARY WEATHER INDEX:  ',$)
      ACCEPT *,M
```

```
      WRITE (6,113)
  113 FORMAT(' ENTER THE SHIELDING THICKNESS IN INCHES OF ',/,
     1' ALUMINUM (OR EQUIVALENT):  ',$)
      ACCEPT *,THK
C
C     CONVERT THE THICKNESS TO G/CM**2 (ALUMINUM EQUIVALENT).
C
      TH=THK*6.8528
      WRITE (6,116) IELM
  116 FORMAT(//' THE ENERGY SPECTRA WILL INCLUDE THE CONTRIBUTION'/
     1 ' OF ELEMENT ',I2,'.')
      IF(NDIF.GT.0) WRITE (6,114) ALPHA,NPT
      IF(NINT.GT.0) WRITE (6,115) BETA,NPT
  114 FORMAT(' THE FILE ',A12,' WILL CONTAIN THE DIFFERENTIAL',/
     1 ,' ENERGY SPECTRUM, TABULATED IN ',I4,' DATA POINTS.')
  115 FORMAT(' THE FILE ',A12,' WILL CONTAIN THE INTEGRAL',/
     1 ,' ENERGY SPECTRUM, TABULATED IN ',I4,' DATA POINTS.')
      WRITE (6,117) Y
  117 FORMAT(' THESE ENERGY SPECTRA WILL BE FOR THE YEAR ',F8.3,'.')
      IF(IT.EQ.0) WRITE (6,118)
  118 FORMAT(' THESE ENERGY SPECTRA WILL BE UNSHIELDED BY THE',/,
     1 ' EARTH''S MAGNETIC FIELD, AND THE CONTRIBUTION FROM TRAPPED',/,
     2 ' PROTONS WILL NOT BE INCLUDED.')
      IF(IT.EQ.1) WRITE (6,119)
  119 FORMAT(' THESE ENERGY SPECTRA WILL INCLUDE THE EFFECTS OF',/,
     1 ' GEOMAGNETIC SHIELDING ACCORDING TO THE GEOMAGNETIC CUTOFF',/,
     2 ' TRANSMITTANCE FUNCTION TABULATED IN GTRANS.DAT.  THE',/,
     3 ' CONTRIBUTION FROM TRAPPED PROTONS WILL BE INCLUDED',/,
     4 ' ACCORDING TO THE ORBIT-AVERAGED TRAPPED PROTON SPECTRA',/,
     5 ' TABULATED IN STASS.DAT.')
      WRITE (6,120) M
  120 FORMAT(' THE INTERPLANETARY WEATHER INDEX IS ',I2,'.')
      WRITE (6,121) TH
  121 FORMAT(' THE SHIELDING THICKNESS IS ',F7.3,' GM/CM**2
     1 ALUMINUM (OR EQUIVALENT).',//)
C
C     SET UP THE ENERGY RANGE AND DIVIDE IT INTO EQUAL LOGARITHMIC STEPS.
C
      EMAX=32000.
      EMIN=10.
      ELNX=ALOG(EMIN)
      DELN=(ALOG(EMAX)-ELNX)/NPT
C
C     COMPUTE THE DIFFERENTIAL FLUX AT EACH ENERGY.
C
      DO 200 I=1,NPT
      EN=EXP(ELNX)
      ELNX=ELNX+DELN
      E(I)=EN
      F(I)=INSIDE(Z,EN,Y,M,IT,TH)
      IF(NDIF.GT.0) WRITE(40,201) F(I),E(I)
  201 FORMAT(2X,E12.5,2X,E12.5)
```

```
 200    CONTINUE
C
C       SUM THE DIFFERENTIAL ENERGY SPECTRUM TO GET THE INTEGRAL ENERGY
C       SPECTRUM (BOX INTEGRATION).
C
        SUM=.6666*INSIDE(Z,EN,Y,M,IT,TH)*EN
        DO 300 I=NPT,2,-1
        SUM=SUM+0.5*(F(I)+F(I-1))*(E(I)-E(I-1))
        IF(NINT.GT.0) WRITE(45,201) SUM,E(I-1)
 300    CONTINUE
        END
```

```
      PROGRAM UPSET

C     THIS PROGRAM COMPUTES THE UPSET RATE DUE TO THE
C     DIRECT IONIZATION OF INDIVIDUAL PARTICLES.  IT ASSUMES
C     THAT FOR EACH BIT THERE EXISTS A SENSITIVE VOLUME.
C     IF AN AMOUNT OF ELECTRICAL CHARGE (>QCRIT) IS CREATED
C     WITHIN THIS VOLUME BY THE IONIZING PARTICLE, THEN AN
C     UPSET WILL OCCUR.  THE SENSITIVE VOLUME IS IDEALIZED AS
C     A PARALLELEPIPED WITH DIMENSIONS X, Y, AND Z.
C     THE INPUTS ARE:
C     THE CRITICAL CHARGE QCRIT IN PICOCOULOMBS,
C     THE DIMENSIONS OF THE SENSITIVE VOLUME IN MICROMETERS,
C     THE NAME OF THE FILE CONTAINING THE INTEGRAL LET
C     SPECTRUM (SPEC.INT IS ASSUMED IF NO NAME IS ENTERED).
C     THE INTEGRAL LET SPECTRUM IS ASSUMED TO BE IN UNITS OF
C     PARTICLES/(SQUARE METER*STERADIAN*SEC) VERSUS
C     MEV*(SQUARE CENTIMETER)/GRAM.
C     THE OUTPUT IS GIVEN IN UPSETS/(BIT*SECOND) AND UPSETS/(BIT*DAY).

C     THIS CALCULATION USES THE METHOD DESCRIBED IN "THE VARIABILITY
C     OF SINGLE EVENT UPSET RATES IN THE NATURAL ENVIRONMENT,"
C     JAMES H. ADAMS, JR., IEEE TRANS. ON NUCL. SCI., NS-30, 4475-
C     4480, DEC., 1983.
C     IT IS OPERATIONALLY EQUIVALENT TO ROCKWELL'S CRIER PROGRAM
C     (PICKEL AND BLANDFORD, IEEE TRANS. ON NUCL. SCI. NS-26, DEC.
C     1979, PP.4735-4739) WHEN USED WITH HEINRICH'S LET SPECTRUM
C     (W. HEINRICH, RADIATION EFFECTS, VOL. 34, PP. 143-8, 1977).

C     THIS PROGRAM CALLS A SUBPROGRAM, DIFPLD, THAT RETURNS
C     THE DIFFERENTAL PATHLENGTH DISTRIBUTION IN THE SENSTIVE
C     VOLUME.
C
      CHARACTER*12 ALPHA,DEFAULT,BLANK
      REAL L(1000),LMIN
      DIMENSION FLUX(1000)
      DATA DSI/2.321/,BLANK/'            '/,DEFAULT/'SPEC.INT'/
C
C     GET THE INPUT DATA.
C
      WRITE(6,1)
 1    FORMAT(' ENTER THE CRITICAL CHARGE IN PICOCOULOMBS:  ',$)
      ACCEPT *, QCRIT
      WRITE(6,2)
 2    FORMAT(' ENTER THE DIMENSIONS OF THE SENSITIVE VOLUME,
     1 X, Y, Z, IN MICROMETERS:  ',$)
      ACCEPT *, X,Y,Z
C
C     CONVERT FROM MICROMETERS TO CENTIMETERS.
C
      X=X*.0001
      Y=Y*.0001
```

```
      Z=Z*.0001
      WRITE(6,3)
 3    FORMAT(' ENTER THE NAME OF THE INTEGRAL LET FILE:  ',$)
      ACCEPT 4, ALPHA
 4    FORMAT(A12)
C
C     IF NO FILE NAME WAS ENTERED, ASSUME 'SPEC.INT'.
C
      IF(ALPHA.EQ.BLANK) ALPHA=DEFAULT
      OPEN(UNIT=1,READONLY,SHARED,STATUS='OLD',FILE=ALPHA)
C
C     READ THE INTEGRAL LET SPECTRUM.
C     FLUX IS IN PARTICLES/(SQUARE METER*STERADIAN*SEC).
C     L IS IN MEV*(SQUARE CENTIMETER)/GRAM.
C
      N=1
 5    CONTINUE
      READ (1,11,END=6) FLUX(N),L(N)
 11   FORMAT(2X,E12.5,2X,E12.5)
      N=N+1
C
C     DON'T OVERFILL THE ARRAYS.
C
      IF(N.LE.1000) GOTO 5
C
C     COMPUTE THE NUMBER OF POINTS IN THE LET SPECTRUM.
C
 6    CONTINUE
      N=N-1
C
C     COMPUTE THE SURFACE AREA OF THE SENSITIVE VOLUME.
C
      S=(2.*X*Y+2.*X*Z+2.*Y*Z)
C
C     CONVERT FROM SQUARE CENTIMETERS TO SQUARE METERS.
C
      S=S*.0001
C
C     CONVERT THE DIMENSIONS OF THE SENSITIVE VOLUME TO G/CM**2.
C
      X=X*DSI
      Y=Y*DSI
      Z=Z*DSI
C
C     COMPUTE THE MAJOR DIAMETER OF THE SENSITIVE VOLUME.
C
      PMAX=SQRT(X*X+Y*Y+Z*Z)
C
C     COMPUTE THE ENERGY (IN MEV) REQUIRED TO PRODUCE QCRIT(IN PC)
C     HOLE-ELECTRON PAIRS IN SILICON.
C
      ENERGY=22.5*QCRIT
```

```
C
C       COMPUTE THE MINIMUM LET THAT CAN PRODUCE AN UPSET.
C
        LMIN=ENERGY/PMAX
        SUM=0.0
        Q=LMIN
C
C       INTEGRATE FROM LMIN TO THE LARGEST LET IN THE SPECTRUM.
C
        DO 10 I=N,1,-1
        IF(L(I).LT.LMIN) GO TO 10
C
C       COMPUTE THE PATHLENGTH CORRESPONDING TO L(I).
C
        D=ENERGY/L(I)
C
C       CARRY OUT THE INTEGRAL.
C
        SUM=SUM+(L(I)-Q)*DIFPLD(D,X,Y,Z)*FLUX(I)/(L(I)**2)
        Q=L(I)
 10     CONTINUE
C
C       COMPUTE THE ERROR RATE.
C
 12     CONTINUE
        ERR=ENERGY*S*3.1416*SUM
        WRITE(6,14)ERR
 14     FORMAT(' ERROR RATE = ',1PE12.5,' IN UPSETS/BIT*SEC.')
C
C       CONVERT TO UPSETS/BIT*DAY.
C
        ERR=ERR*86400.
        WRITE(6,15)ERR
 15     FORMAT(' ERROR RATE = ',1PE12.5,' IN UPSETS/BIT*DAY.')
        END
```

```
      FUNCTION DIFPLD(S,L,W,H)
C
C          THIS FUNCTION RETURNS THE PROBABILITY DENSITY FOR PATHS
C     OF LENGTH S THROUGH A PARALLELEPIPED OF DIMENSIONS
C     L, W, AND H.  S, L, W, AND H MUST BE IN THE SAME UNITS.
C          THIS IS AN EXACT SOLUTION, DUE TO M. D. PETROFF OF
C     ROCKWELL INTERNATIONAL (SEE J. C. PICKEL AND J. T. BLANDFORD,
C     IEEE TRANS. ON NUCL. SCI. NS-27, 1006(1980)) WITH
C     SIMPLIFICATIONS DUE TO WARREN BENDEL OF NRL (PRIVATE
C     COMMUNICATION).  THE EQUATION NUMBERS REFER TO THE APPENDIX
C     OF PICKEL AND BLANDFORD'S PAPER.
C
      REAL L
C
C     EQUATION (A-7)
C
      AP=3.*(H*W+H*L+L*W)
C
C     EQUATION (A-8)
C
      DIFPLD=(G(S,L,W,H)+G(S,W,L,H)+G(S,L,H,W)+G(S,W,H,L)+
     1 G(S,H,W,L)+G(S,H,L,W))/(3.1416*AP)
      RETURN
      END
```

```
      FUNCTION G(S,X,Y.Z)
      REAL KSQ
C
C     PRELIMINARY DEFINITIONS
C
      KSQ=X*X+Y*Y
      TSQ=X*X+Z*Z
      T=SQRT(TSQ)
      RSQ=KSQ+Z*Z
      R=SQRT(RSQ)
      V=12.*X*Y*Z*Z
      PSQ=S*S-Z*Z
      QSQ=S*S-X*X-Z*Z
      IF((S.GE.0.0).AND.(S.LT.Z)) GO TO 10
      IF((S.GE.Z) .AND.(S.LT.T))GO TO 20
      IF((S.GE.T) .AND.(S.LE.R))GO TO 30
      G=0.0
      RETURN
C
C     EQUATION (A-9)
C
 10   G=8.*Y*Y*Z/KSQ-S*(3.*X*Y/(R*T))**2
      RETURN
C
C     EQUATION (A-10)
C
 20   G=S*(3.*Y/SQRT(KSQ))**2-S*(3.*X*Y/(T*R))**2
     1 -X*(SQRT(PSQ)/S)*(8.+4.*Z*Z/(S*S))
     2 +(V*ATAN(Y/X)-(Y*Z*Z/SQRT(KSQ))**2)/(S*S*S)
      RETURN
C
C     EQUATION (A-11)
C
 30   G=-S*(3.*X*Z/(R*SQRT(KSQ)))**2
     1 +(X*X*Z*Z*(Z*Z/KSQ-3.)+V*ATAN(Y/X))/(S*S*S)
     2 +Y*Z*Z*(SQRT(QSQ)/S)*(8./TSQ+4./(S*S))
     3 -(V/(S*S*S))*ACOS(X/SQRT(PSQ))
      RETURN
      END
```